I.O.S.

WAVES RECORDED OFF SOUTH UIST IN THE HEBRIDES

by
B C H FORTNUM

Data for March 1976 to February 1978
at position 57° 18′ N, 07° 38′ W

Summary Analysis and Interpretation Report

Report No 115

1981

INSTITUTE OF
OCEANOGRAPHIC
SCIENCES

NATURAL ENVIRONMENT RESEARCH COUNCIL

INSTITUTE OF OCEANOGRAPHIC SCIENCES

Wormley, Godalming,
Surrey, GU8 5UB.
(0428 - 79 - 4141)

(Director: Dr. A.S. Laughton)

Bidston Observatory,
Birkenhead,
Merseyside, L43 7RA.
(051 - 653 - 8633)

(Assistant Director: Dr. D.E. Cartwright)

Crossway,
Taunton,
Somerset, TA1 2DW.
(0823 - 86211)

(Assistant Director: M.J. Tucker)

WAVES RECORDED OFF SOUTH UIST
IN THE HEBRIDES

by
B.C.H.FORTNUM

Data for March 1976 to February 1978
at position 57°18′N, 07°38′W

Summary Analysis and Interpretation Report

Report No 115

1981

The preparation of this report and the collection of the data contained in it have been financed by the Departments of Energy and of Industry

Institute of Oceanographic Sciences
Crossway
Taunton
Somerset TA1 2DW
UK

CONTENTS

LIST OF FIGURES

1. INTRODUCTION

1.1 Site description

The site at which the wave measurements were taken is shown on the map in figure 1.1. It is approximately 15 kilometres west of the island of South Uist in the Outer Hebrides, where the water depth is about 42 metres; its position is 57°18′N, 007°38′W.

1.2 Description of measuring and recording systems

The wave measurements were made by a Waverider buoy and the first buoy was laid on 28 February 1976 using the RV Challenger. The mooring used was similar to that described in HUMPHERY(1975), except that it was modified to suit local conditions. The chain linking the anchor and sub-surface float was up-rated to 9mm, and its length adjusted so that the float was approximately 15m below the surface. The total length of mooring components above the float was increased to 35m to allow the Waverider to follow the larger waves anticipated at the South Uist site. Waverider maintenance visits would normally be possible only in summer; therefore heavy zinc sacrificial anodes were used to protect metal parts where appropriate. The Waverider buoy measures the vertical acceleration of the water surface; this acceleration is integrated twice on the buoy to give the elevation of the water surface above the mean water level, which is then transmitted by a radio link to the receiving equipment located on a hill (Rueval, 87m OD) on the island of South Uist. This information about the water surface elevation is sampled twice each second and recorded digitally on magnetic tape by a Rapco data logger. Each data record contains 2088 values of elevation (covering approximately 17 minutes), and the time between starts of successive records is 3 hours. (In addition, data are recorded in analogue form by a chart recorder and as an fm signal on magnetic tape, purely for back-up purposes. The fm records may be used to replace missing or invalid Rapco records, but before an fm record can be used in the Rapco validation and analysis system, it must be subjected to a digitisation process; this produces a digital record identical in format to that of the Rapco records.) Tape translation is carried out at the Taunton laboratory using a replay unit interfaced to a DEC PDP-11 computer.

1.3 Details of calibration and maintenance

(i) Buoy no 6459 laid 28 February 1976; previously calibrated 22 April 1975; sensitivity -2.2 per cent.
(ii) Buoy no 6459 removed from mooring, and buoy no 6242 fitted to existing mooring 3 August 1976; previously calibrated 13 April 1976; sensitivity -0.5 per cent.
(iii) Buoy no 6242 removed and buoy no 6850 fitted to new sub-surface mooring 18 April 1977; sensitivity -1.5 per cent.
(iv) Buoy no 6850 removed from mooring, and buoy no 6459 fitted to existing mooring 10 August 1977; previously calibrated 4 April 1977; sensitivity -4 per cent.
Routine servicing of the equipment (including changing charts, magnetic tapes and cassettes) is carried out on site by a local agent. Major servicing is carried out by IOS personnel at intervals of approximately 6 months, or whenever a significant fault is reported.

1.4 Wave data coverage and return (figures 1.4(a) - 1.4(f))

(Corrected page)

1.4 Wave data coverage and return (figures 1.4(a) - 1.4(f))
The period covered by the data is 5 March 1976 to 28 February 1978. For this period 603 of the 5812 possible Rapco records (i.e. 10.4%) were either missing or classified invalid. However 118 of these missing/invalid records have been replaced using data from the fm back-up system, and so the number of records used in the preparation of this report is 5327 (an overall data return of 91.7%). No attempt has been made to correct any bias which may have resulted from missing/invalid records, because of the uncertain reliability of available techniques. (Simple gap-filling by linear interpolation, up to a maximum of 7 consecutive records, has been carried out for the purpose of persistence calculations only: see section 3.6.) The approximate times when missing/invalid records occurred may be derived from the plots in figure 1.4 which show Hs as a time series. On these plots each vertical line represents a valid record, and the height of the line is proportional to the value of Hs for that record: therefore these plots also indicate the variation of Hs with time. A previous report on data from this site is FORTNUM et al (1979).

2. WIND DATA - COMPARISON WITH THE LONG-TERM AVERAGE
The meteorological station nearest to the wave measurement site is Benbecula (57°28′N, 007°22′W) where wind data have been analysed for a 15 year period from March 1963 to February 1978. Winds approaching from directions which have very limited fetches associated with them have not been considered, so that only winds in the sector from 170° to 010° have been considered in this report (including a proportion of calms and variables). The data used are three-hourly synoptic wind speeds.

2.1 Monthly variation of wind speeds (figure 2.1)
For each month, the mean of the monthly means of wind speed is plotted. There are four months for which the mean wind speed for 1976-1978 is more than 10% different from the mean for 1963-1978: they are March, August, December and February. Only one of these months (March) has a mean wind speed which is higher than the 'long-term' monthly mean (by 16%); for December and February the means are 23% and 27% respectively below their 'long-term' monthly mean wind speeds.

2.2 Yearly variation of wind speeds (figure 2.2)
The year-to-year variability of wind conditions is illustrated in this figure. It shows, for each year, the maximum value of wind speed, and also the means of the next N highest wind speeds, where N = 5, 10, 20, 50, 100 (thus the highest 186 wind speeds are represented). It can be seen that 1976 is generally the calmest of the 15 years shown, and that 1977 experienced comparatively low maximum wind speeds whilst its mean wind speed is comparatively high.

wind speed is comparatively high.

South Uist 76/78 -2-

3. WAVE DATA - DESCRIPTION AND DISCUSSION OF THE PRESENTATIONS

Where figures show seasonal data, the seasons are defined as follows:

spring - March, April, May
summer - June, July, August
autumn - September, October, November
winter - December, January, February

The maximum value of Hs in these two years of data is 9.06 metres; the associated value of Tz is 10.42 seconds, and of Hmax(3hr) is about 16.9 metres.

3.1 Statistics of variations of wave heights

3.1.1 Monthly variation of Hs (figure 3.1.1)

For each month, the mean of the monthly means of significant wave height is plotted. Three months (July, August and February) show very little variation between the means for each year; for the remaining nine months the variations between years are comparatively large, the standard deviation being between 13% (April) and 26%(January) of the mean.

3.1.2 Yearly variation of Hs (figure 3.1.2)

The year-to-year variability of wave conditions is illustrated in this figure. It shows, for each year, the maximum value of Hs, and also the means of the next N highest values of Hs, where N = 5, 10, 20, 50, 100 (thus the highest 186 values of Hs are represented). The figure simply shows that the highest values of Hs were greater in the second year than in the first.

3.2 Statistics of wave heights

3.2.1 Occurrence of Hs (figures 3.2.1.1-3.2.1.5)

The percentage occurrence of Hs is shown on histograms. The most frequently occurring values of Hs may be seen, from figure 3.2.1.5, to lie between 1.5 and 2.0 metres, accounting for 17.7% of the total.

3.2.2 Exceedance of Hs and Hmax(3hr) (figures 3.2.2.1-3.2.2.5)

These graphs may be used to estimate the fraction of the time during which Hs was greater than, or less than, a given height. For instance, from figure 3.2.2.4 it may be seen that during winter the significant wave height exceeded 4 metres for approximately 15 per cent of the time.

3.3 Design wave heights

The methods used to calculate the design wave height (the most probable height of the highest wave with a return period of 50 years) are described in Appendix III. The results obtained by the different methods are given below.

3.3.1 Weibull distribution of Hs (figure 3.3.1)

The parameters of the Weibull distribution which most closely fits the data are A = 0.15 metre, B = 2.29 metres and C = 1.55, and this distribution is represented by the straight line in figure 3.3.1. Extrapolation of this line to a return period of 50 years gives a value of

Hs of 11.5 metres. The value of Tz associated with this Hs is approximately 11.5 seconds, resulting in a value for the design wave height of 21.3 metres.

3.3.2 Fisher-Tippett I distribution of Hs (figure 3.3.2)

The parameters of the Fisher-Tippett I distribution which most closely fits the data are a = 1.44 $metre^{-1}$ and b = 4.90, and this distribution is represented by the straight line in figure 3.3.2. (The parameters have been chosen for a best fit to the top 6 data points, as the other data points appear to be scattered about at least one other straight line.) Extrapolation of this line to a return period of 50 years gives a value of Hs of 11.6 metres. The value of Tz associated with this Hs is 11.5 seconds, resulting in a value for the design wave height of 21.6 metres.

3.3.3 Fisher-Tippett III distribution of Hs (figure 3.3.3)

The parameters of the Fisher-Tippett III distribution which most closely fits the data are A = 15.0 metres, B = 13.76 metres and C = 9.76, and this distribution is represented by the straight line in figure 3.3.3. Extrapolation of this line to a return period of 50 years gives a value of Hs of 10.9 metres. The value of Tz associated with this Hs is approximately 11 seconds, resulting in a value for the design wave height of 20.4 metres.

3.3.4 Individual wave model (figure 3.3.4)

The value of steepness used in the wave-by-wave method of determining design wave heights (as described in Appendix III) is 1:18, and the inverse mean period is 0.161 Hz. Using these values and the Fisher-Tippett III parameters given in section 3.3.3, the data which appear in figure 3.3.4 are obtained; by interpolation the design wave height is found to be 22.5 metres. A higher value of design wave height is expected from this method than from the methods described above, for the reasons stated in Appendix III.

3.4 Statistics of wave periods

The percentage occurrences of each of three wave period parameters (Tz, Tbar or Te) are shown on a histogram.

3.4.1 Occurrence of Tz (figures 3.4.1.1-3.4.1.5)

The most frequently occurring values of Tz in the data set lie between 6.0 and 6.5 seconds (14.1% of the total), and all values of Tz lie between 2.5 and 12.5 seconds (figure 3.4.1.5).

3.4.2 Occurrence of Tbar (figures 3.4.2.1-3.4.2.5)

For Tbar, the modal class is 6.5 to 7.0 seconds (12.5% of the total), and the range is from 2.5 to 14.0 seconds (figure 3.4.2.5).

3.4.3 Occurrence of Te (figures 3.4.3.1-3.4.3.5)

For Te, the modal class is 7.5 to 8.0 seconds (11.7%), and the range is from 3.5 to 16.0 seconds (figure 3.4.3.5).

3.5 Statistics of wave height and period combined
These figures (sometimes called "scatter" plots) show the numbers of wave records having particular combinations of values of Hs and period parameters (Tz, Tbar or Te). The numbers of wave records are presented as parts per thousand (the total number of valid observations being shown on each figure), except for those which would be less than one part per thousand; these are shown instead as single occurrences and are distinguished by being underlined.

3.5.1 Occurrences of Hs and Tz combined (figures 3.5.1.1-3.5.1.5)
On these figures points of equal occurrences are joined by contour lines to give an indication of the bivariate probability distribution of Hs and Tz, and to illustrate the correlation between them. A wave "steepness" (as defined in Appendix III) can be calculated for each (Hs,Tz) pair. It may be seen from the figures that all (Hs,Tz) pairs calculated for the South Uist data set have "steepnesses" less steep than 1:13, and a line is drawn on each figure showing this limiting "steepness". (Wave "steepnesses" as shown in this figure are significantly less than the maximum of 1:7 for an individual wave, since Hs and Tz are parameters averaged over a number of waves most of which have steepnesses less than this maximum.)

3.5.2 Occurrences of Hs and Tbar combined (figures 3.5.2.1-3.5.2.5)
These figures show data boundaries similar to those of wave "steepness" in figures 3.5.1.1 to 3.5.1.5, although the physical significance of these boundaries is not so obvious.

3.5.3 Occurrences of Hs and Te combined (figures 3.5.3.1-3.5.3.5)
On these figures lines of constant wave power per unit length of wave crest are shown (in kW/m), using the formula applicable to deep water (see Appendix II). (It should be noted that using the deep water formula instead of the depth-dependent formula results in an underestimate of the wave energy; the magnitude of this underestimate depends on the depth of the water and on the form of the spectrum, but it is typically about 10% at this site.)

3.6 Statistics of persistence of wave conditions
These figures show the means and standard deviations of the durations of storms and calms against each threshold value of Hs, and also the percentage of the total duration occupied by each event. Gaps in the data series of 7 or less records are filled (for the purpose of persistence calculations only) by linear interpolation; larger gaps are not filled, effectively reducing the series to a number of smaller sub-series, each with a correspondingly smaller total duration. (For storms, the curves showing percentage of time occupied by the events are, for all practical purposes, the same as those showing percentage exceedance of Hs as described in section 3.2.2.)

3.6.1 Persistence of calms of Hs (figures 3.6.1.1-3.6.1.5)
Information about, for example, calms of Hs less than 1.3 metres at the South Uist site during winter can be derived from figure 3.6.1.3. The mean duration of such calms was approximately 25 hours (with a standard deviation of 21 hours); they occupied about 10% of the total duration of

4236 hours, i.e. about 420 hours; and therefore there were 16 or 17 such calm events during this period.

3.6.2 Persistence of storms of Hs (figures 3.6.2.1-3.6.2.5)
Similar information can be derived for storms. For Hs of 4.5 metres during summer, figure 3.6.2.2 shows that the mean duration of such storms was approximately 10 hours (with a standard deviation of 5 hours); the total time occupied was 1% of 4410 hours, i.e. about 44 hours; and therefore the number of such storm events in this period was 4 or 5.

3.7 Distribution of wave energy with Hs and Te (figures 3.7.1-3.7.5)
For each wave record the wave energy per metre of wave crest is calculated from Hs and Te, using the formula applicable to deep water (see note in section 3.5.3). For each class of (Hs,Te) the energy from all records with Hs and Te values falling within that class is summed. The total energy within each class is then expressed in parts per thousand of the overall total energy and presented in these figures (a zero indicates less than one part per thousand, which on figure 3.7.5, for instance, means less than 585 kWh/m for the two-year period). In figure 3.7.5 it can be seen that a large proportion of the wave energy measured at the site during this two-year period is associated with the intermediate values of Hs and Te.

4. ACKNOWLEDGEMENTS

Contributions have been made towards the collection, analysis and presentation of the South Uist wave data by several members of the Applied Wave Research Group and of the Instrument Engineering Group, both based at the Taunton laboratory of the Institute of Oceanographic Sciences. The Meteorological Office kindly supplied the wind data.

5. REFERENCES

FORTNUM B C H, HUMPHERY J D and PITT E G 1979. Contoured wave data off South Uist. Institute of Oceanographic Sciences, Report No 71.

HUMPHERY J D 1975. Waverider moorings and their modification at IOS. 42-46 in Technology of Buoy Systems. London: Society for Underwater Technology.

APPENDIX I

Method of system calibration

I.1 Method of calibration of Waverider buoys using the facilities of the National Maritime Institute, Hythe

The Waverider is clamped between two rigid parallel bars, which are supported at their mid-points on bearings mounted at the apexes of two supporting A-frames. The Waverider is driven through a vertical circle, 3 metres in diameter, by a variable speed motor through belt-drives. The buoy is maintained in the vertical position throughout by chain-drives. Rig-speed is electronically controlled, and is monitored by a tachometer giving angular velocity in revolutions per minute. However all IOS calibrations are made using a stop-watch to time several revolutions; an average rotation period is then calculated. Height-modulated radio emissions are received from the buoy on a standard Waverider receiver. The receiver converts the signals into a pen-deflection on a chart recorder, and into an analogue voltage output. Early IOS calibrations were expressed simply as a percentage of the nominal value of sensitivity (see section 1.3), after amplitude corrections had been made for imperfect electronic integrator response at the longer rig-rotation periods (greater than 10 seconds). The procedure has now been refined however; buoys and receivers are calibrated separately to high accuracy, and a combined figure in volts per metre of buoy displacement is presented.

APPENDIX II

Definitions of wave parameters and their derivations from spectral moments

II.1 Definition of spectral moments
The nth moment of a continuous spectrum is

$$m_n = \int_0^\infty f^n S(f)\, df$$

where $S(f)$ is the spectral density at frequency f.

For the discrete spectra produced from the digital time series, the following equation has been used in the calculation of the spectral moments.

$$m_n = \frac{10}{T} \sum_{i=i_L}^{i_U} f_i^{\,n} S_i$$

where S_i is the ith spectral estimate above zero frequency, and T is the record length in seconds.
For all the data, $i_L = 5$; ($f_5 = .0444$Hz)
For the first year's data, $i_U = 70$; ($f_{70} = .6792$Hz)
For the second year's data, $i_U = 65$; ($f_{65} = .6304$Hz)

II.2 Derivation of wave parameters
The wave parameters presented in this report are derived from the spectral moments using the following identities.

$$Hs = 4\sqrt{m_0}$$

$$Tz = \sqrt{\frac{m_0}{m_2}}$$

$$\bar{T}\ (\text{Tbar}) = \frac{m_0}{m_1}$$

$$Te = \frac{m_{-1}}{m_0} \quad .$$

Wave power may be calculated from the spectra using the expression

$$P = \int S(f)\, V_g(f,d)\, df$$

where V_g is the group velocity at frequency f and in water of depth d.

An approximation to this expression has been used in this report, based on the assumption that the wave measurements were made in deep water: in this case

$$V_g(f,d) = V_g(f) = \frac{g}{4\pi f}$$

which leads to

$$P' = 0.49\, Hs^2\, Te$$

where P' is in kilowatts per metre of wave crest
Hs is in metres
Te is in seconds.

APPENDIX III

Details of methods used for calculating design wave heights

III.1 By finding the long-term distribution of Hs

III.1.1 Hs is used as a measure of the "sea-state" (i.e. the intensity of wave activity), and it is sampled every 3 hours. It is assumed that a set of Hs data for one year, or an integral number of years, is representative of the wave climate.
For each value of Hs, the probability that this value will not be exceeded is calculated; this probability is then plotted against Hs. The axes are scaled according to an extreme-value distribution, so that data with a perfect fit would appear as a straight line on the diagram. This procedure is carried out using extreme-value distributions defined in the following ways

Weibull

$$\text{Prob}(\text{Hs} \leqslant h) = \begin{cases} 1 - \exp\left[-\left(\frac{h-A}{B}\right)^C\right], & \text{for } h > A \\ 0, & \text{for } h \leqslant A \end{cases}$$

where B and C are positive, and A represents a lower bound on h.

Fisher-Tippett I (first asymptote)

$$\text{Prob}(\text{Hs} \leqslant h) = \exp\left[-\exp(-ah+b)\right].$$

Fisher-Tippett III (third asymptote)

$$\text{Prob}(\text{Hs} \leqslant h) = \begin{cases} \exp\left[-\left(\frac{A-h}{B}\right)^C\right], & \text{for } h \leqslant A \\ 1, & \text{for } h > A \end{cases}$$

where B and C are positive, and A represents an upper bound on h. (See FISHER AND TIPPETT(1928) and GUMBEL (1958) for the derivations of these distributions.)

For each extreme-value distribution the best-fit straight line is drawn; this line is then extrapolated to the desired probability (see section III.1.2) and the corresponding value of Hs is read off as the "design sea-state".

III.1.2 To calculate the "sea-state" which will be exceeded only once in N years, a storm duration of D hours needs to be assumed. The probability that a randomly chosen time will be within this storm is then

$$\frac{D}{24 \times 365.25 \times N}$$

IOS uses D = 3 hours (this choice is discussed in section III.1.5) which gives

$$\text{Probability} = \frac{3.422 \times 10^{-4}}{N}$$

$$= 6.845 \times 10^{-6} \quad \text{for} \quad N = 50 \text{ years.}$$

III.1.3 The value of Tz for the "design sea-state" is required before the highest wave in the storm can be calculated. This is derived from the bivariate distribution of Hs and Tz (figure 3.5.1.5). A line is drawn across this at the "design sea-state" value of Hs and the most likely value of Tz (the modal value) is then estimated using extrapolations of the probability contours.

III.1.4 The most probable value of the highest zero-up-cross wave in the storm is then derived by assuming that the heights of such waves follow a Rayleigh distribution whose probability density function is

$$\text{prob}(h) = \frac{2h}{(Hrms)^2} \exp\left[-\left(\frac{h}{Hrms}\right)^2\right]$$

where $Hrms \approx \frac{Hs}{\sqrt{2}}$.

Exact theory is not available for zero-up-cross wave heights, but this distribution has been found to be an adequate fit to measured data. If there are n waves in the recording interval (3hr), then the probability that the highest wave, H, in three hours is less than h is

$$\text{Prob}(H \leqslant h) = \left\{1 - \exp\left[-\left(\frac{h}{Hrms}\right)^2\right]\right\}^n$$

with a corresponding probability density function

$$\frac{2n}{(Hrms)^2} h \exp\left[-\left(\frac{h}{Hrms}\right)^2\right] \left\{1 - \exp\left[-\left(\frac{h}{Hrms}\right)^2\right]\right\}^{n-1} .$$

The most probable value (the mode) of this probability density function is usually used and is given by

$$Hmax(3hr) = Hrms\sqrt{\Psi}$$

where Ψ is a function of Tz which may be found using either figure 7 or equation 6.1-2 in TANN(1976).

III.1.5 In choosing the value of storm duration D, it should be noted that the effect of increasing D is to decrease the value of Hs for a given return period N. However, it also increases the ratio of Hmax(3hr) to Hs. It is found that in practice these effects roughly cancel and typically the value of Hmax(3hr) changes by only 3 per cent for a change of D from 3 to 15 hours. The choice of D is therefore not critical.

Many details of the above procedures may be found in TANN(1976).

III.2 By a wave-by-wave method

III.2.1 BATTJES(1970) shows that the probability that a randomly chosen wave will have a height H greater than h is

$$\text{Prob}(H>h) = \frac{\int_0^\infty \int_0^\infty R(h, Hs)\, Tz^{-1}\, p(Tz, Hs)\, dHs\, dTz}{\int_0^\infty \int_0^\infty Tz^{-1}\, p(Tz, Hs)\, dHs\, dTz} \quad \ldots\ldots\ldots\ldots (1)$$

where $R(h, Hs)$ is the Rayleigh cumulative probability function and $p(Tz, Hs)$ is the joint probability density function of Hs and Tz.

III.2.2 TANN makes the following suggestion in an unpublished manuscript. In order that values of Hs higher than those actually measured may be represented in the calculation of this probability, the values of Hs are assumed to have a long-term cumulative probability function $F(Hs)$, and a probability density function $f(Hs) = F'(Hs)$.

For each value of Hs throughout the long-term distribution, an average value of Tz^{-1} is used (denoted by $\overline{T_{Hs}^{-1}}$). It is defined as

$$\overline{T_{Hs}^{-1}} = \int_0^\infty Tz^{-1}\ \frac{p(Tz, Hs)}{P(Hs)}\ dTz$$

where $P(Hs) = f(Hs)$.

Therefore

$$\int_0^\infty Tz^{-1}\, p(Tz, Hs)\, dTz = \overline{T_{Hs}^{-1}}\, f(Hs)$$

which, when substituted into equation (1), allows the probability of exceedance to be written

$$\text{Prob}\,(H>h) = \frac{\int_0^\infty R(h, Hs)\, \overline{T_{Hs}^{-1}}\, f(Hs)\, dHs}{\int_0^\infty \overline{T_{Hs}^{-1}}\, f(Hs)\, dHs} \ .$$

The value of $\overline{T_{Hs}^{-1}}$ used with each value of Hs is chosen to satisfy the condition of constant wave "steepness", where the relationship between "steepness"(1:s), water depth(d), Hs and Tz is

$$Tz = \sqrt{\frac{2\pi s Hs}{g}\ \coth\left(\frac{2\pi d}{sHs}\right)}\ .$$

The value for the steepness used in this report is given in section 3.3.4.

The long-term distribution used in the computation for this report is the Fisher-Tippett III extreme-value distribution, whose probability density function is

$$f(Hs) = \frac{C}{A-Hs}\left(\frac{A-Hs}{B}\right)^{C} \exp\left[-\left(\frac{A-Hs}{B}\right)^{C}\right] .$$

The constants A,B,C are determined graphically as described in section III.1.1, and their values as used in this report are given in section 3.3.3.

III.2.3 Thus the probability of a wave exceeding each particular wave height may be found, and this probability may be converted into a return period of N years using the formula

$$N = \frac{1}{365.25 \times 24 \times 3600 \times T_{ave}^{-1} \times Prob}$$

where $T_{ave}^{-1} = \frac{1}{\text{average period}}$.

The value of the average wave period is contained in section 3.3.4. Since T_{ave}^{-1} is a non-analytic function of Prob, the simplest way of solving the problem is to calculate Prob for various values of h, calculate N for each of these values of Prob, and then interpolate to find the height h corresponding to the required value of N (in this case 50 years).

Whereas the method described in section III.1 assumes that the highest wave in a 50-year period will come from the most stormy 3-hour period in 50 years, the individual wave method takes into account the probability that storms other than the highest may provide the wave with a 50-year return period. Consequently the height of a 50-year wave as estimated by this method is likely to be greater than that estimated from the method of using a long-term distribution of Hs.

III.3 References

BATTJES J A 1970. Long-term wave height distribution at seven stations around the British Isles. National Institute of Oceanography, Internal Report No A44.

FISHER R A AND TIPPETT L H C 1928. Limiting forms of frequency distribution of the largest or smallest member of a sample. Proceedings of the Cambridge Philosophical Society 24, 180-190.

GUMBEL E J 1958. Statistics of Extremes. New York: Columbia University Press. 371 pp.

TANN H M 1976. The estimation of wave parameters for the design of offshore structures. Institute of Oceanographic Sciences, Report No 23.

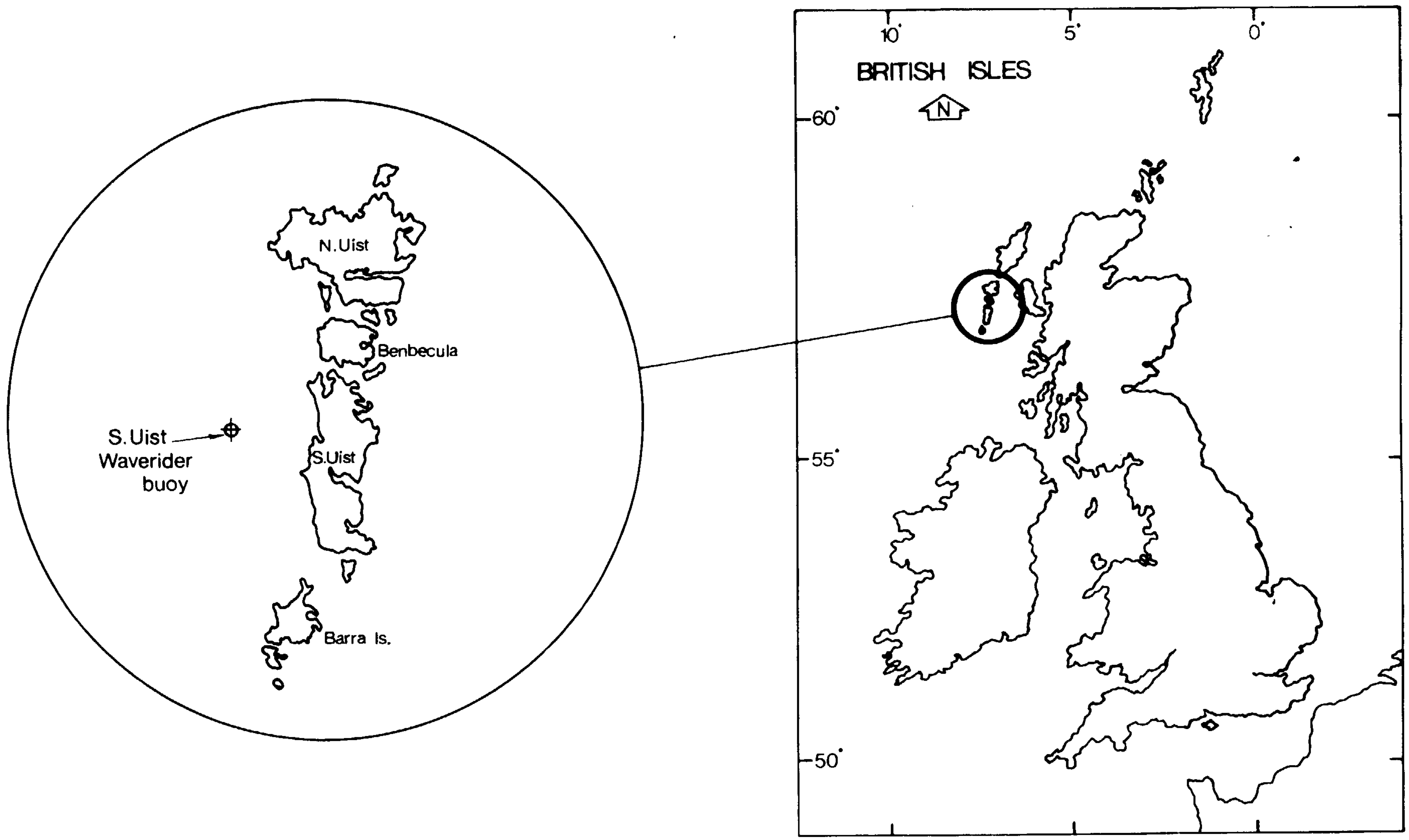

SU768

Location map of S.Uist Wave Recorder

FIG 1.1

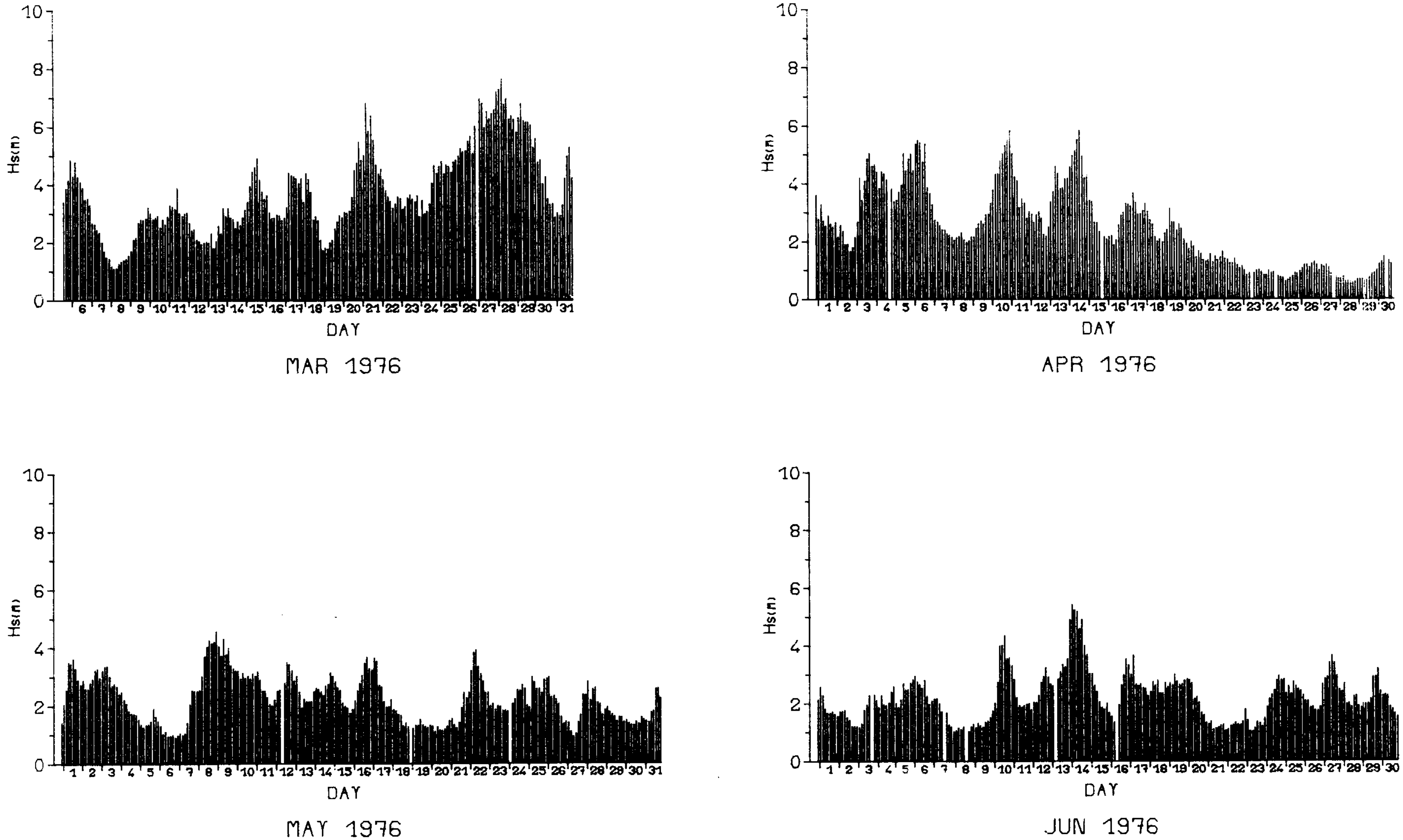

TIME SERIES OF Hs

SOUTH UIST MAR 1976 - FEB 1978

FIG 1.4(a)

SU768

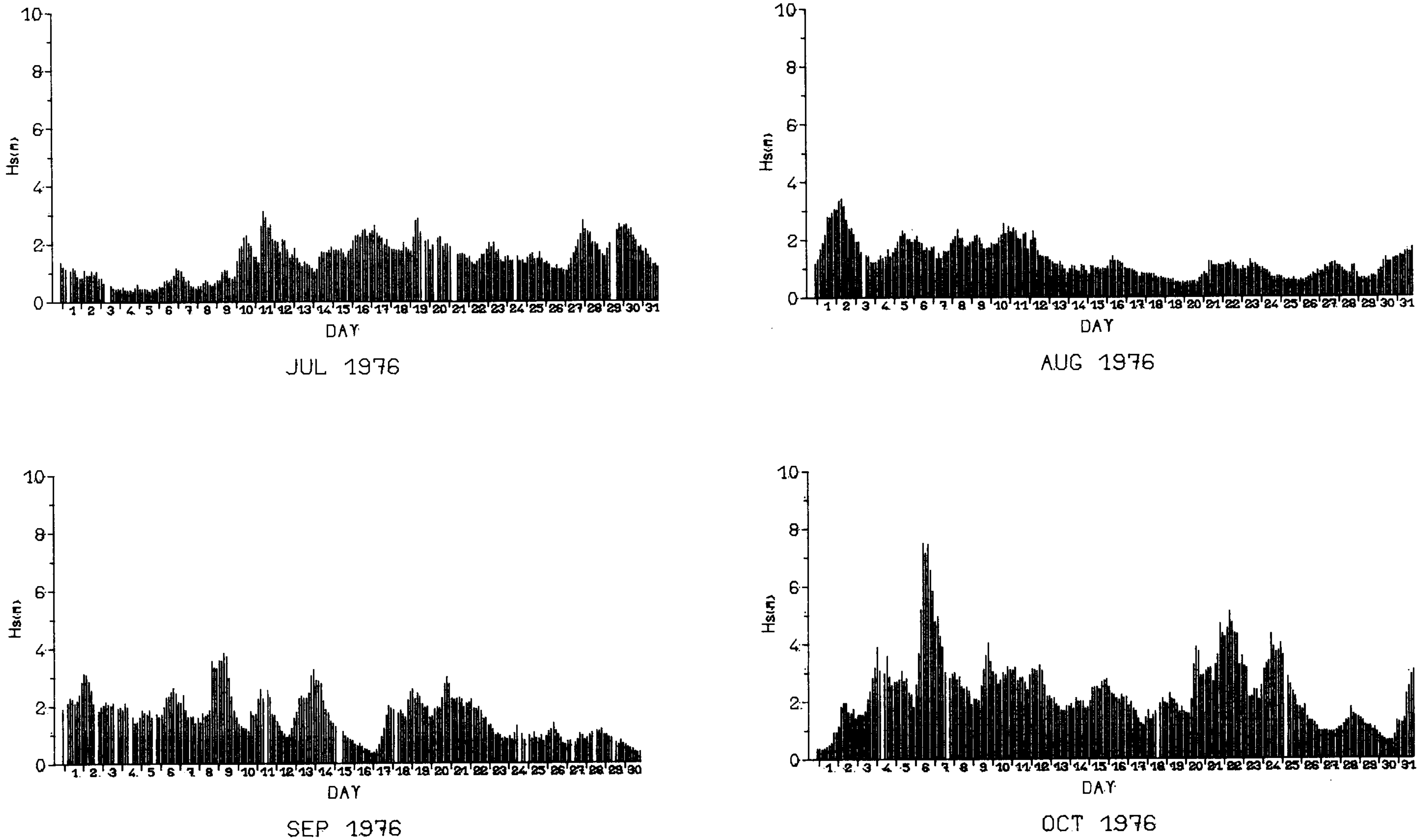

TIME SERIES OF Hs

SOUTH UIST MAR 1976 - FEB 1978

FIG 1.4(b)

SU768

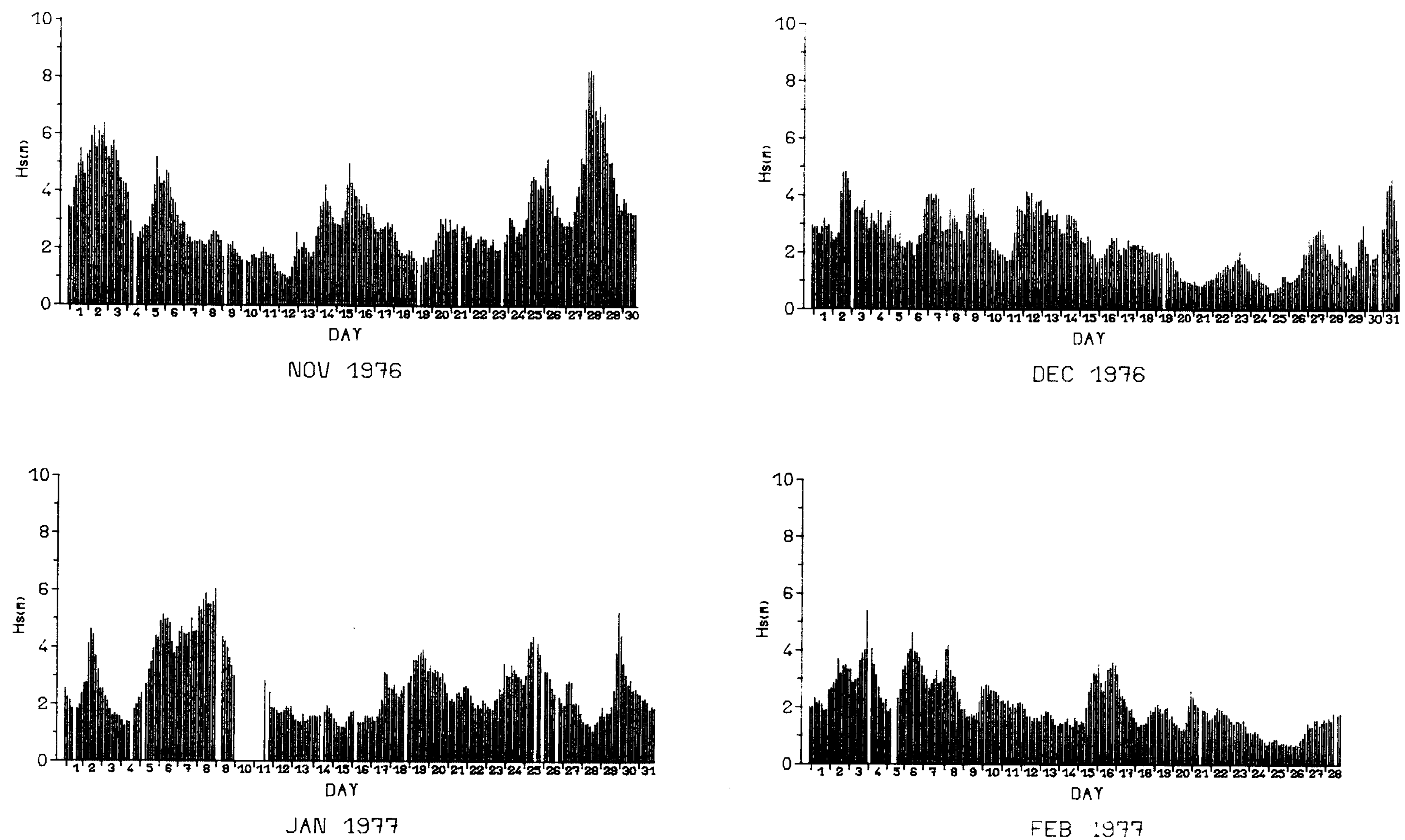

TIME SERIES OF Hs

SOUTH UIST MAR 1976 - FEB 1978

FIG 1.4(c)

SU768

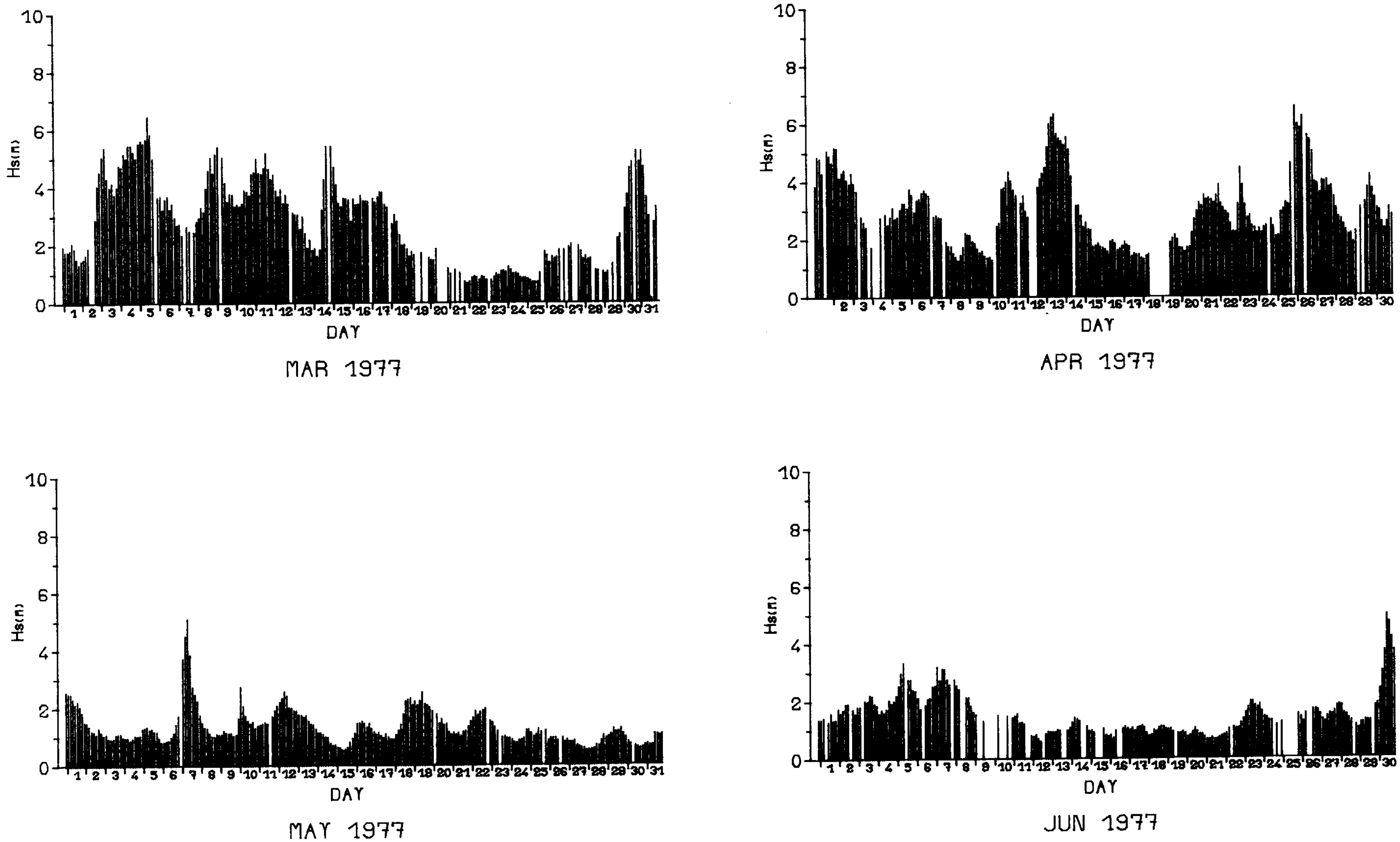

TIME SERIES OF Hs

SOUTH UIST MAR 1976 - FEB 1978

FIG 1.4(d)

SU768

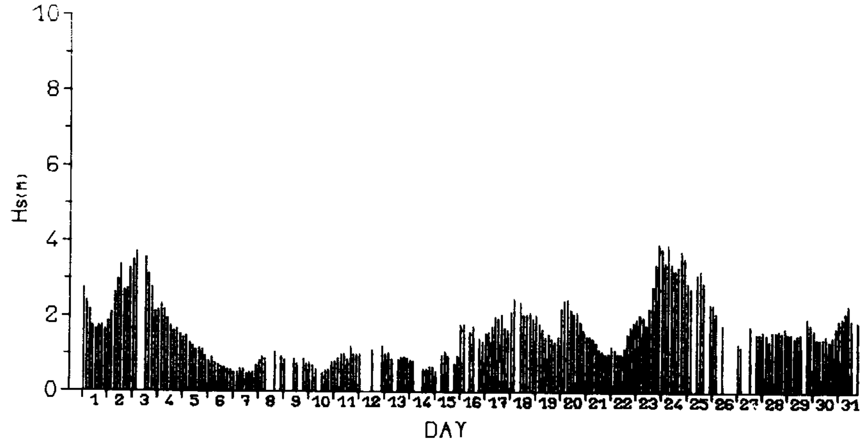

JUL 1977

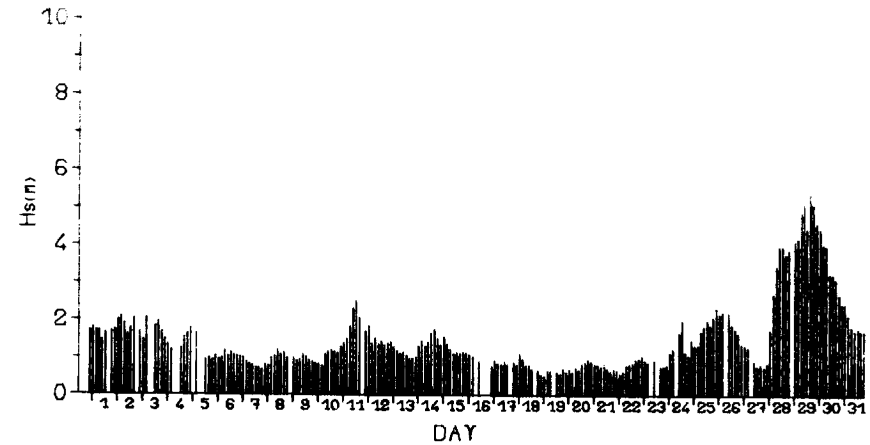

AUG 1977

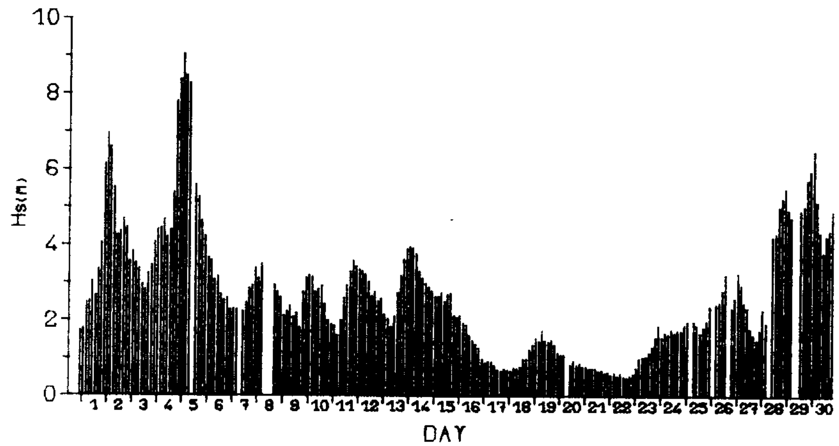

SEP 1977

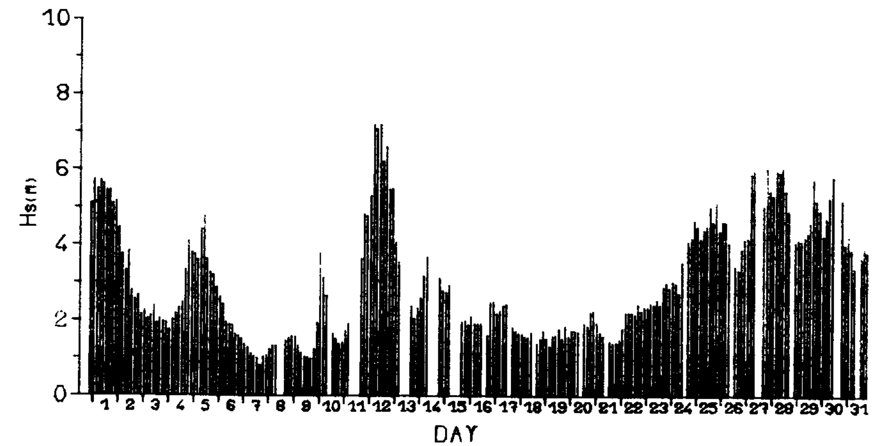

OCT 1977

TIME SERIES OF Hs

SOUTH UIST MAR 1976 - FEB 1978

FIG 1.4(e)

SU768

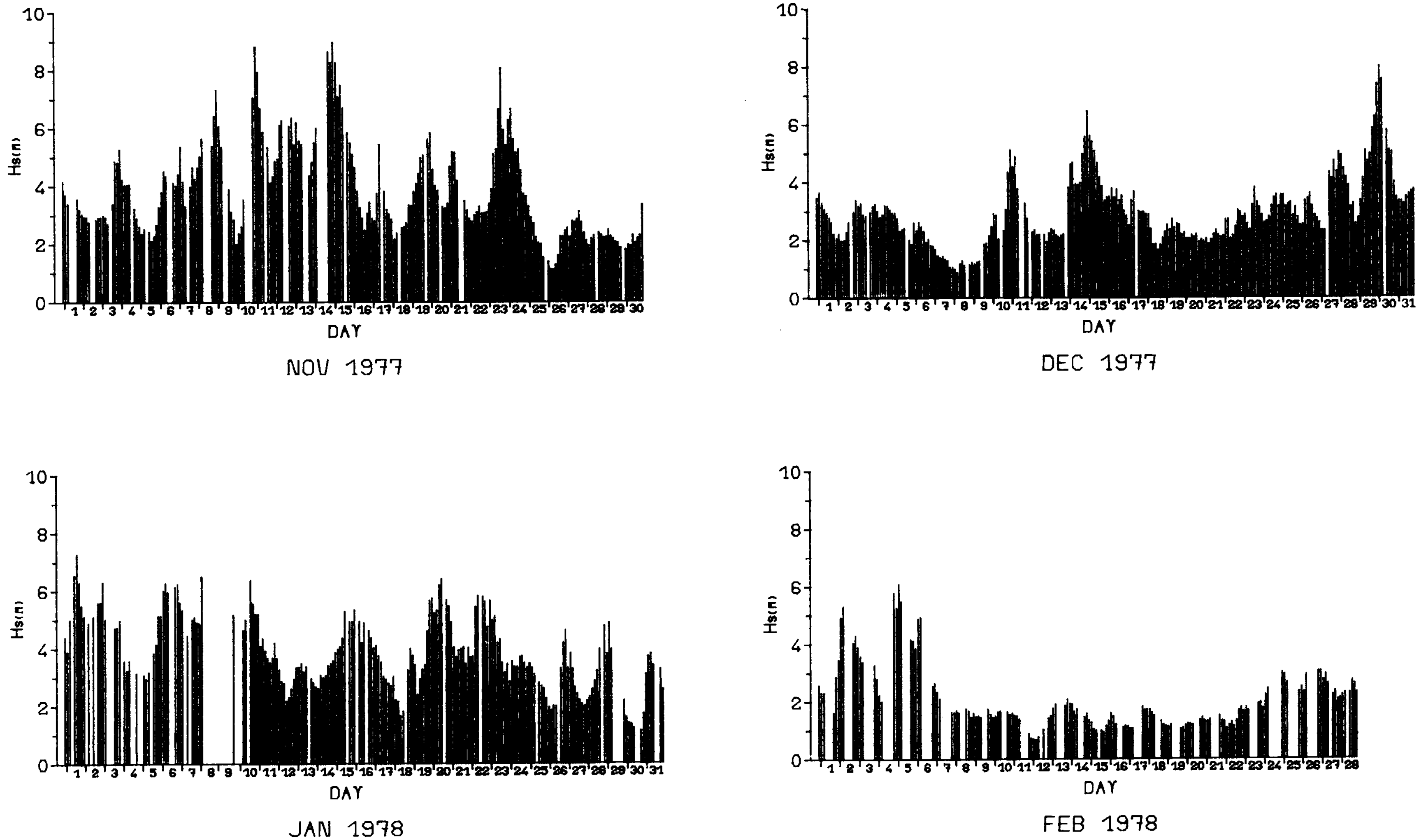

TIME SERIES OF Hs

SOUTH UIST MAR 1976 - FEB 1978

FIG 1.4(f)

SU768

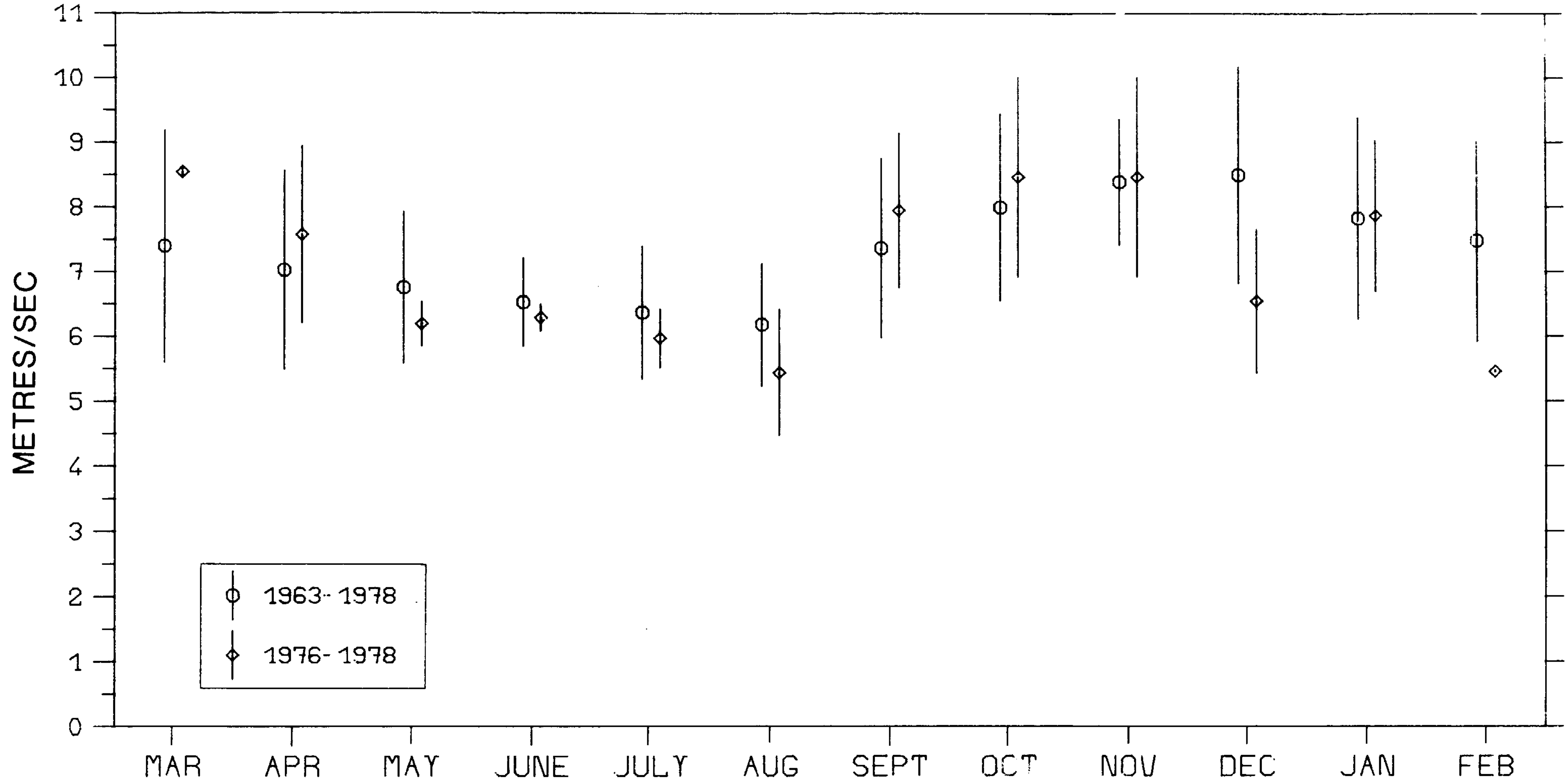

MEAN AND STANDARD DEVIATION OF THE MONTHLY MEAN OF
WIND SPEED

BENBECULA 1963 - 1978

FIG 2.1

SU768

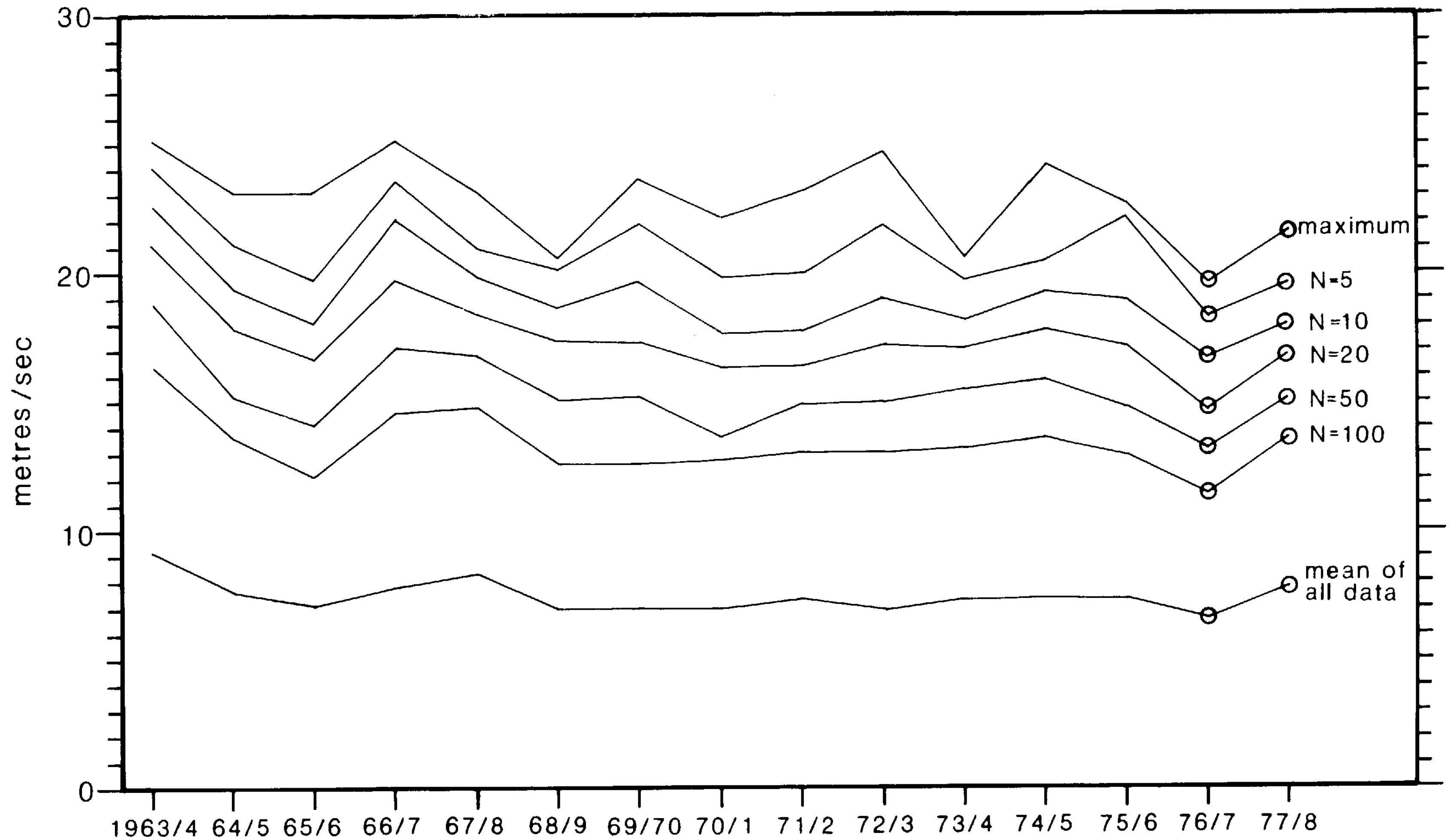

Mean of N largest values of wind speed

Benbecula March 1963 - February 1978

SU768

FIG 2.2

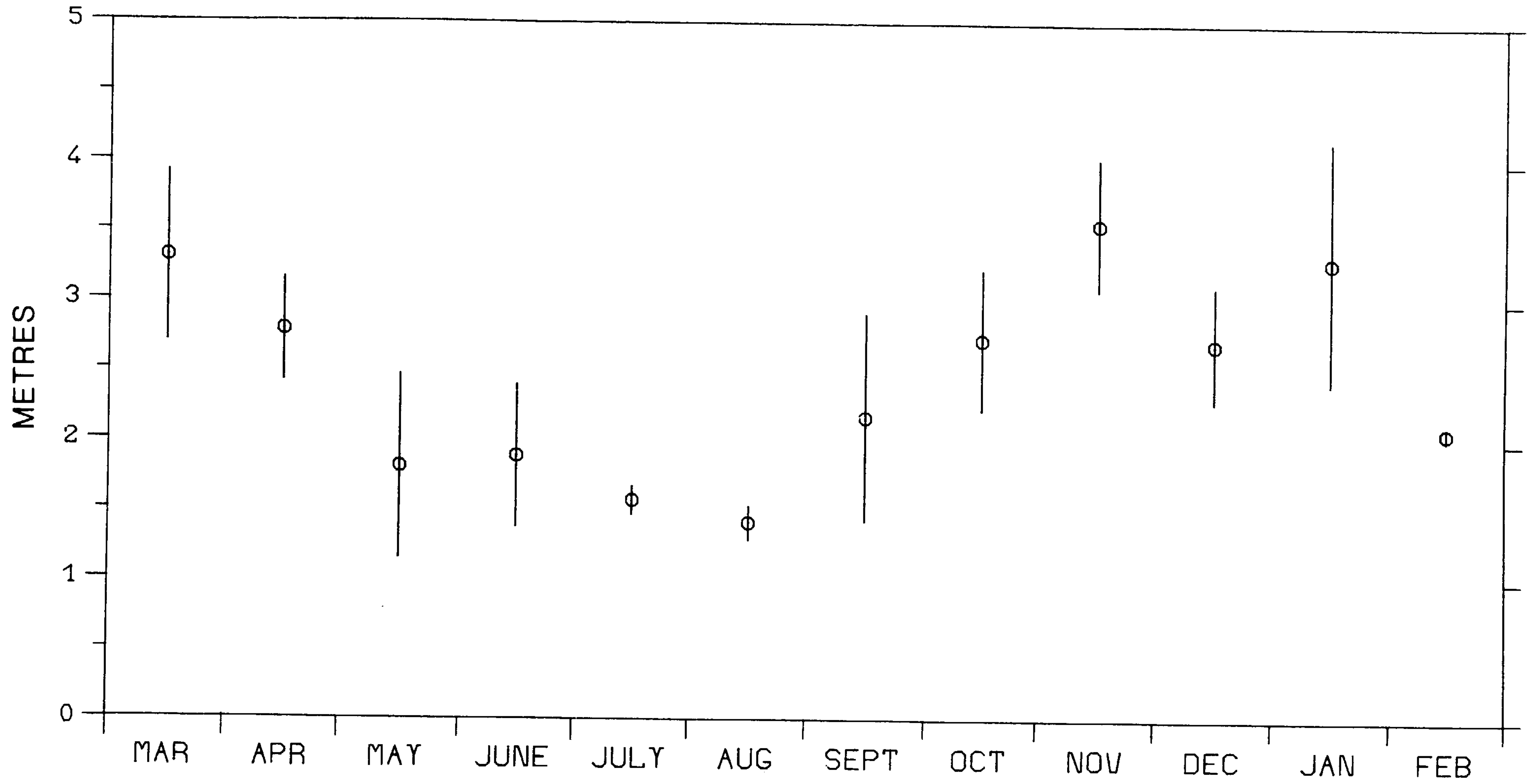

MEAN AND STANDARD DEVIATION OF THE MONTHLY MEAN OF
SIGNIFICANT WAVE HEIGHT
SOUTH UIST 1976 - 1978

FIG 3.1.1

SU768

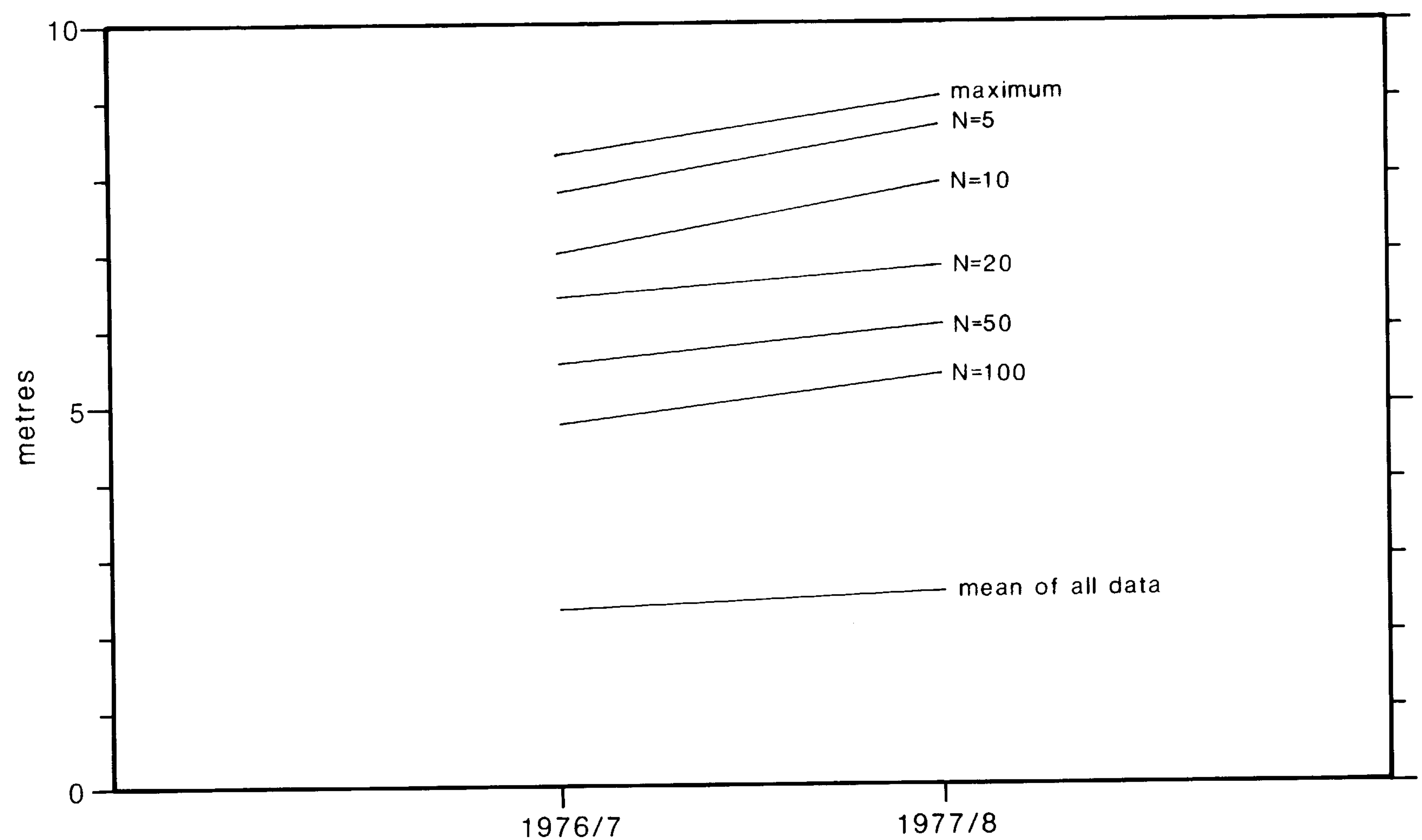

Mean of N largest values of significant wave height
South Uist March 1976 - February 1978

FIG 3.1.2

SU768

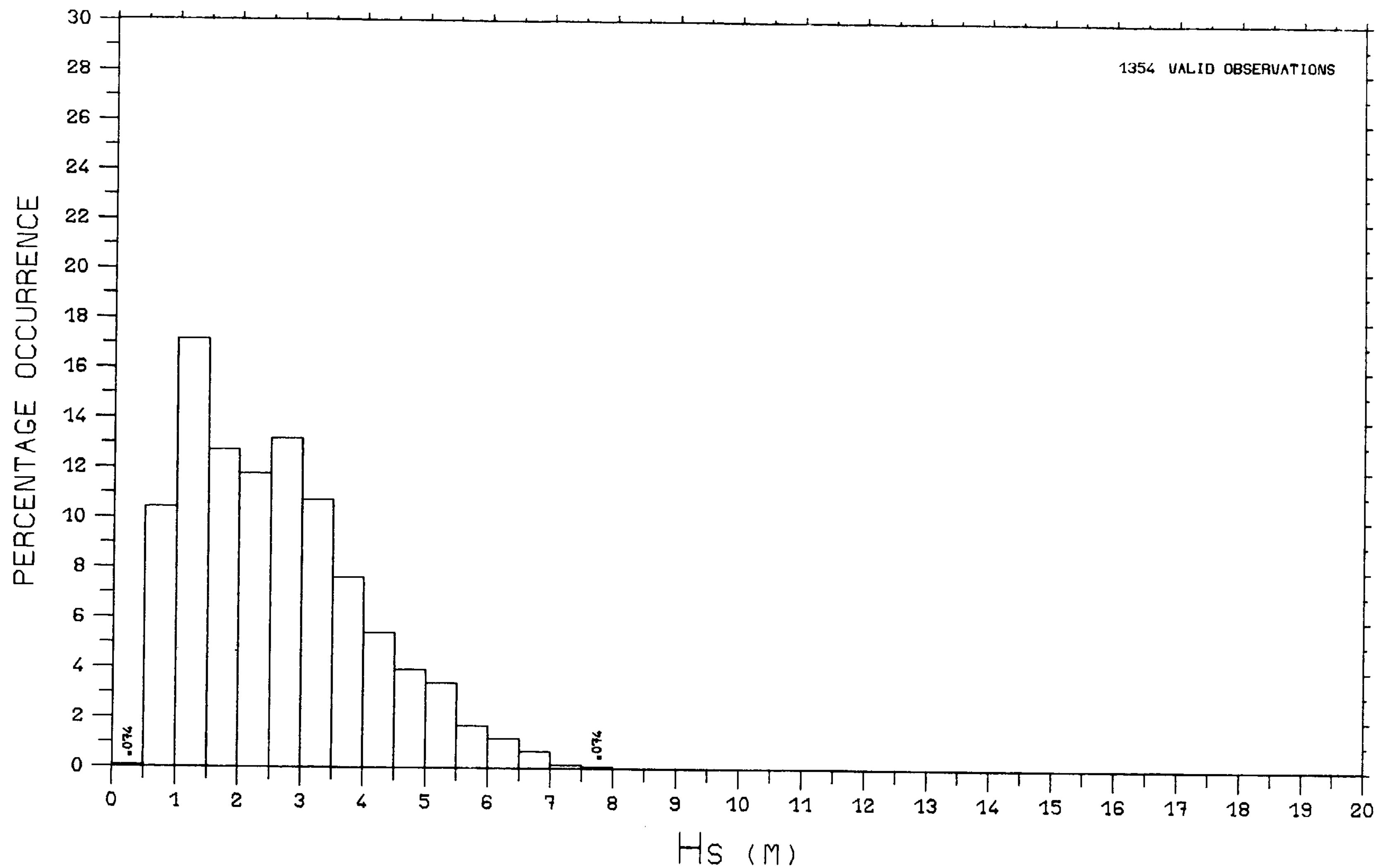

PERCENTAGE OCCURRENCE OF Hs

SU768

SOUTH UIST SPRING 1976 , 1977

FIG 3.2.1.1

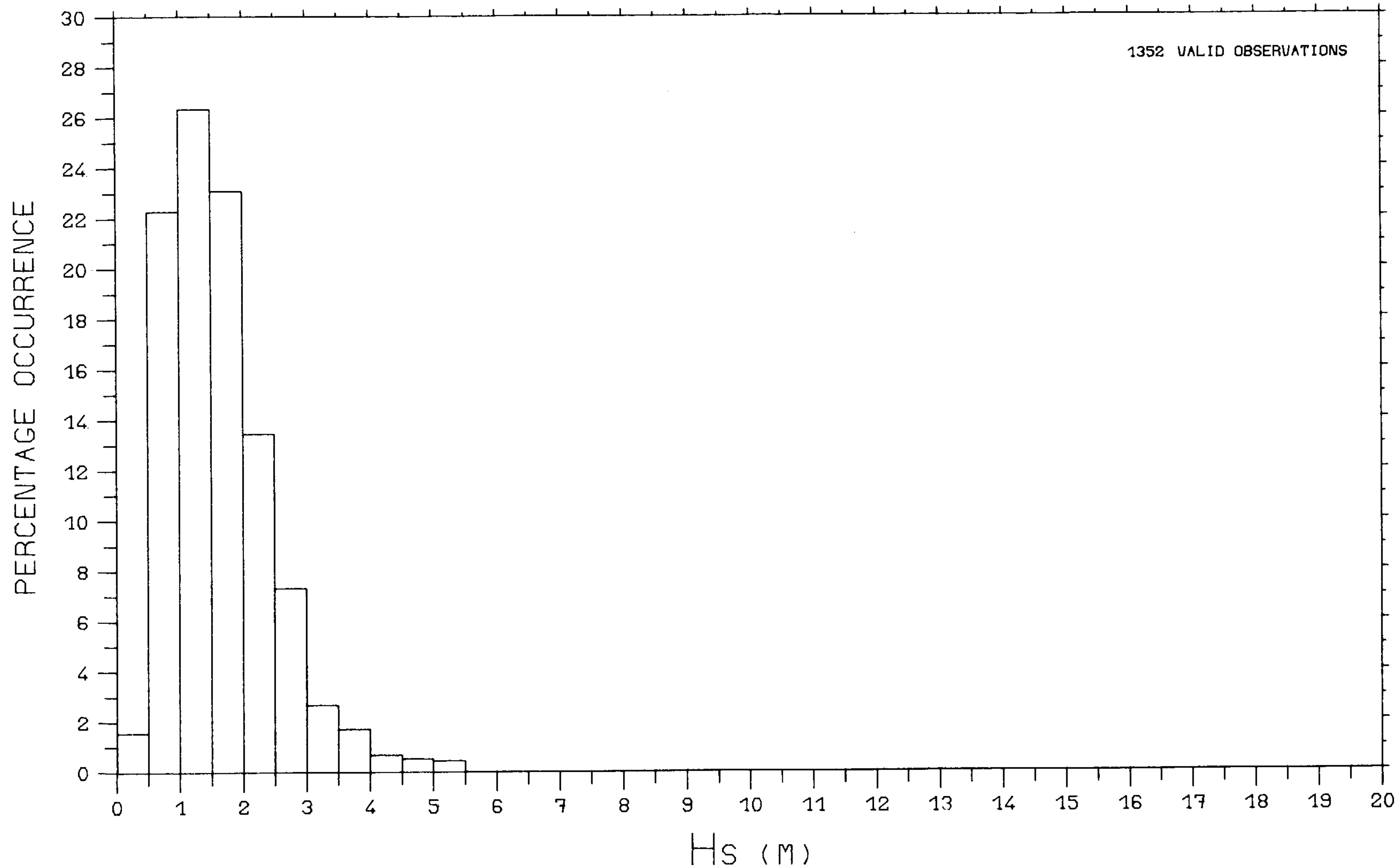

PERCENTAGE OCCURRENCE OF Hs

SOUTH UIST SUMMER 1976 , 1977

FIG 3.2.1.2

SU768

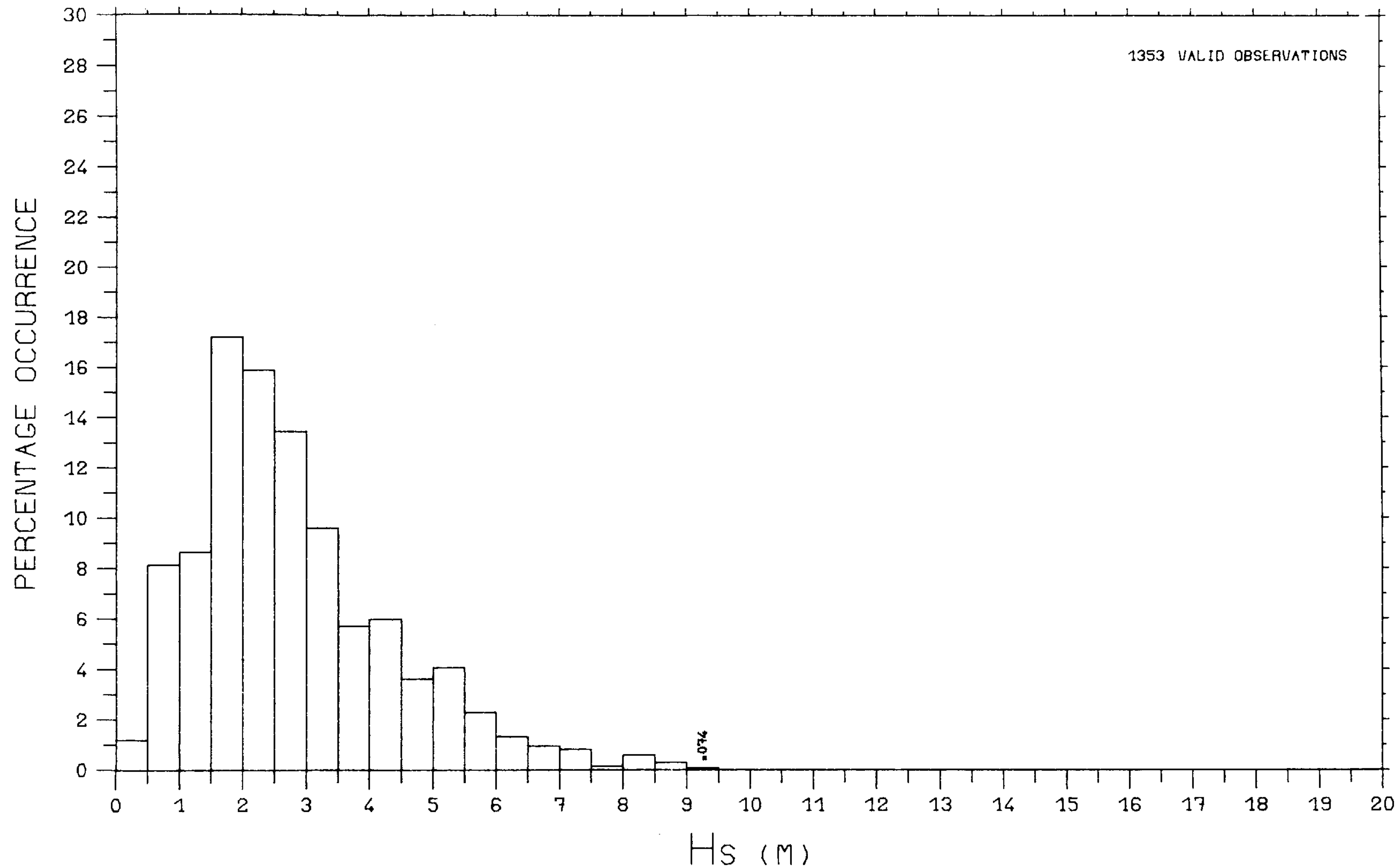

PERCENTAGE OCCURRENCE OF Hs

SOUTH UIST AUTUMN 1976 , 1977

FIG 3.2.1.3

SU768

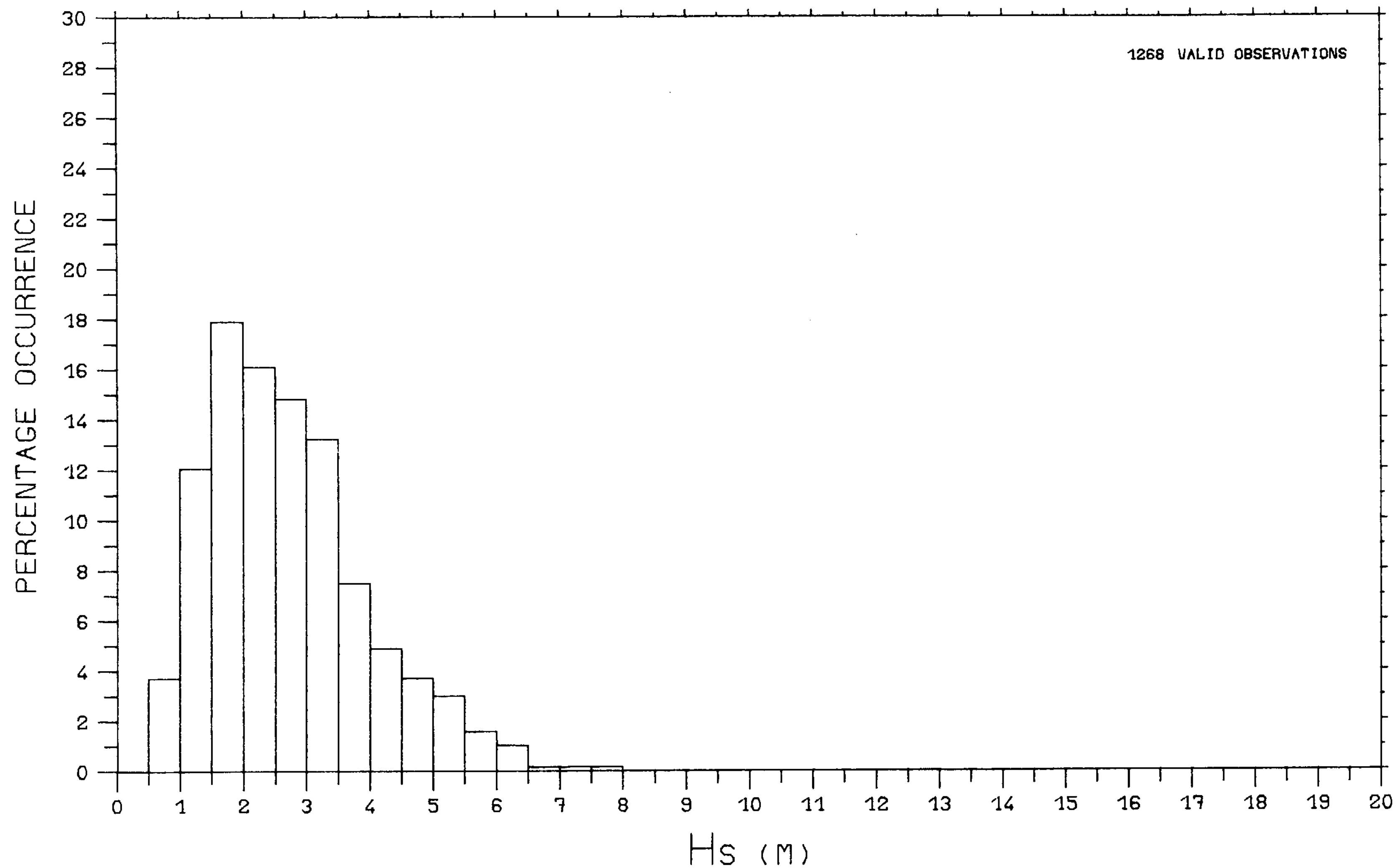

PERCENTAGE OCCURRENCE OF Hs

SOUTH UIST WINTER 1976/7,1977/8

FIG 3.2.1.4

SU768

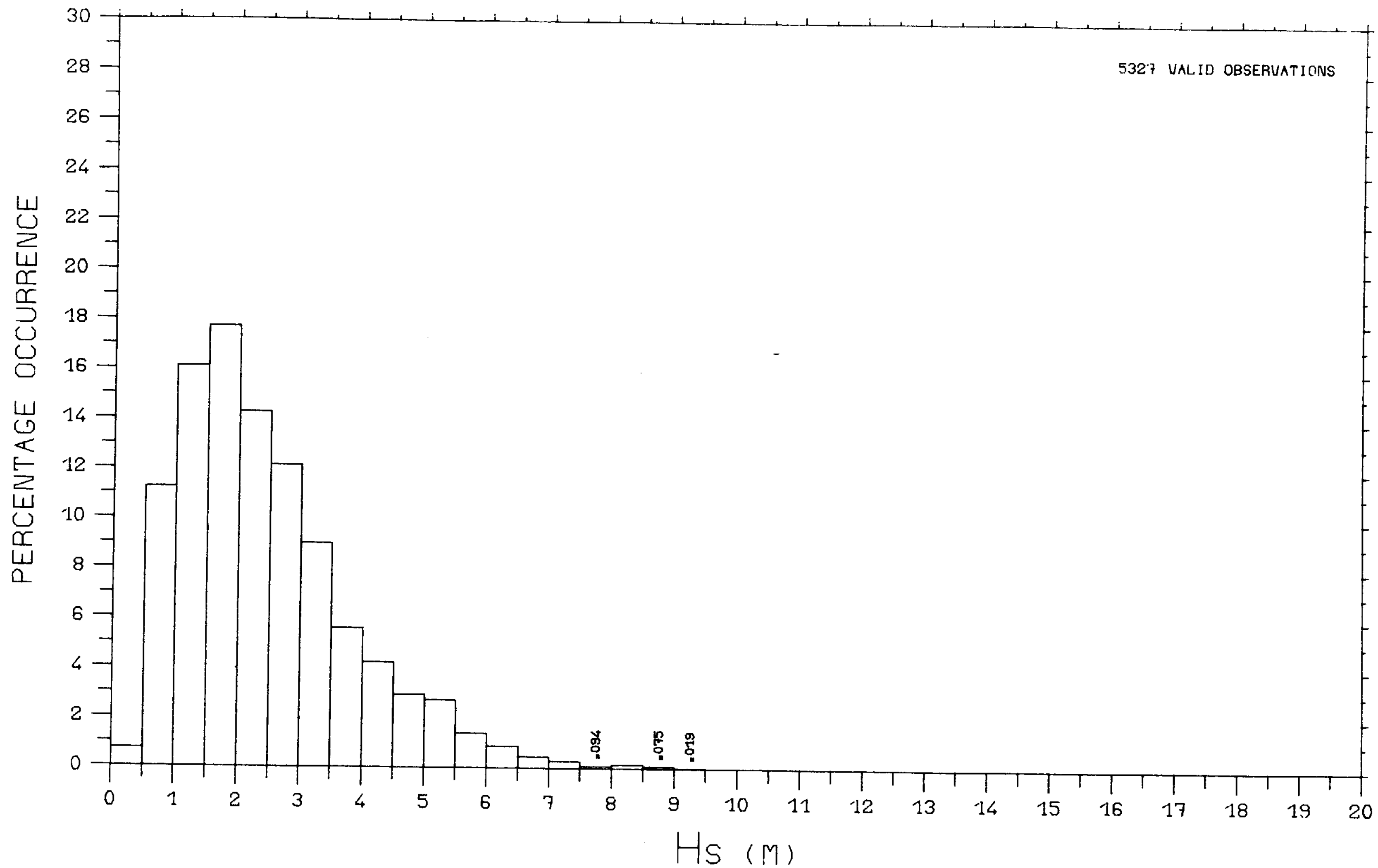

PERCENTAGE OCCURRENCE OF Hs

SU768 SOUTH UIST MAR 1976 - FEB 1978

FIG 3.2.1.5

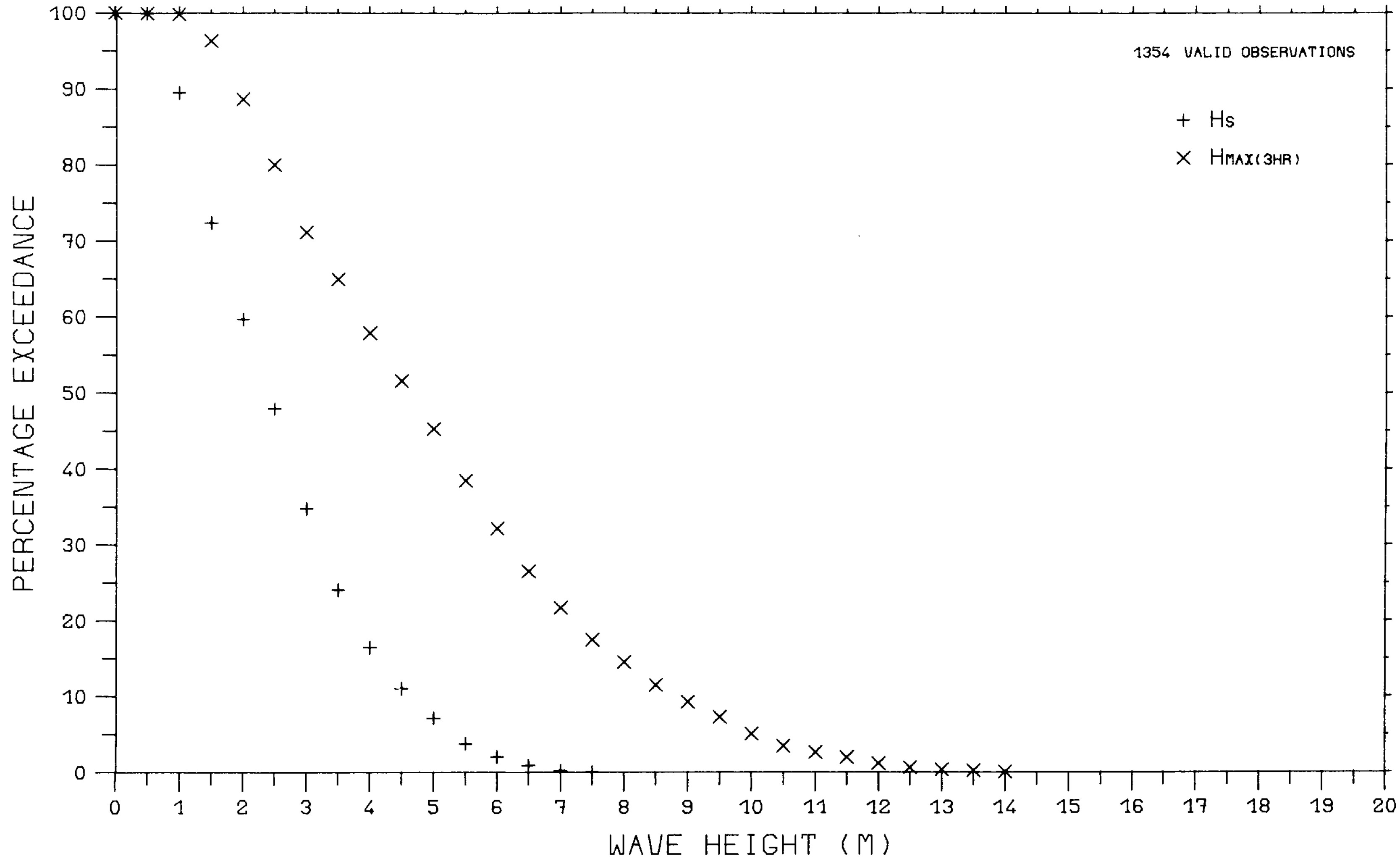

PERCENTAGE EXCEEDANCE OF Hs AND HMAX(3HR)

SOUTH UIST SPRING 1976 , 1977

FIG 3.2.21

SU768

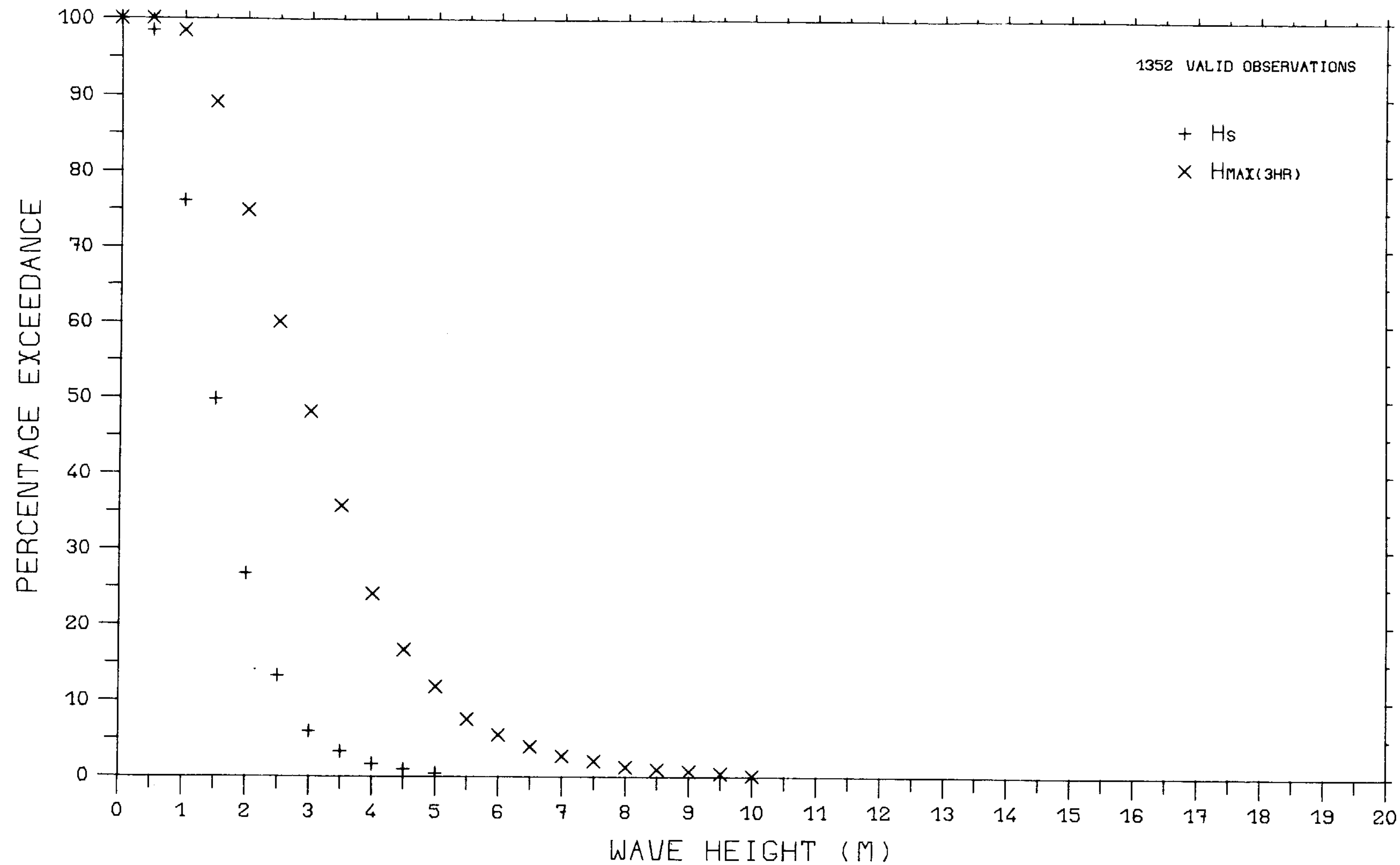

PERCENTAGE EXCEEDANCE OF H_S AND $H_{MAX(3HR)}$

SOUTH UIST SUMMER 1976 , 1977

FIG 3.2.2.2

SU768

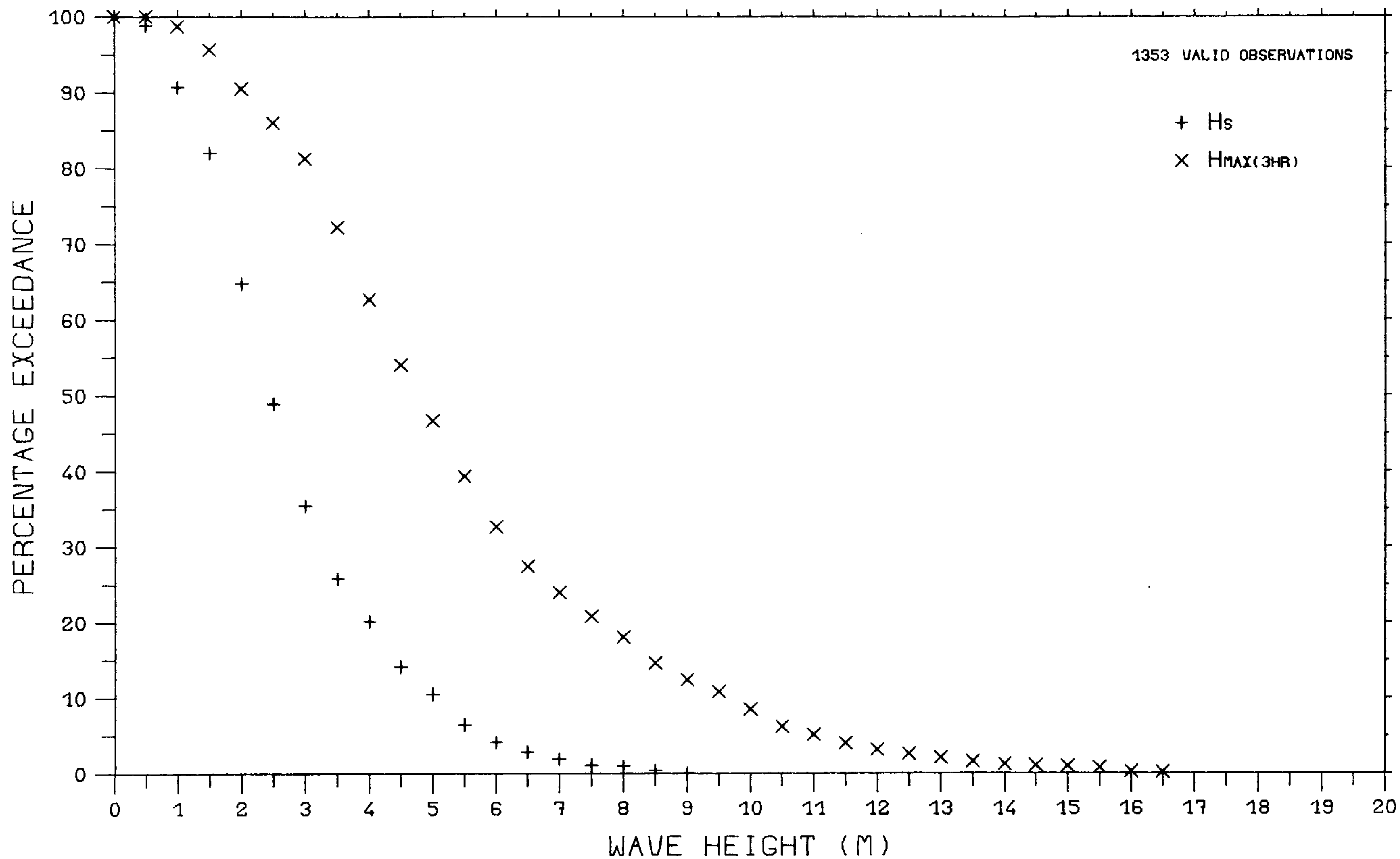

PERCENTAGE EXCEEDANCE OF Hs AND HMAX(3HR)

SOUTH UIST AUTUMN 1976 , 1977

FIG 3.22.3

SU768

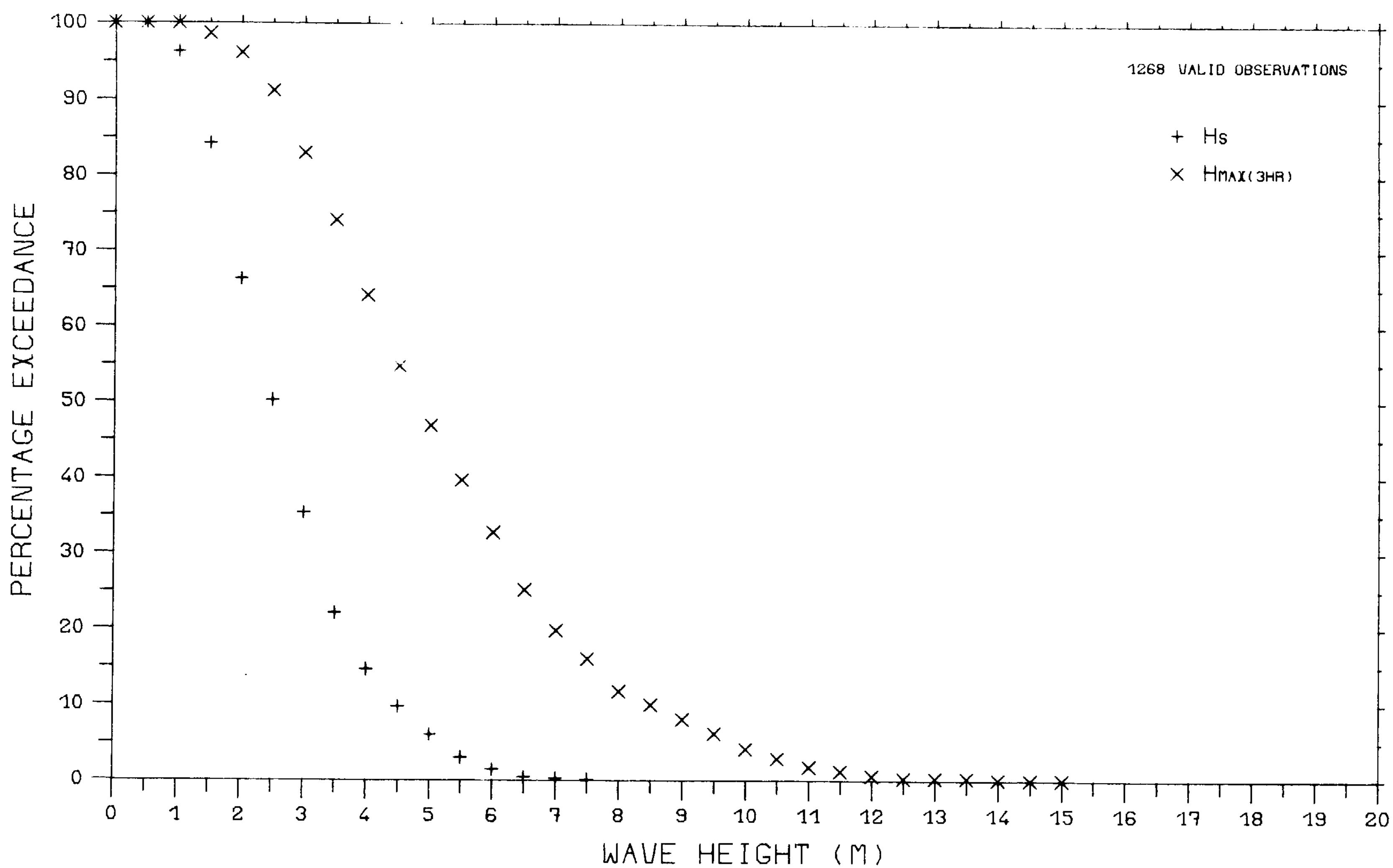

PERCENTAGE EXCEEDANCE OF H_S AND $H_{MAX(3HR)}$

SOUTH UIST WINTER 1976/7,1977/8

FIG 3.2.24

SU768

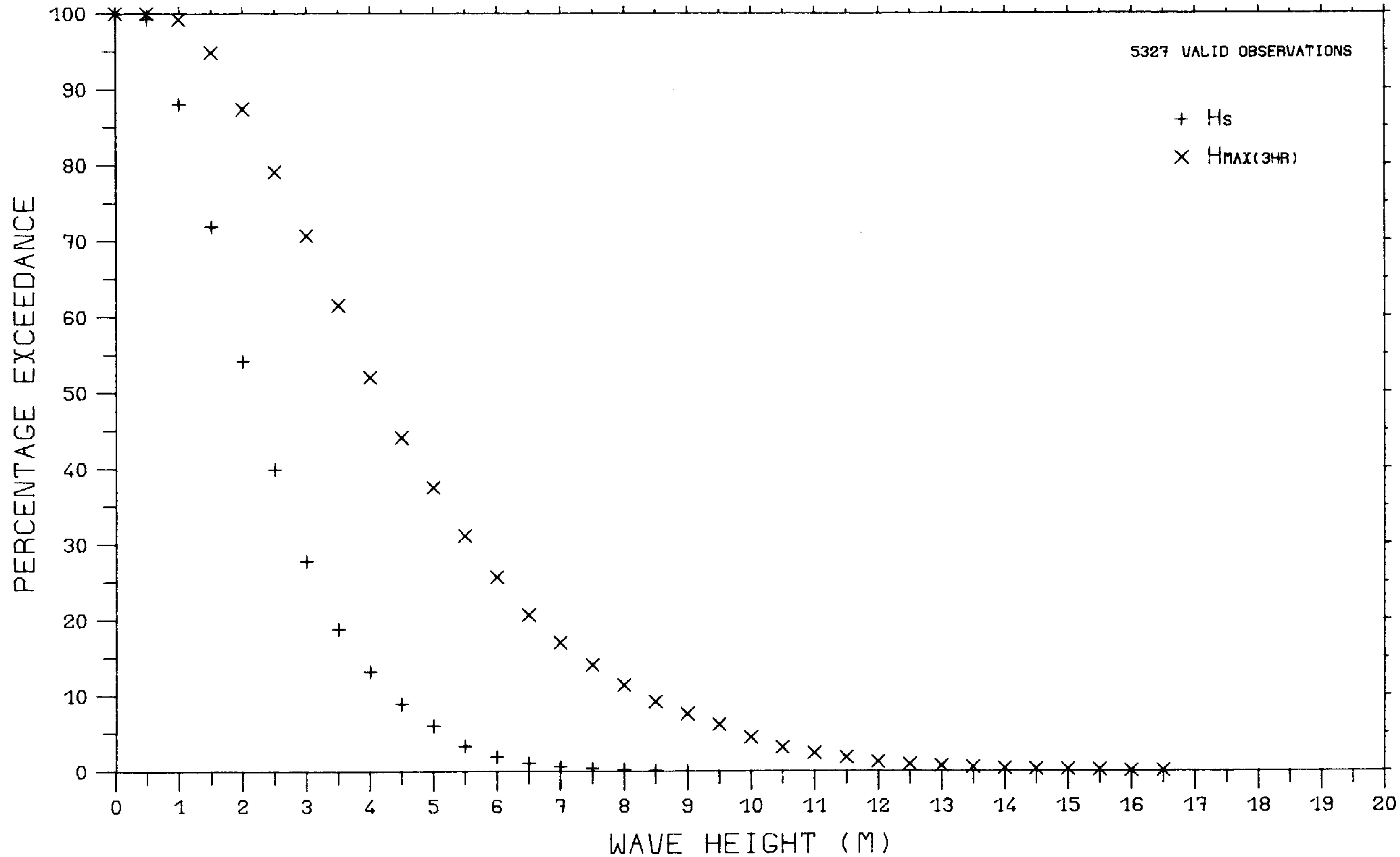

PERCENTAGE EXCEEDANCE OF Hs AND HMAX(3HR)

SOUTH UIST MAR 1976 - FEB 1978

FIG 3.2.2.5

SU768

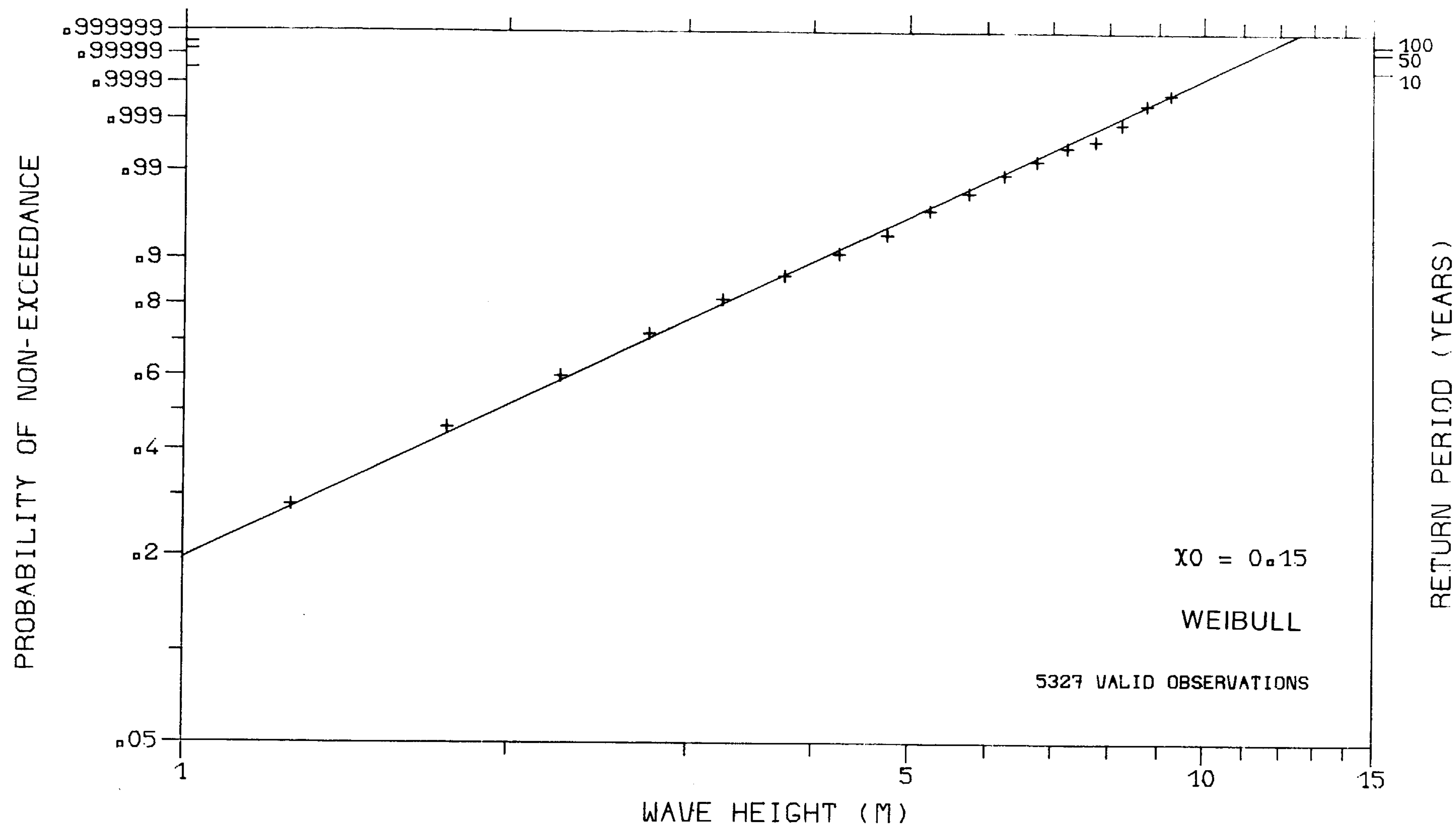

CUMULATIVE DISTRIBUTION OF WAVE HEIGHT, HS

SOUTH UIST MARCH 1976-FEBRUARY 1978

FIG 3.3.1

SU768

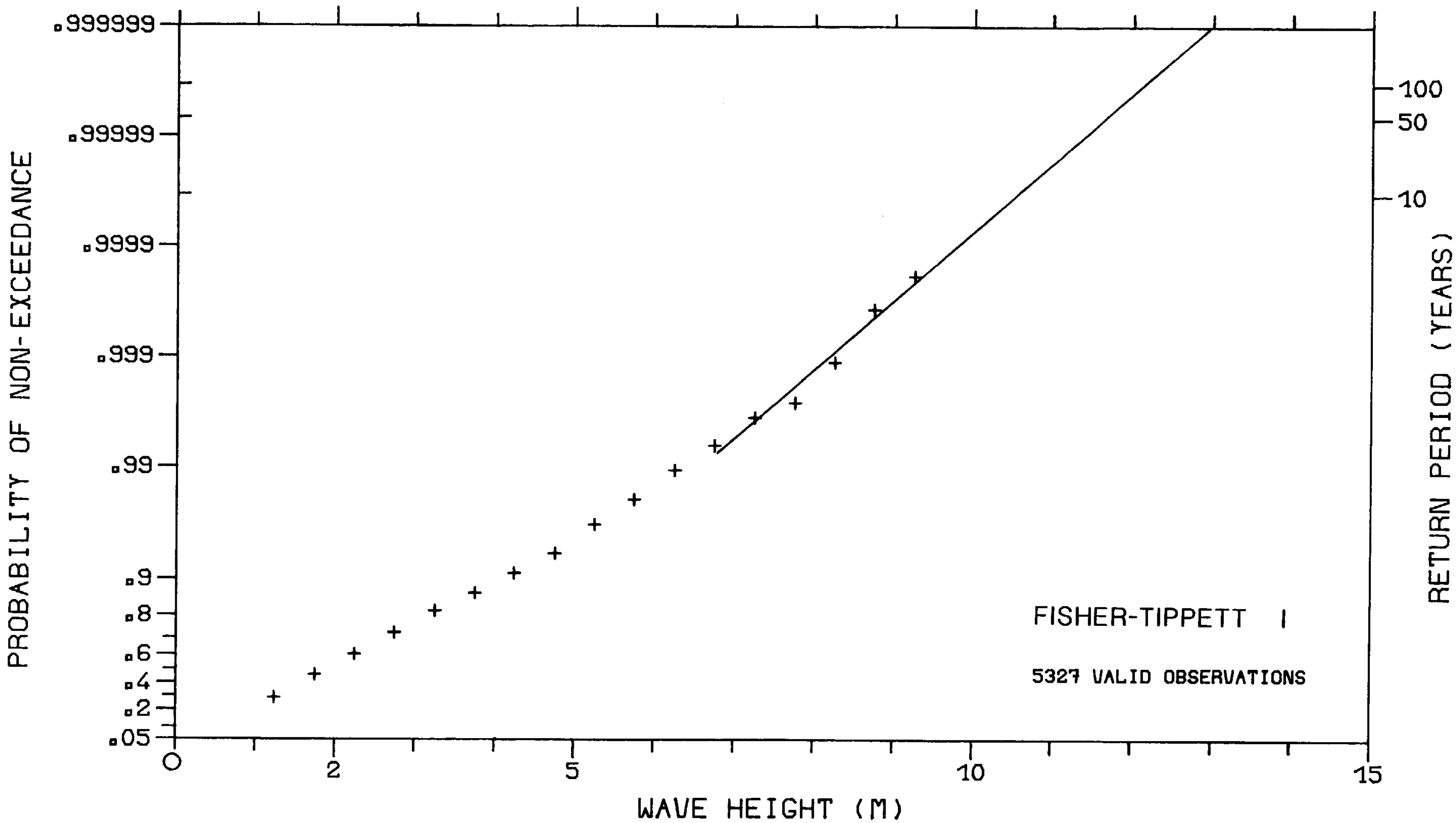

CUMULATIVE DISTRIBUTION OF WAVE HEIGHT-HS

SOUTH UIST MARCH 1976-FEBRUARY 1978

FIG 3.3.2

SU768

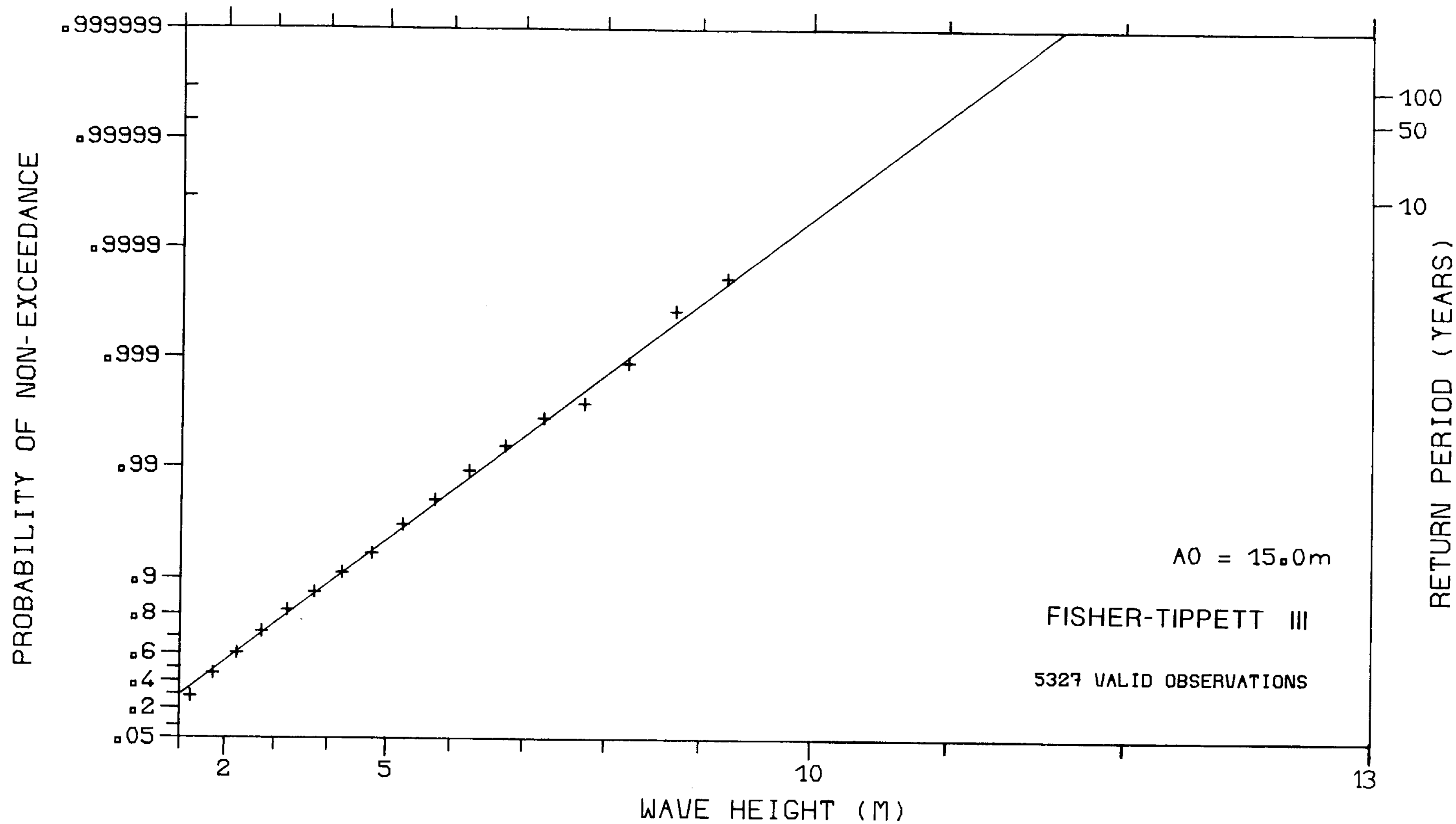

CUMULATIVE DISTRIBUTION OF WAVE HEIGHT-HS

SOUTH UIST MARCH 1976-FEBRUARY 1978

FIG 3.3.3

SU768

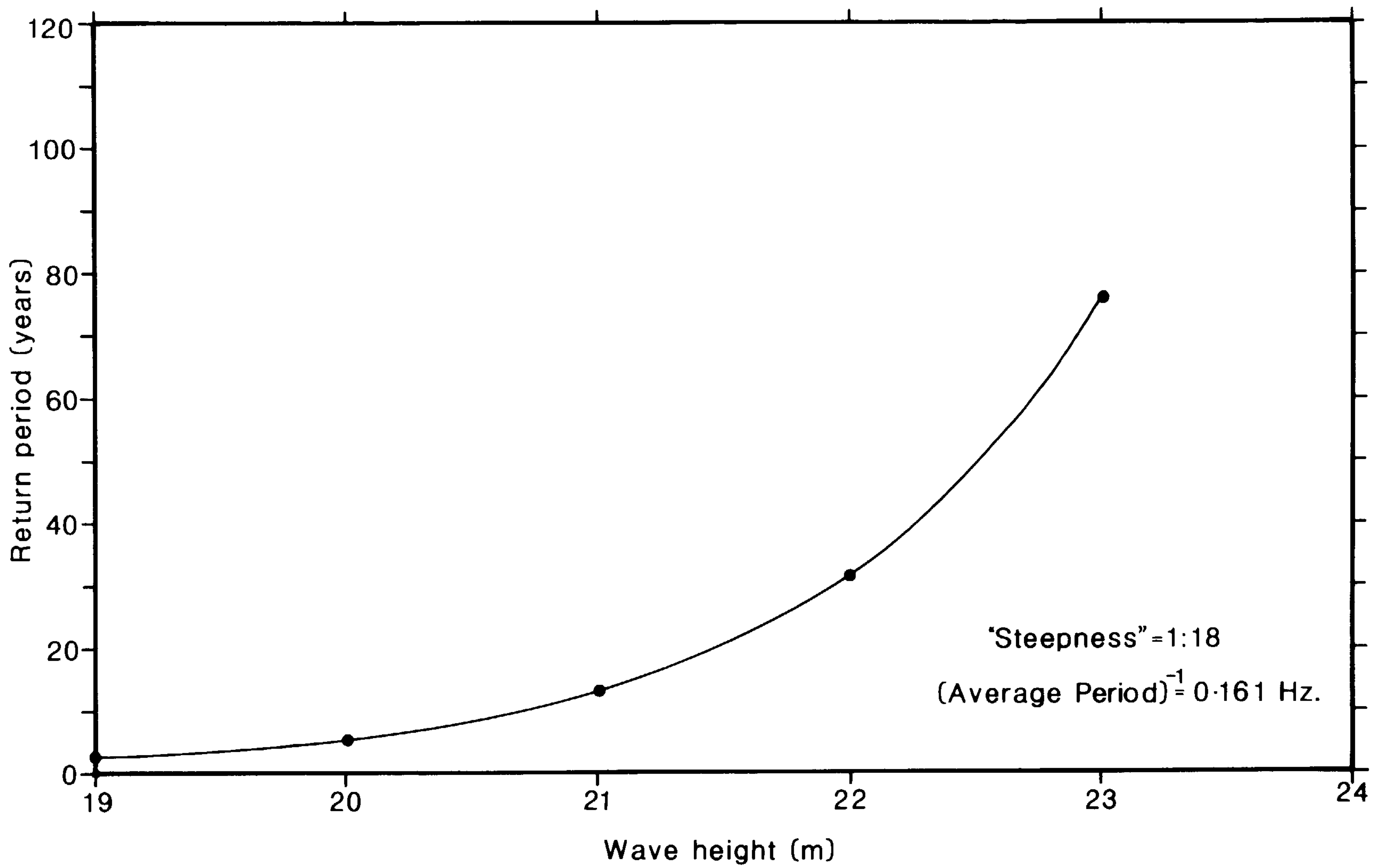

RETURN PERIOD v. WAVE HEIGHT - INDIVIDUAL WAVE MODEL

SOUTH UIST MAR. 1976 - FEB. 1978

FIG 3.3.4

SU768

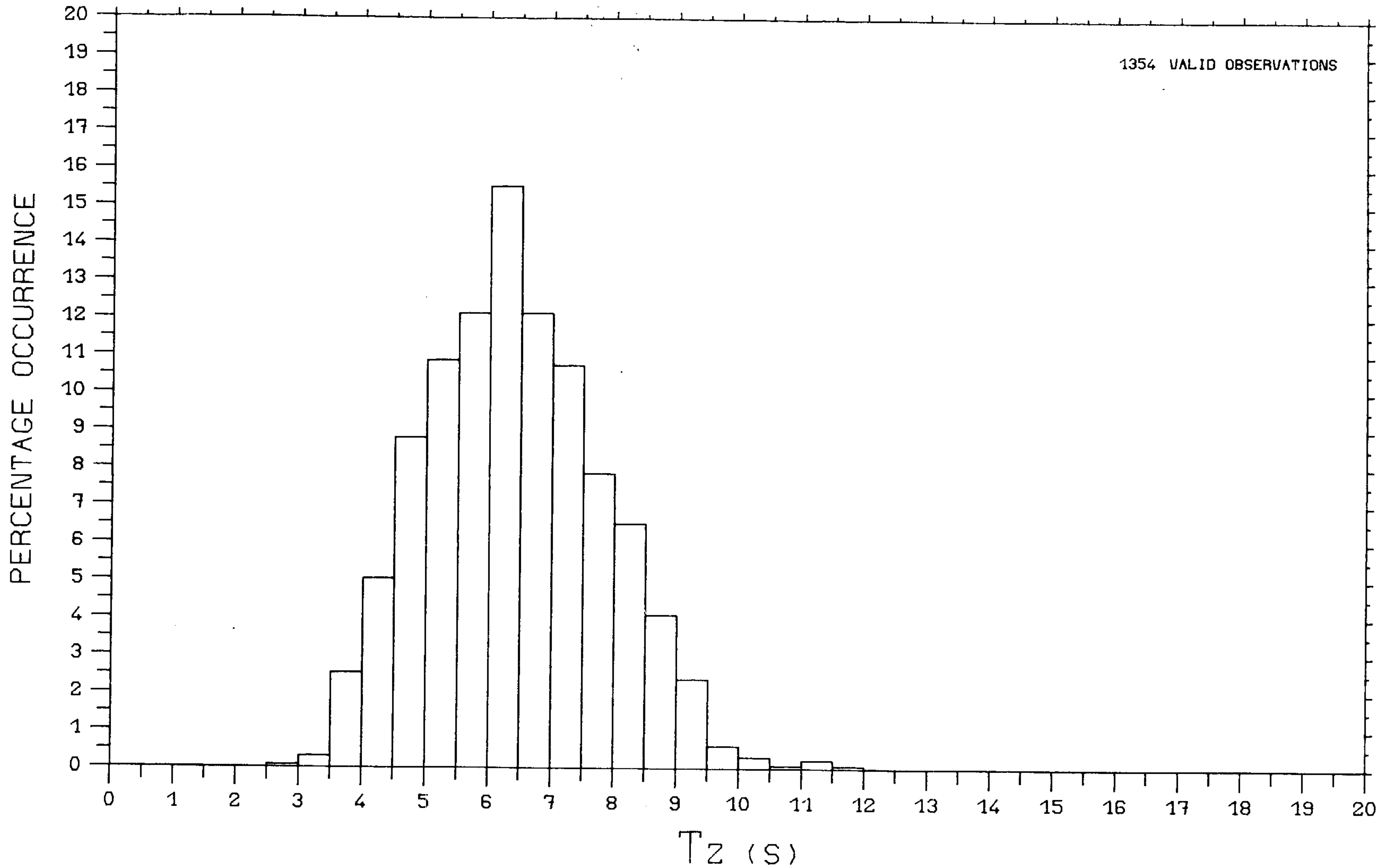

PERCENTAGE OCCURRENCE OF T_Z

SU768

SOUTH UIST SPRING 1976 , 1977

FIG 3.4.1.1

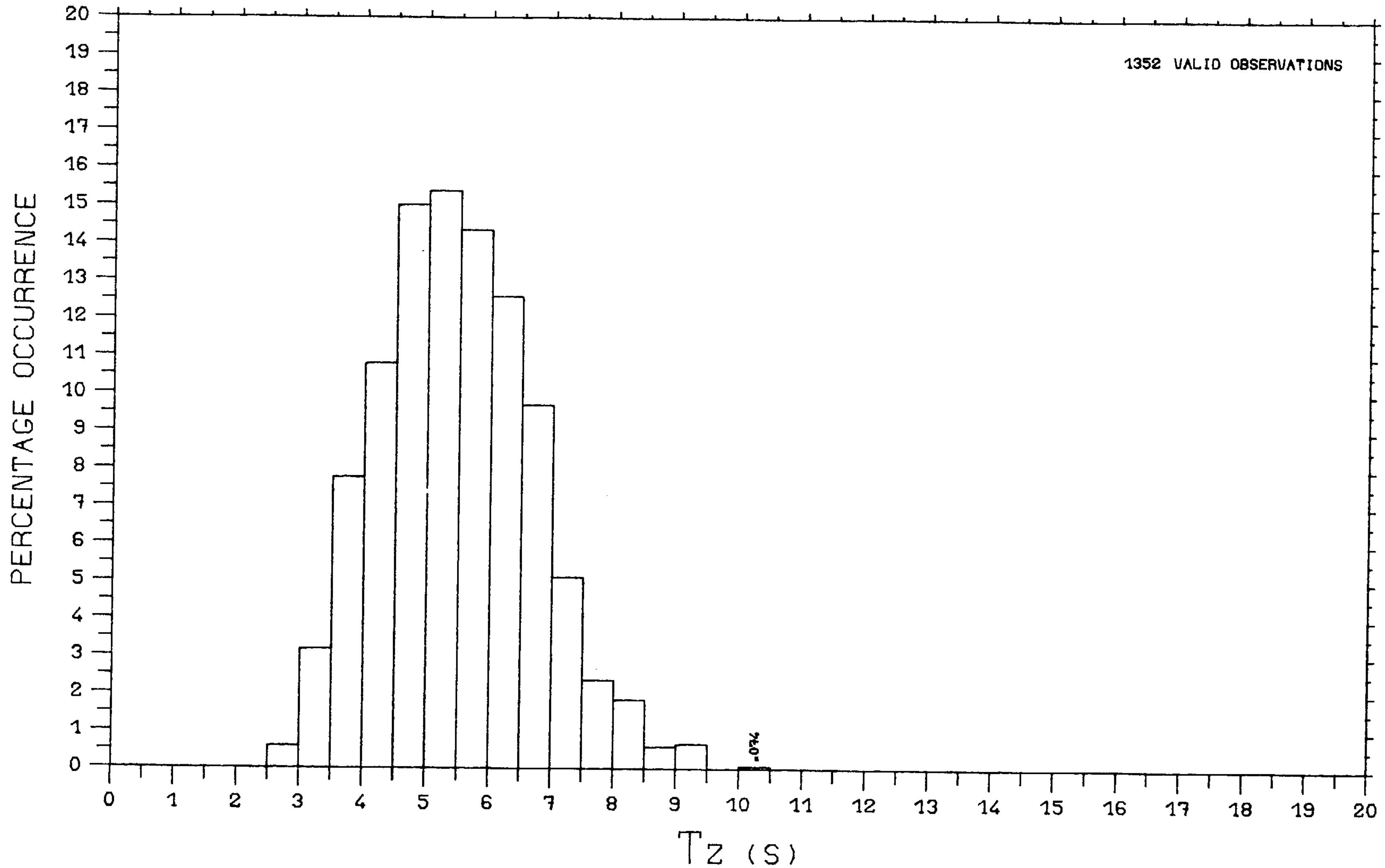

PERCENTAGE OCCURRENCE OF T_z

SOUTH UIST SUMMER 1976 , 1977

FIG 3.4.1.2

SU768

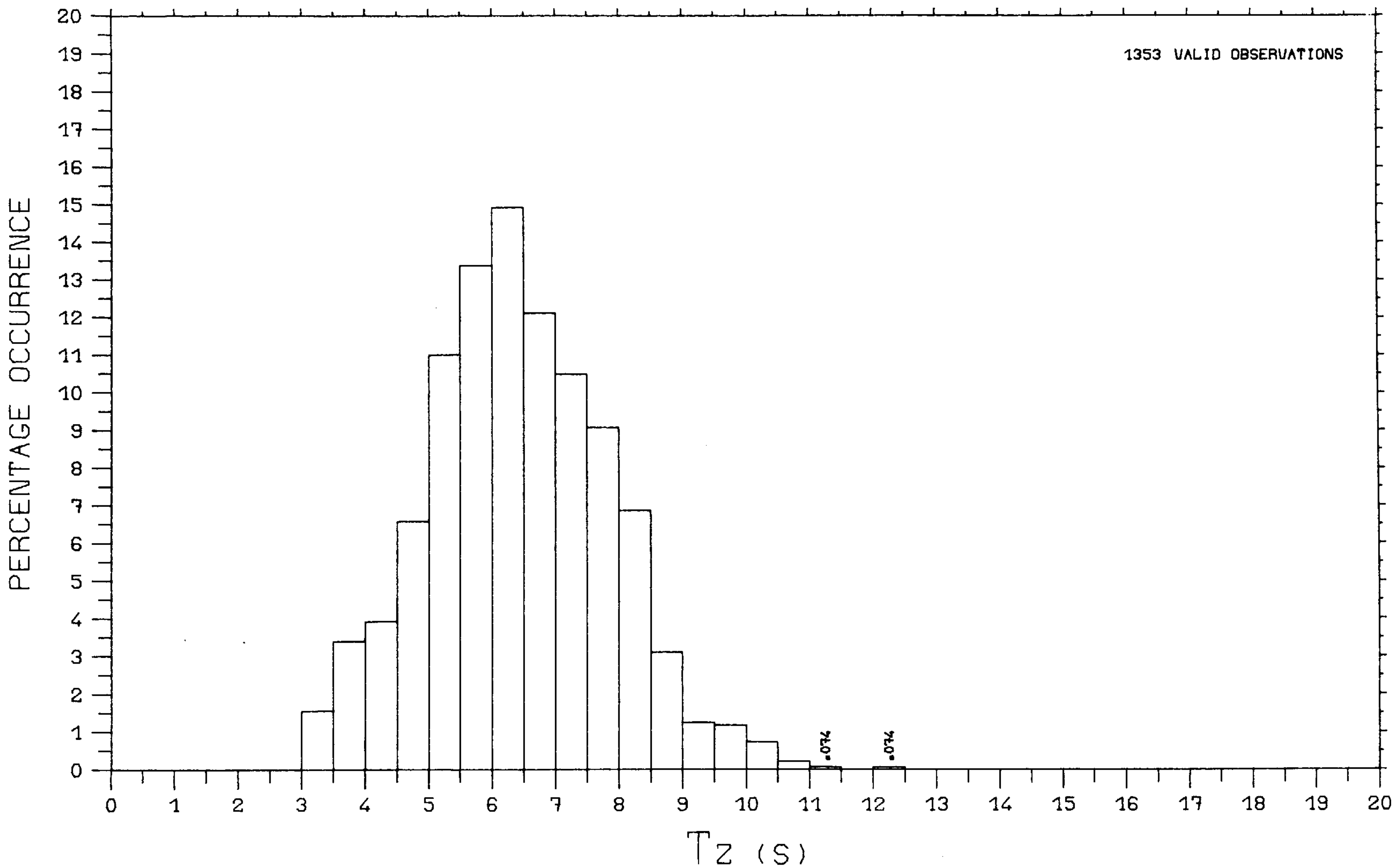

PERCENTAGE OCCURRENCE OF T_z

SOUTH UIST AUTUMN 1976 , 1977

FIG 3.4.1.3

SU768

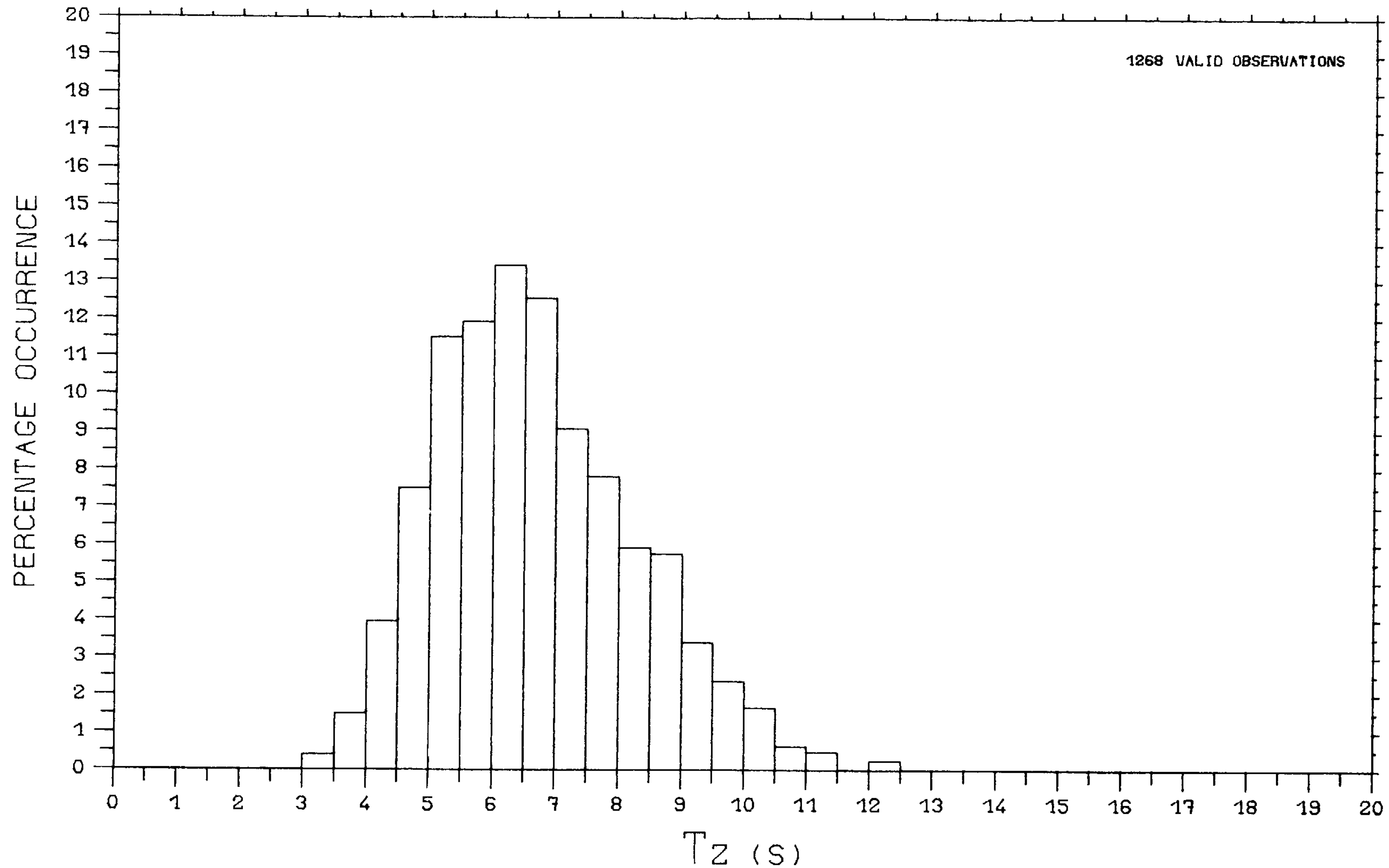

PERCENTAGE OCCURRENCE OF T_Z

SOUTH UIST WINTER 1976/7, 1977/8

FIG 3.4.1.4

SU768

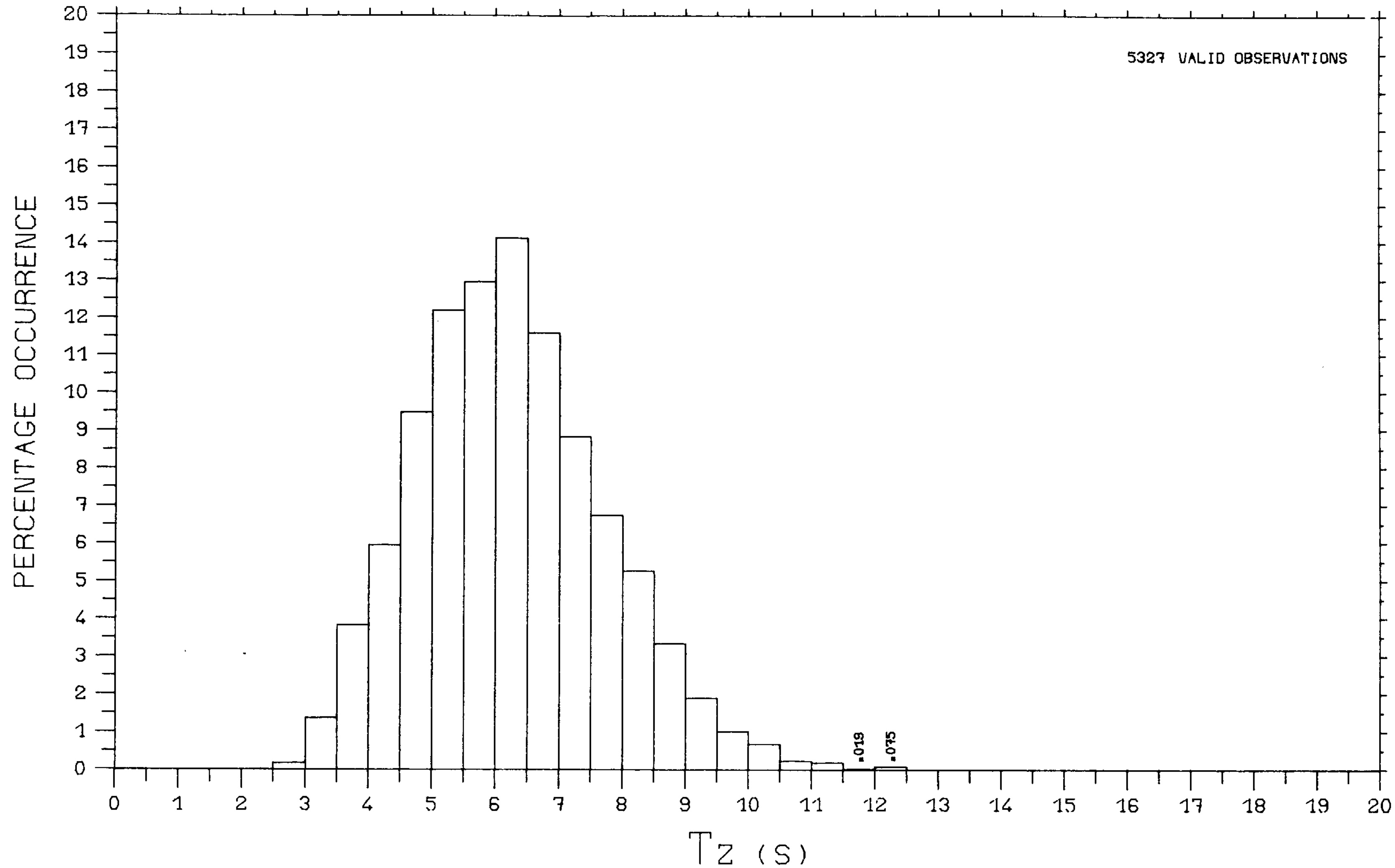

PERCENTAGE OCCURRENCE OF Tz

SOUTH UIST MAR 1976 - FEB 1978

FIG 3.4.1.5

SU768

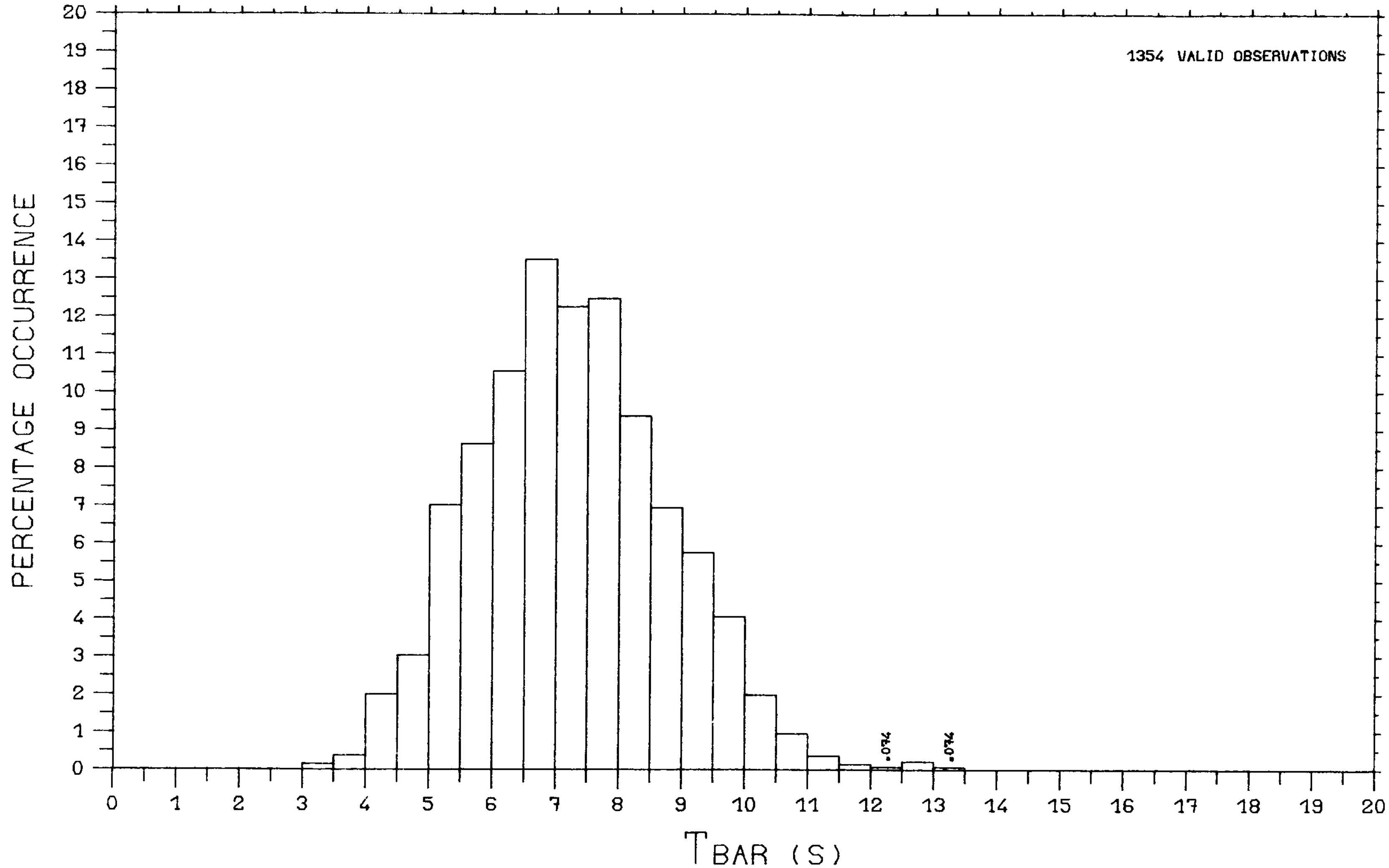

PERCENTAGE OCCURRENCE OF TBAR

SOUTH UIST SPRING 1976 , 1977

FIG 3.4.2.1

SU768

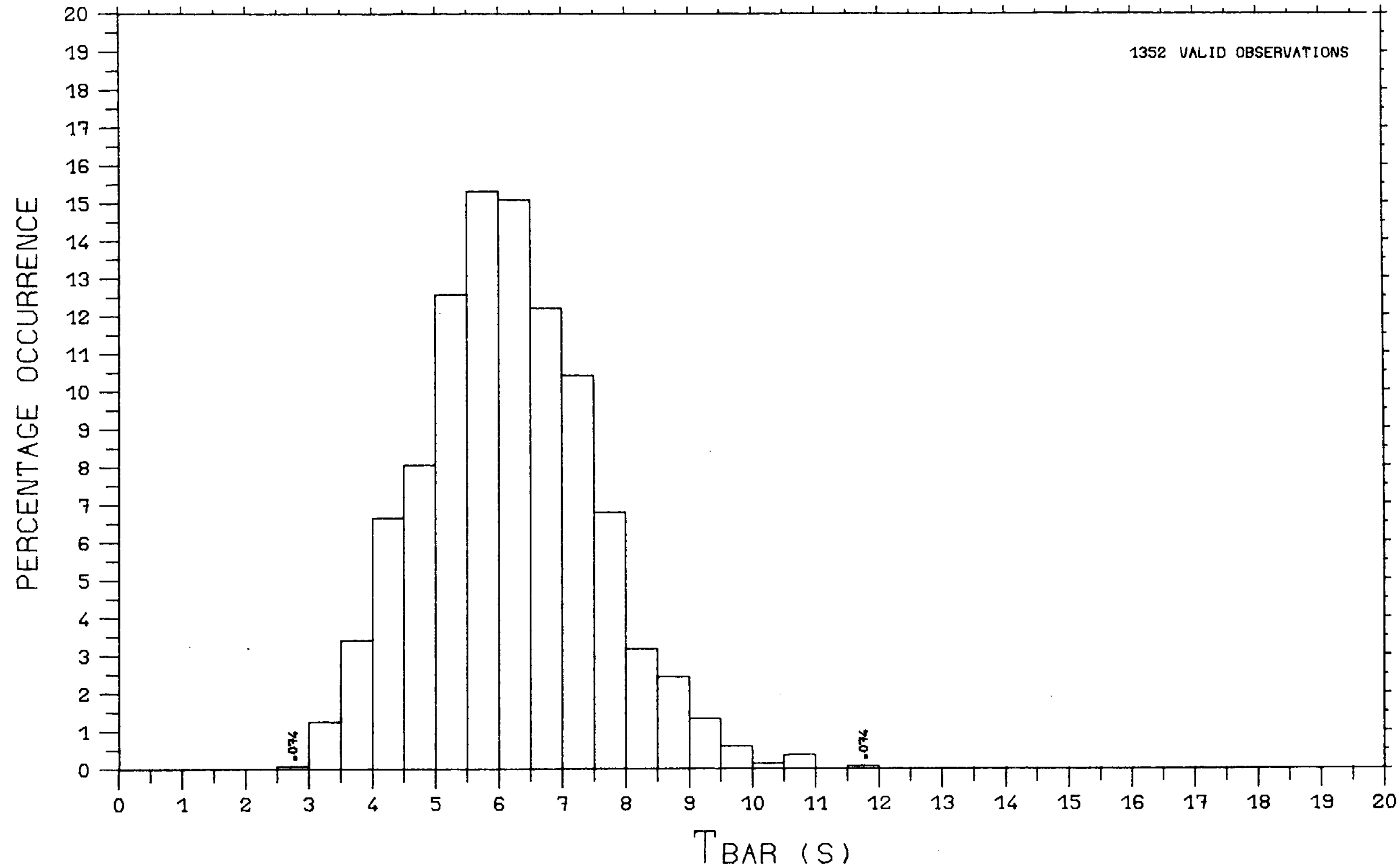

PERCENTAGE OCCURRENCE OF TBAR

SOUTH UIST SUMMER 1976 , 1977

FIG 3.4.2.2

SU768

(Corrected fig)

PERCENTAGE OCCURRENCE

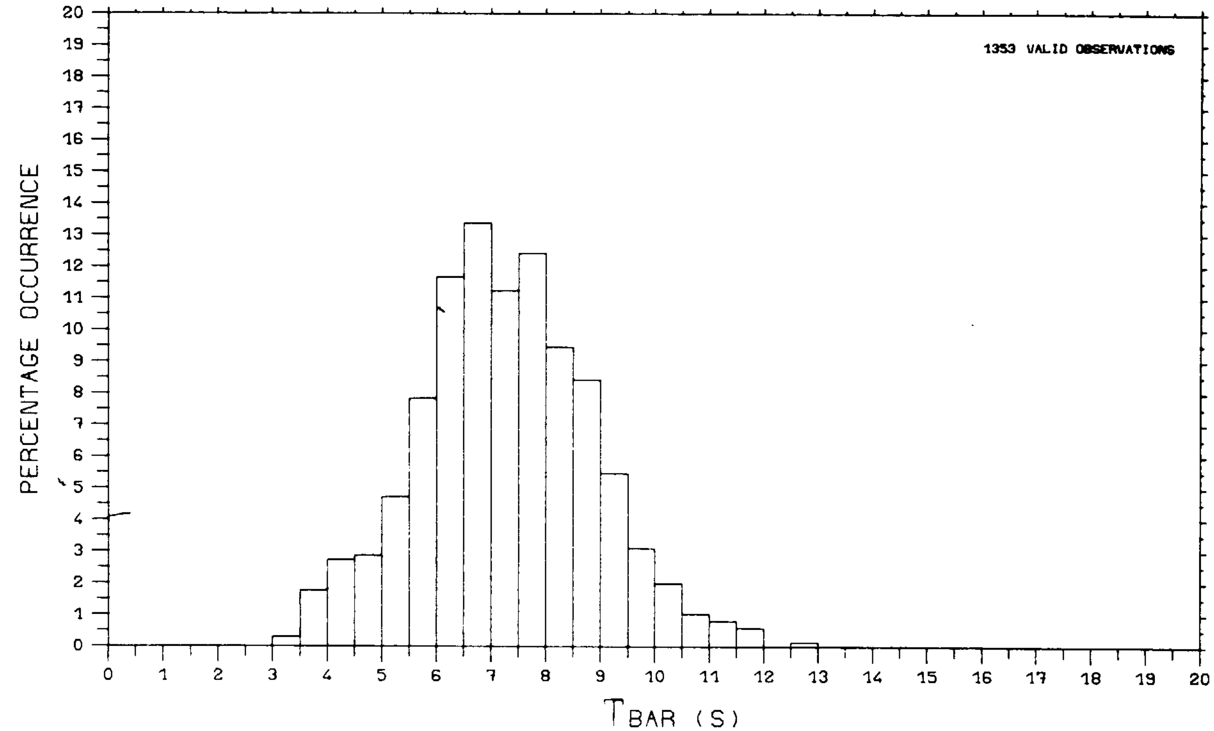

PERCENTAGE OCCURRENCE OF T_{BAR}

SU768

SOUTH UIST AUTUMN 1976 , 1977
FIG 3.4.2.3

SU768

SOUTH UIST AUTUMN 1976 , 1977
FIG 3.4.2.3

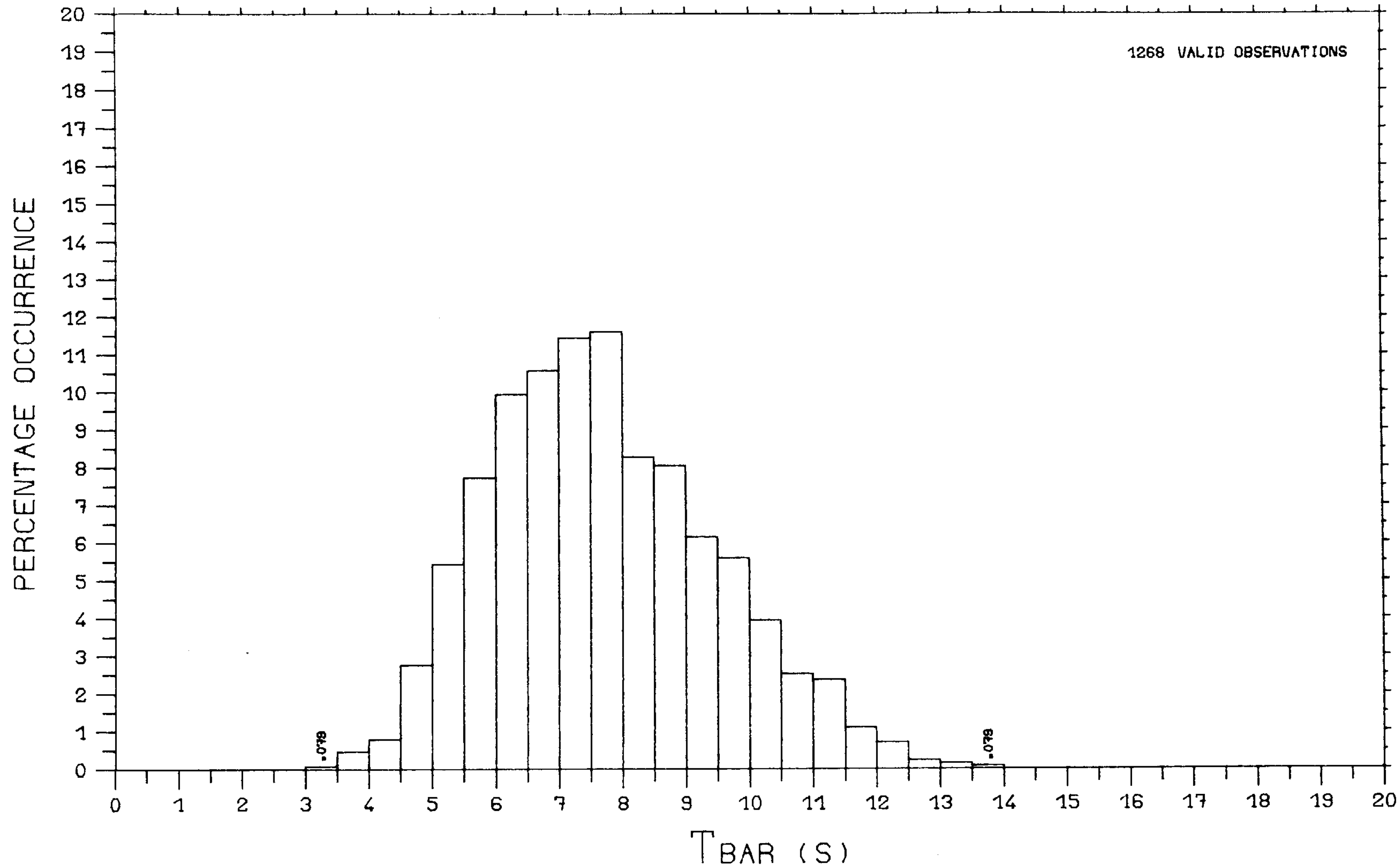

PERCENTAGE OCCURRENCE OF T_{BAR}

SOUTH UIST WINTER 1976/7, 1977/8

FIG 3.4.2.4

SU768

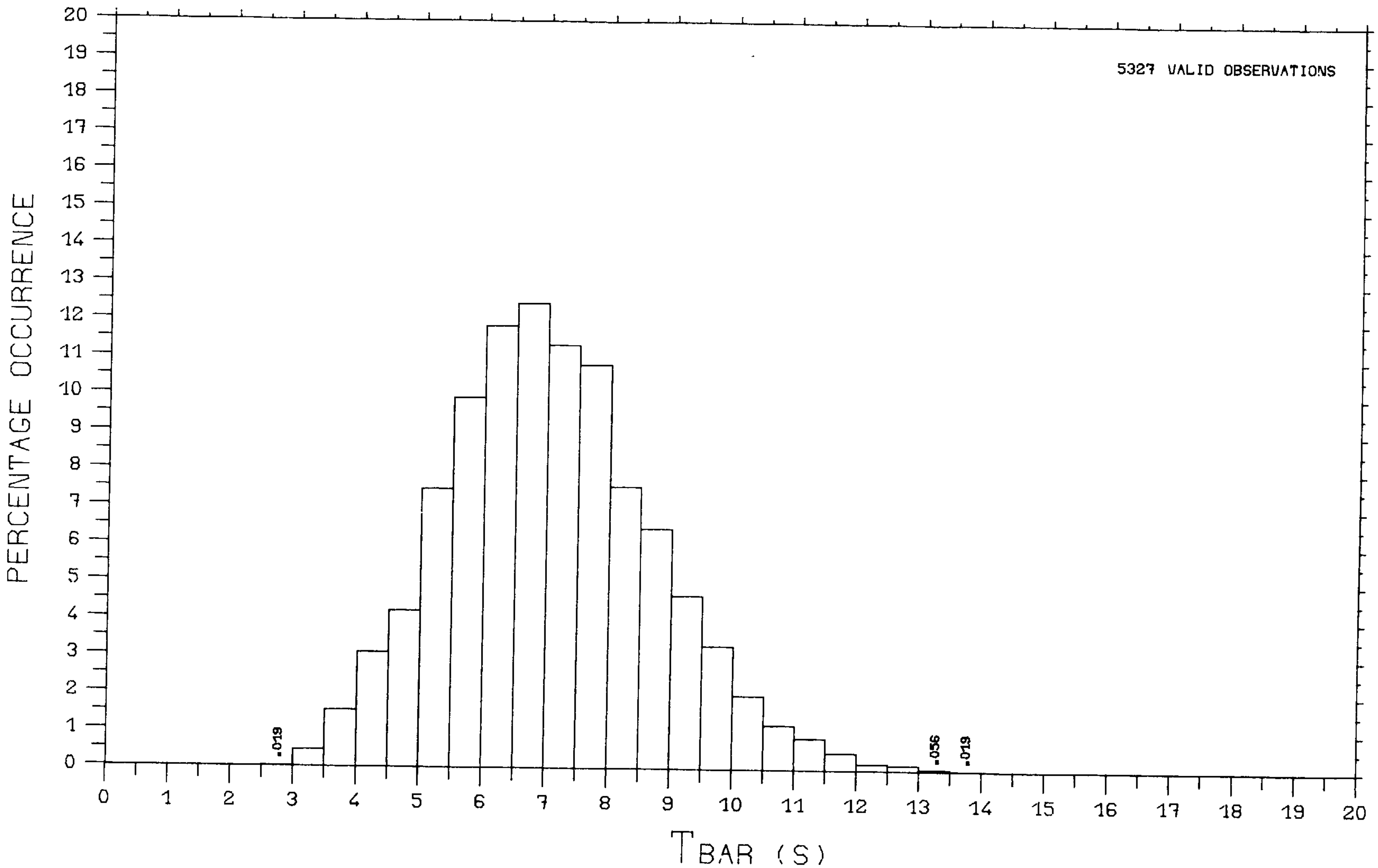

PERCENTAGE OCCURRENCE OF T_{BAR}

SOUTH UIST MAR 1976 - FEB 1978

FIG 3.4.2.5

SU768

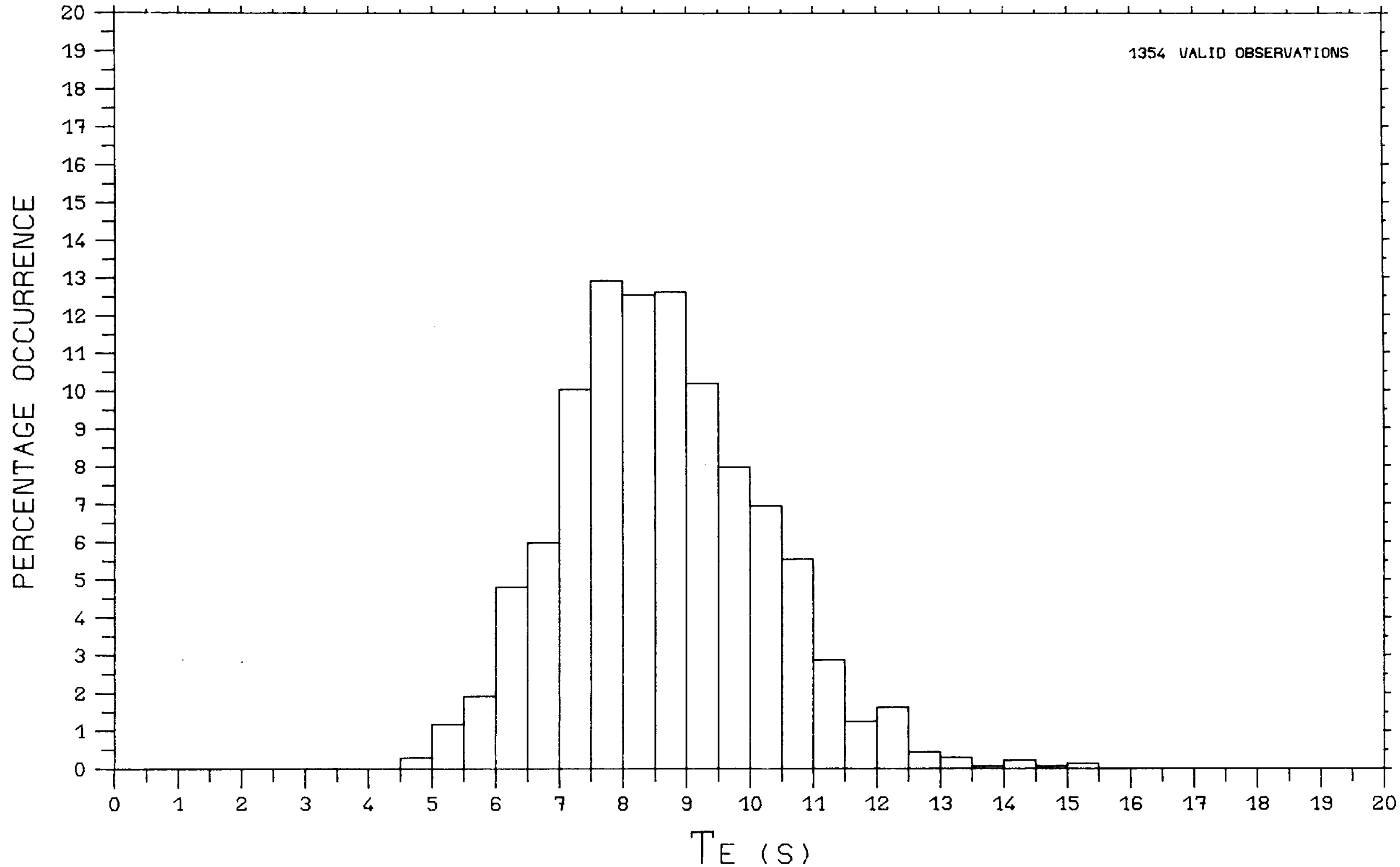

PERCENTAGE OCCURRENCE OF T_E

SOUTH UIST SPRING 1976 , 1977

FIG 3.4.3.1

SU768

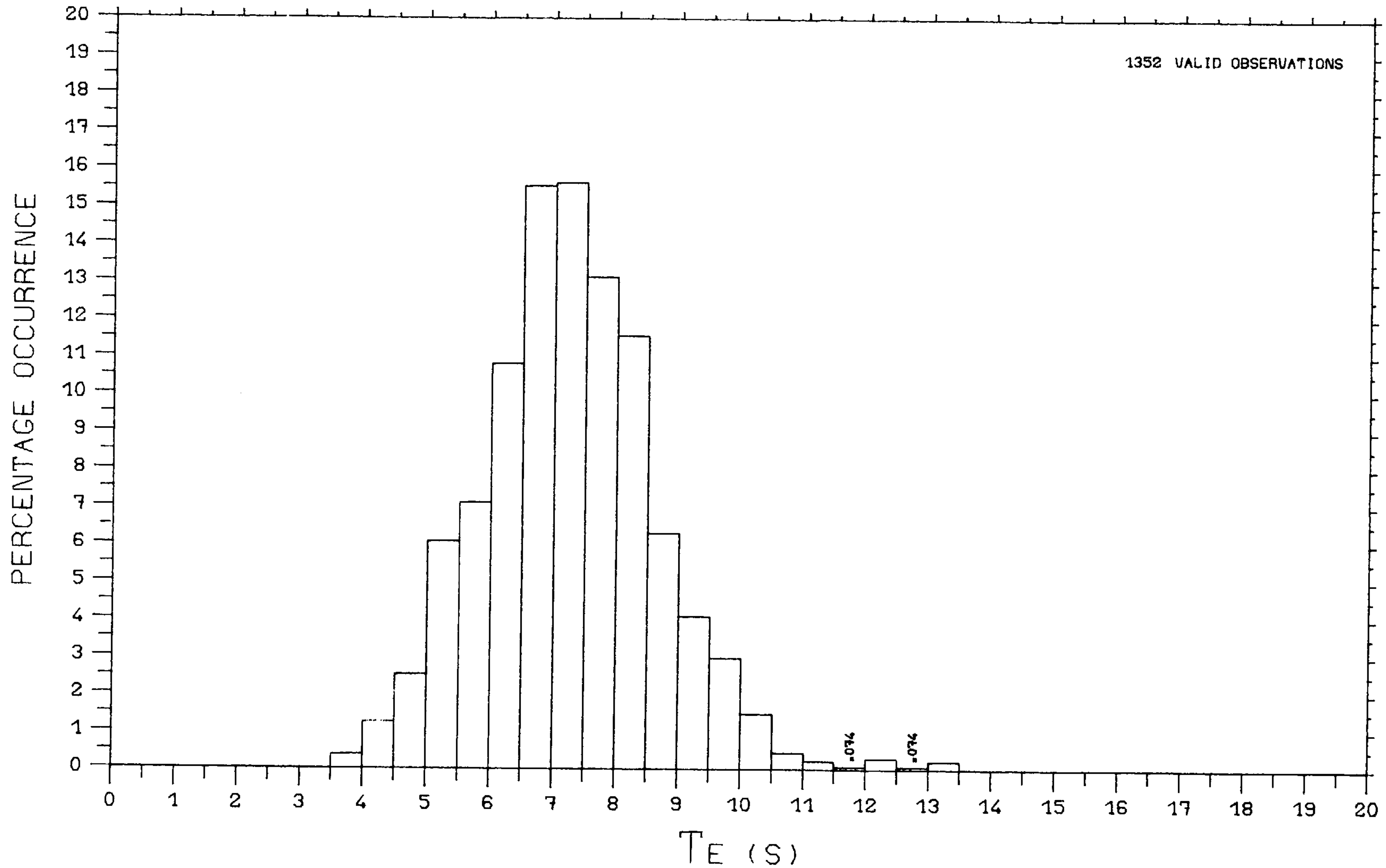

PERCENTAGE OCCURRENCE OF T_E

SOUTH UIST SUMMER 1976 , 1977

FIG 3.4.3.2

SU768

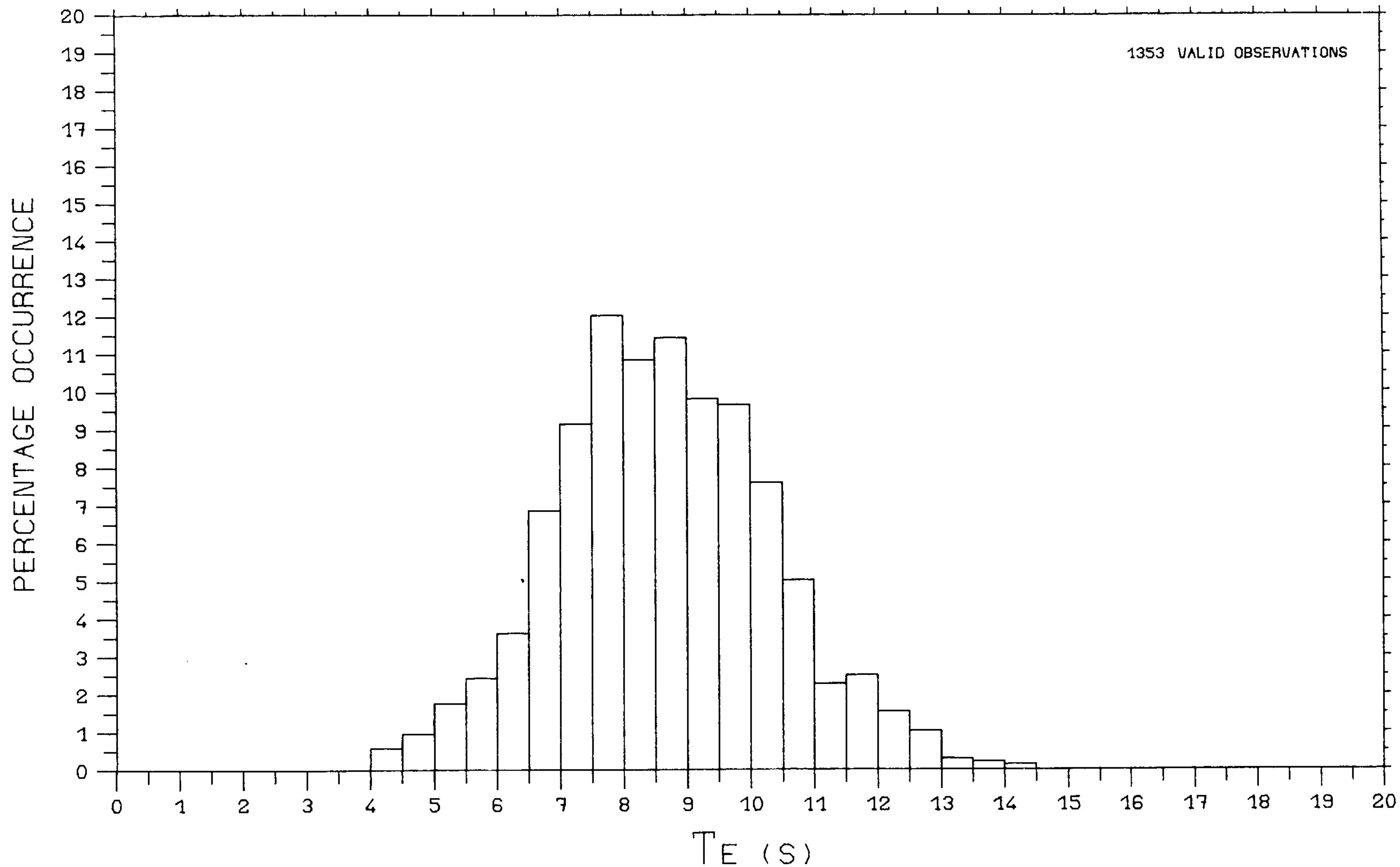

PERCENTAGE OCCURRENCE OF T_E

SOUTH UIST AUTUMN 1976 , 1977

FIG 3.4.3.3

SU768

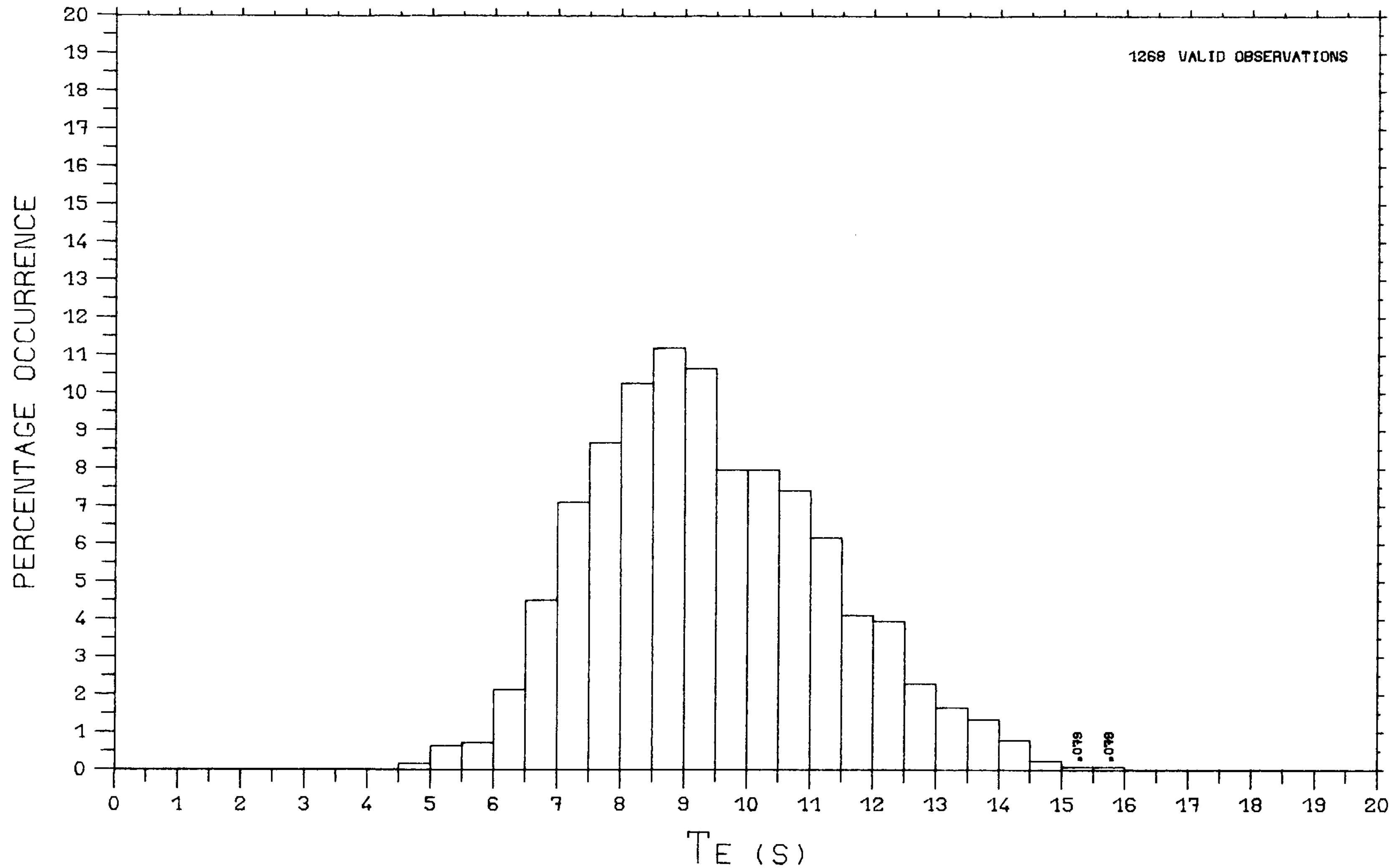

PERCENTAGE OCCURRENCE OF TE

SU768

SOUTH UIST WINTER 1976/7,1977/8

FIG 3.4.3.4

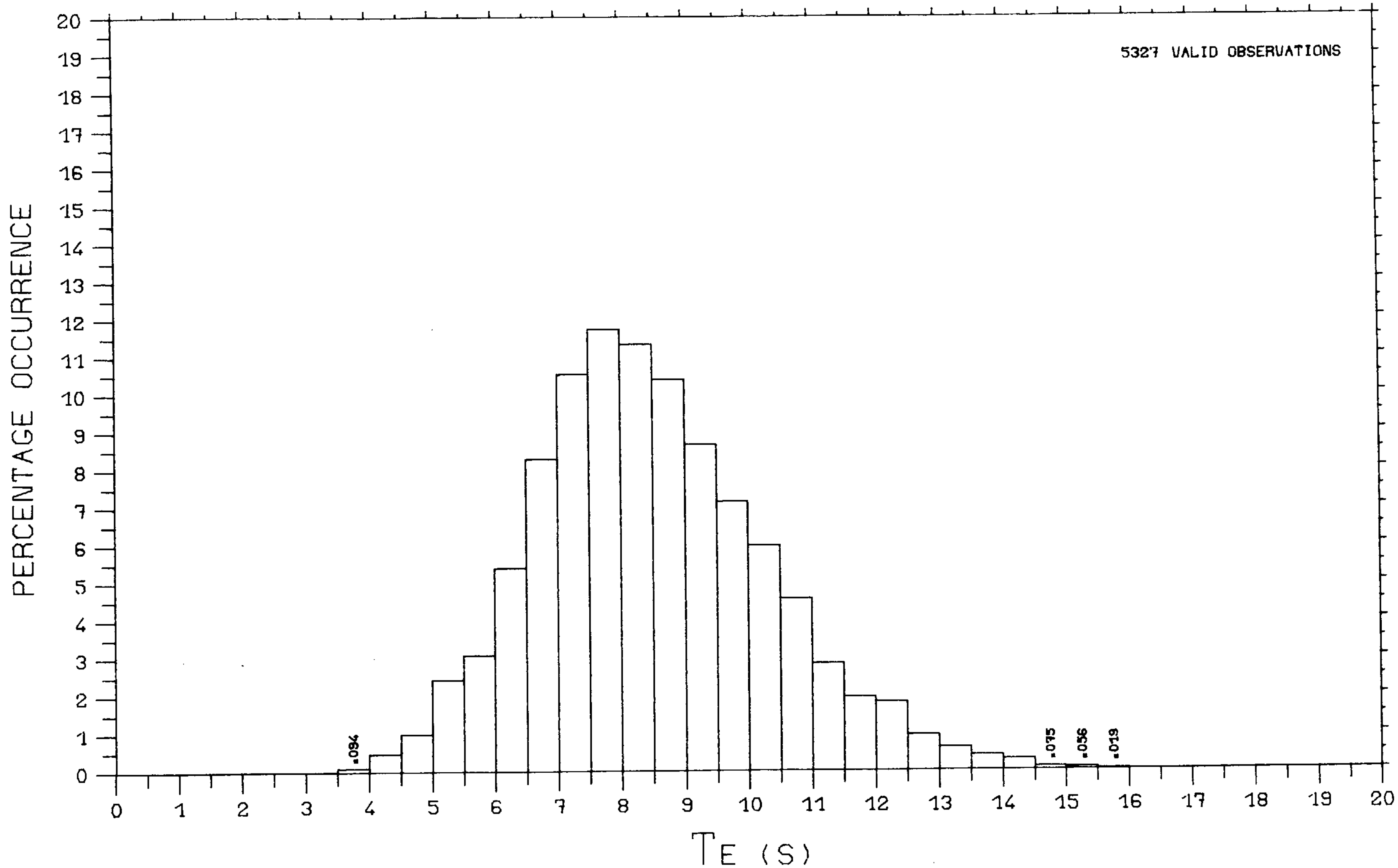

PERCENTAGE OCCURRENCE OF T_E

SOUTH UIST MAR 1976 - FEB 1978

FIG 3.4.3.5

SU768

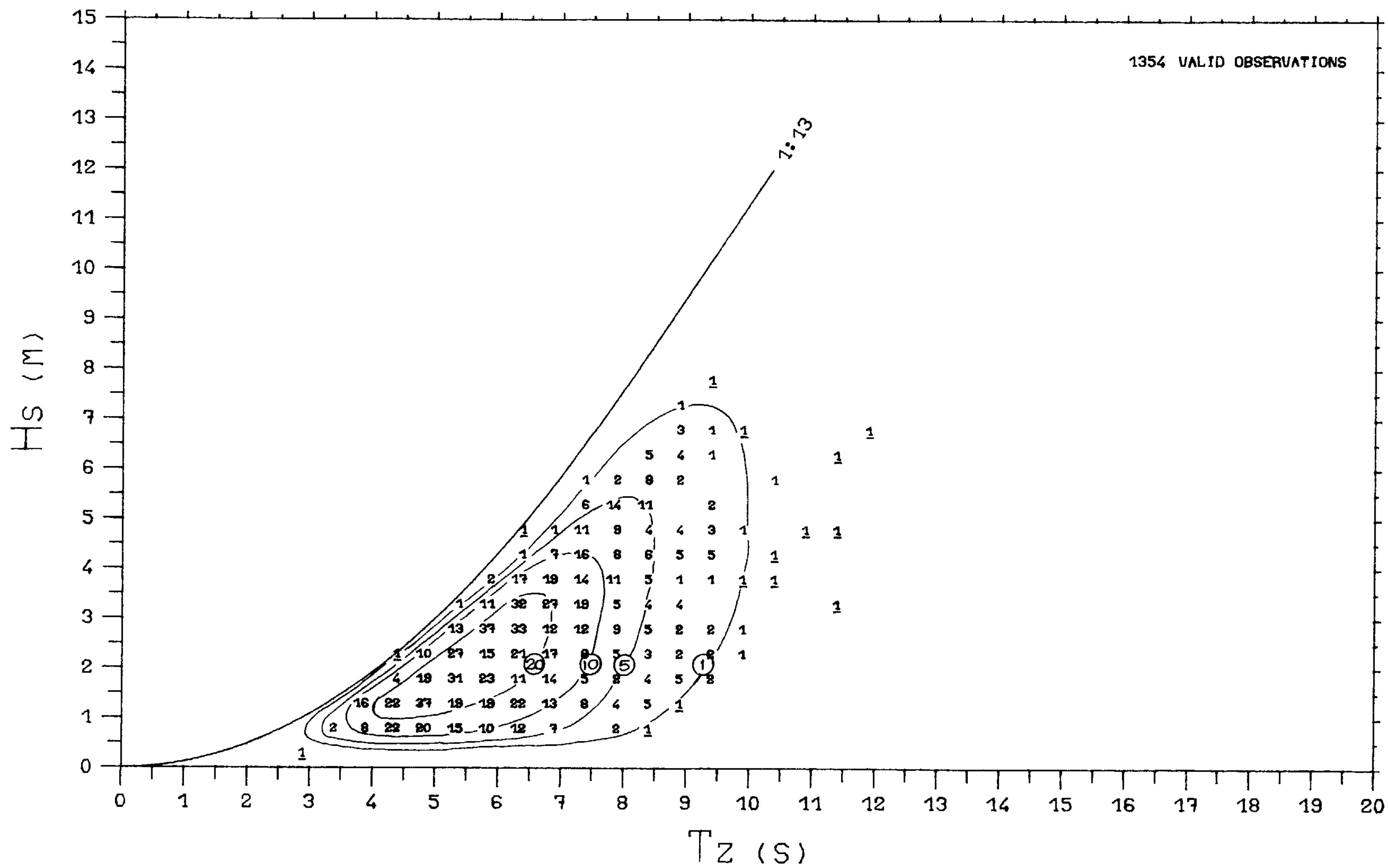

SCATTER DIAGRAM OF HS AND TZ (PPT)

SU768

SOUTH UIST SPRING 1976 , 1977

FIG 3.5.1.1

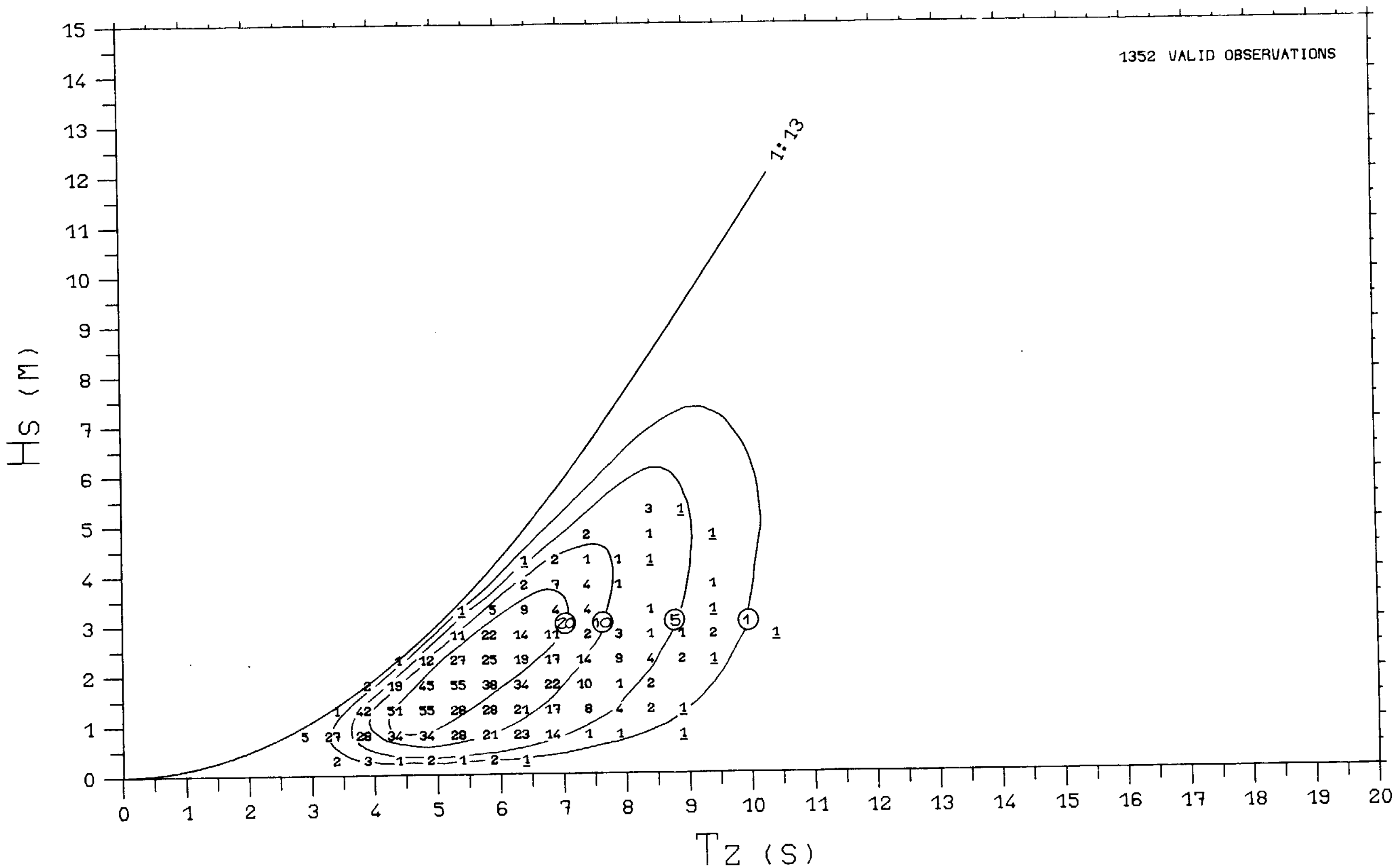

SCATTER DIAGRAM OF HS AND TZ (PPT)

SOUTH UIST SUMMER 1976 , 1977

FIG 3.5.1.2

SU768

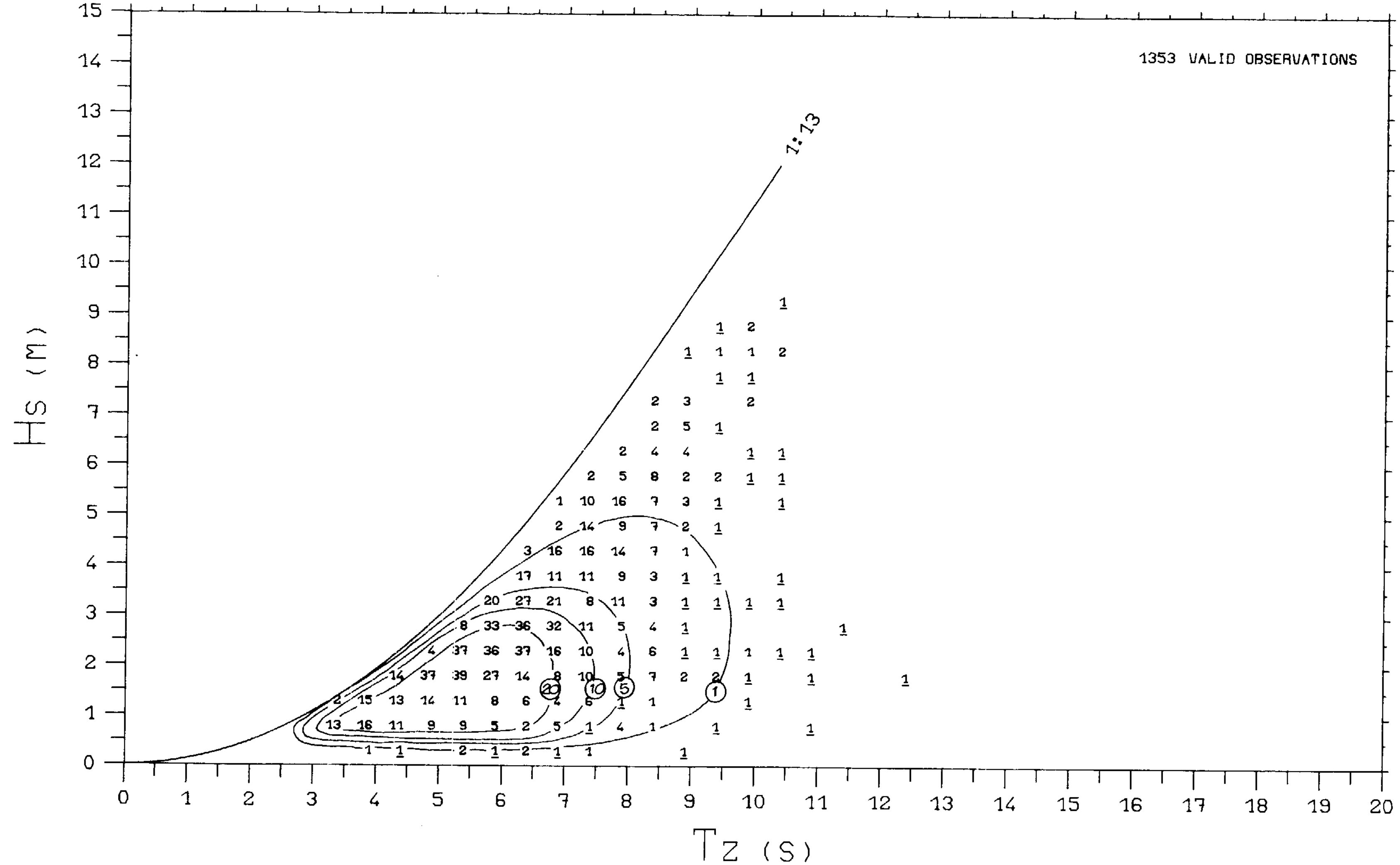

SCATTER DIAGRAM OF Hs AND Tz (PPT)

SOUTH UIST AUTUMN 1976 , 1977

FIG 3.5.1.3

SU768

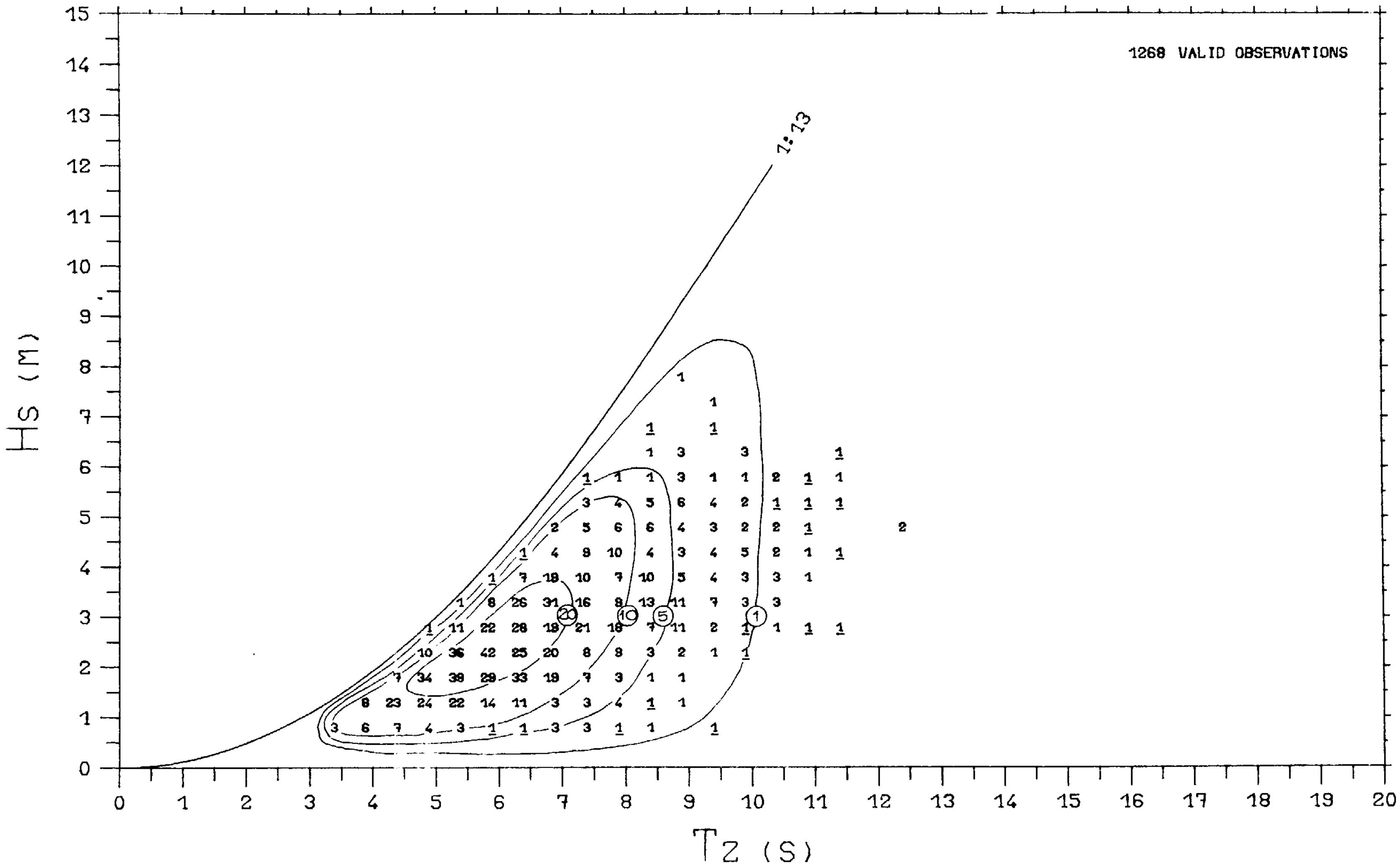

SCATTER DIAGRAM OF Hs AND Tz (PPT)

SU768

SOUTH UIST WINTER 1976/7, 1977/8

FIG 3.5.1.4

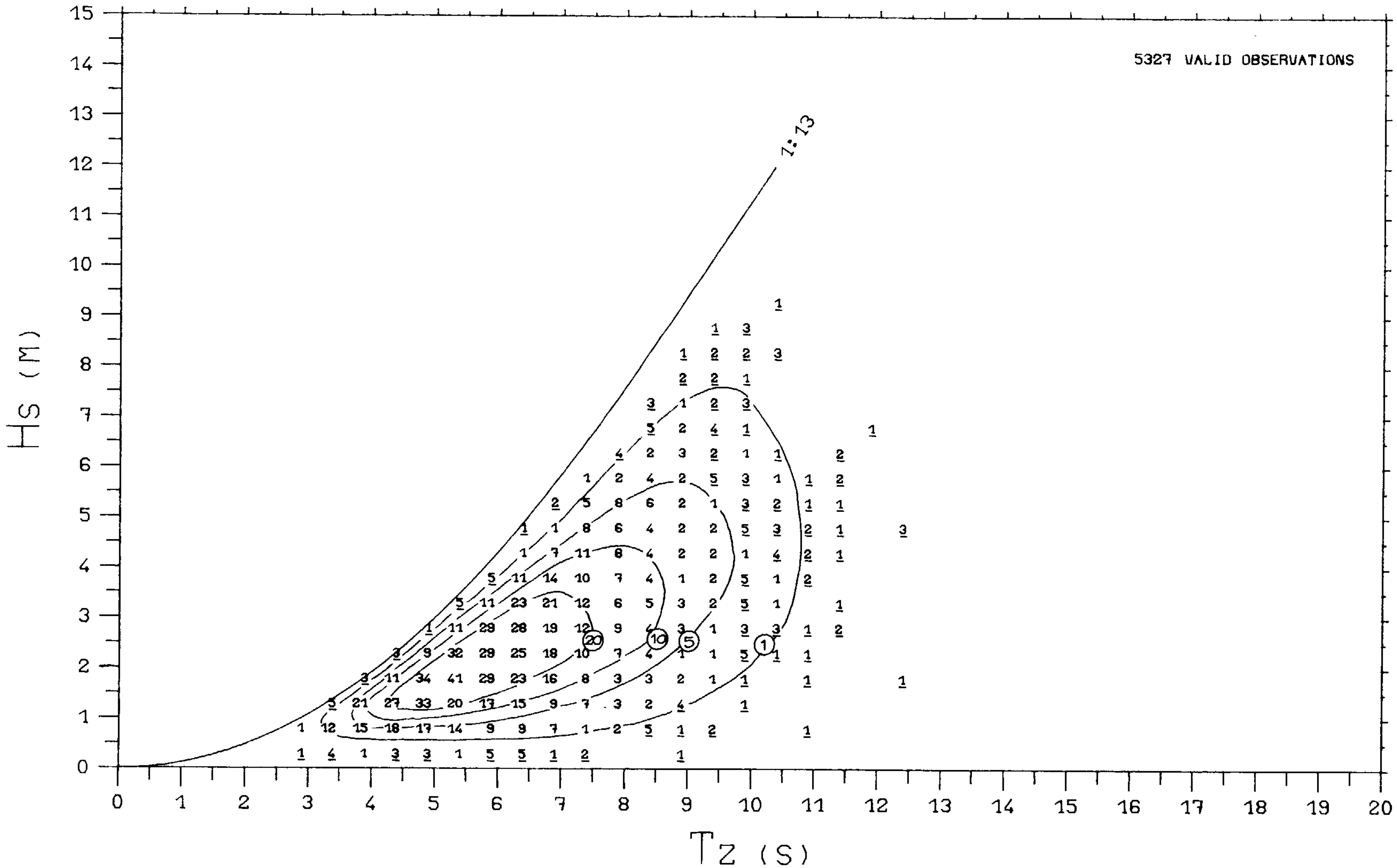

SCATTER DIAGRAM OF Hs AND Tz (PPT)

SU768

SOUTH UIST MAR 1976 - FEB 1978

FIG 3.5.1.5

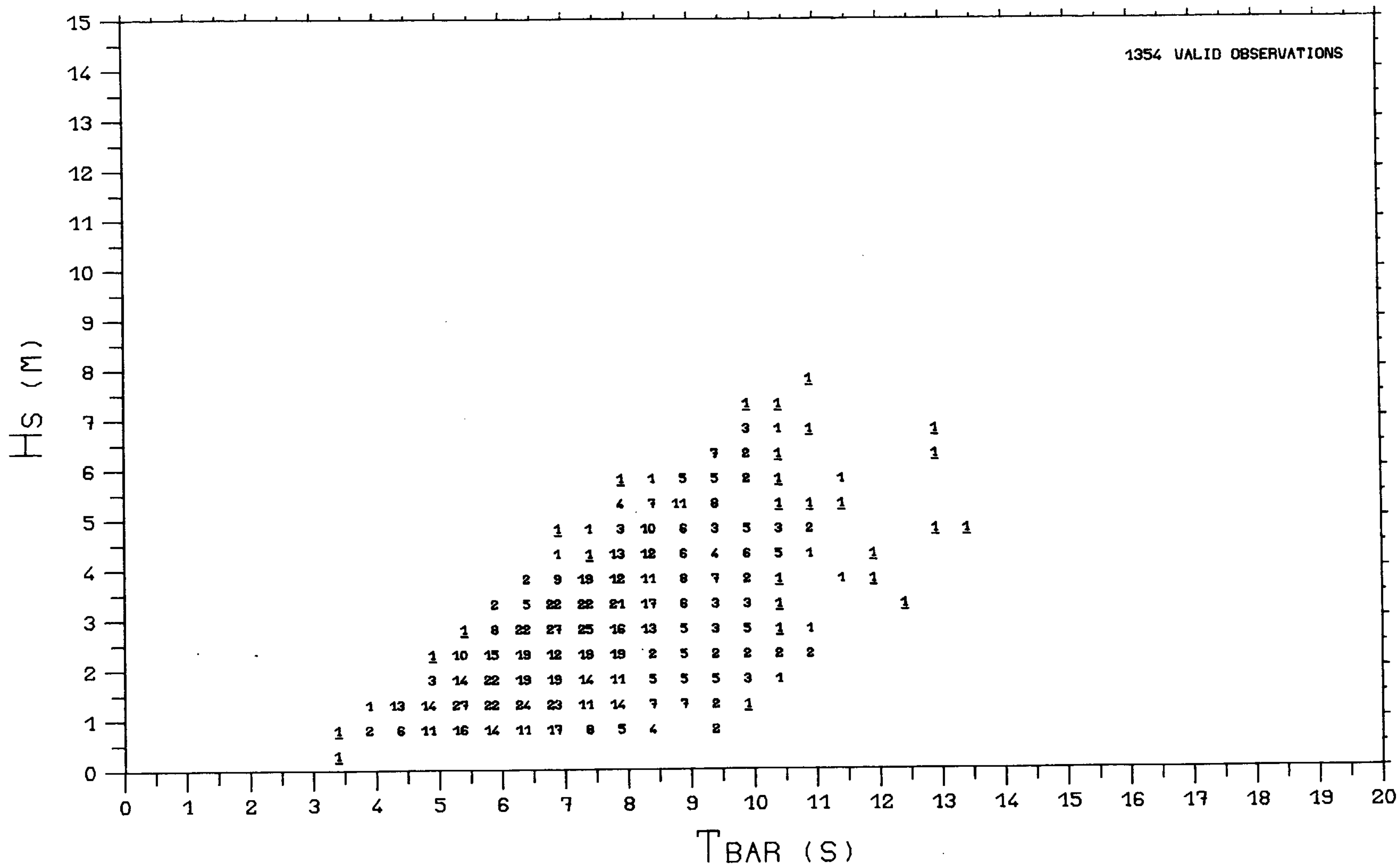

SCATTER DIAGRAM OF H_S AND T_{BAR} (PPT)

SOUTH UIST SPRING 1976 , 1977

FIG 3.5.2.1

SU768

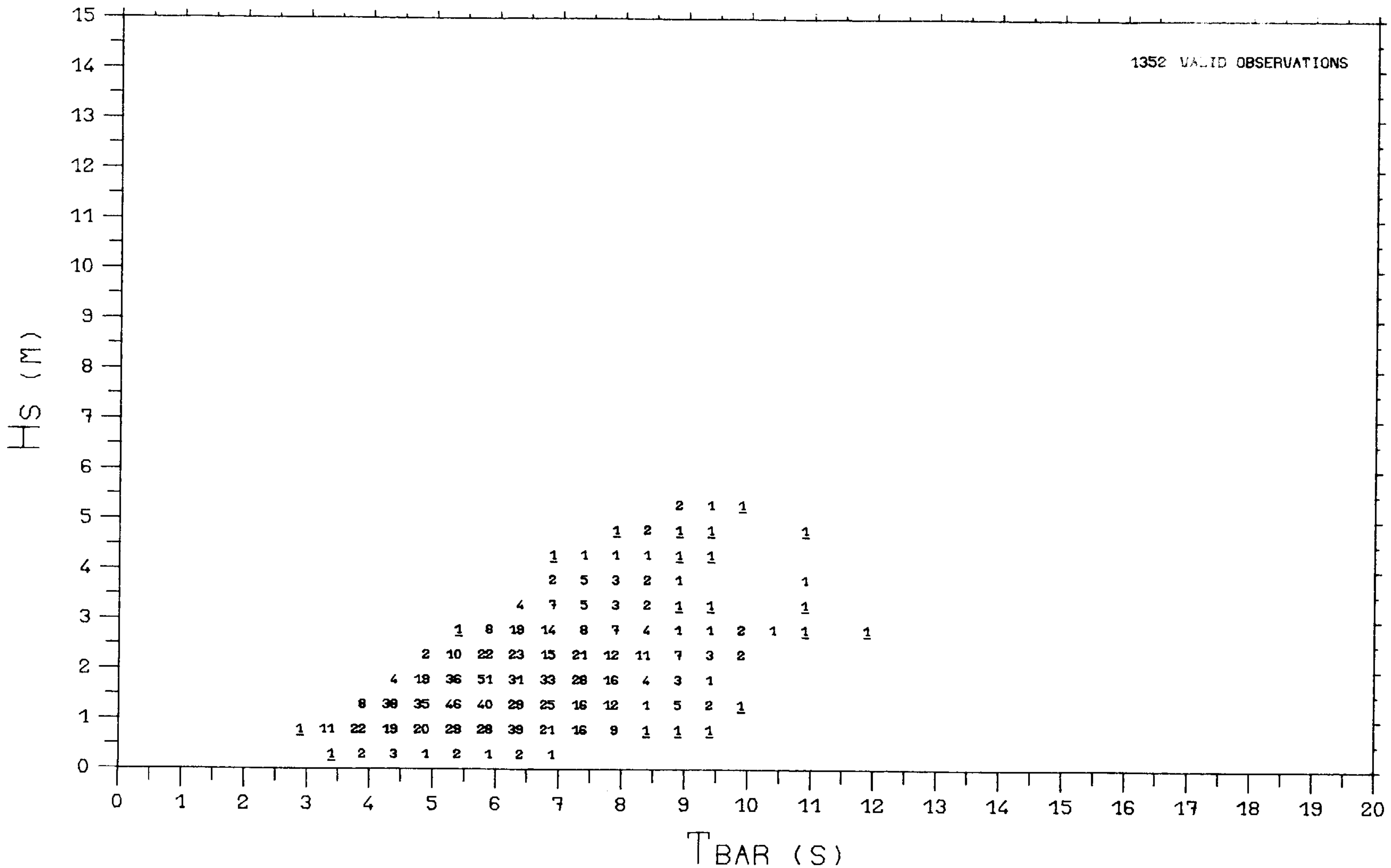

SCATTER DIAGRAM OF H_S AND T_{BAR} (PPT)

SU768

SOUTH UIST SUMMER 1976 , 1977

FIG 3.5.2.2

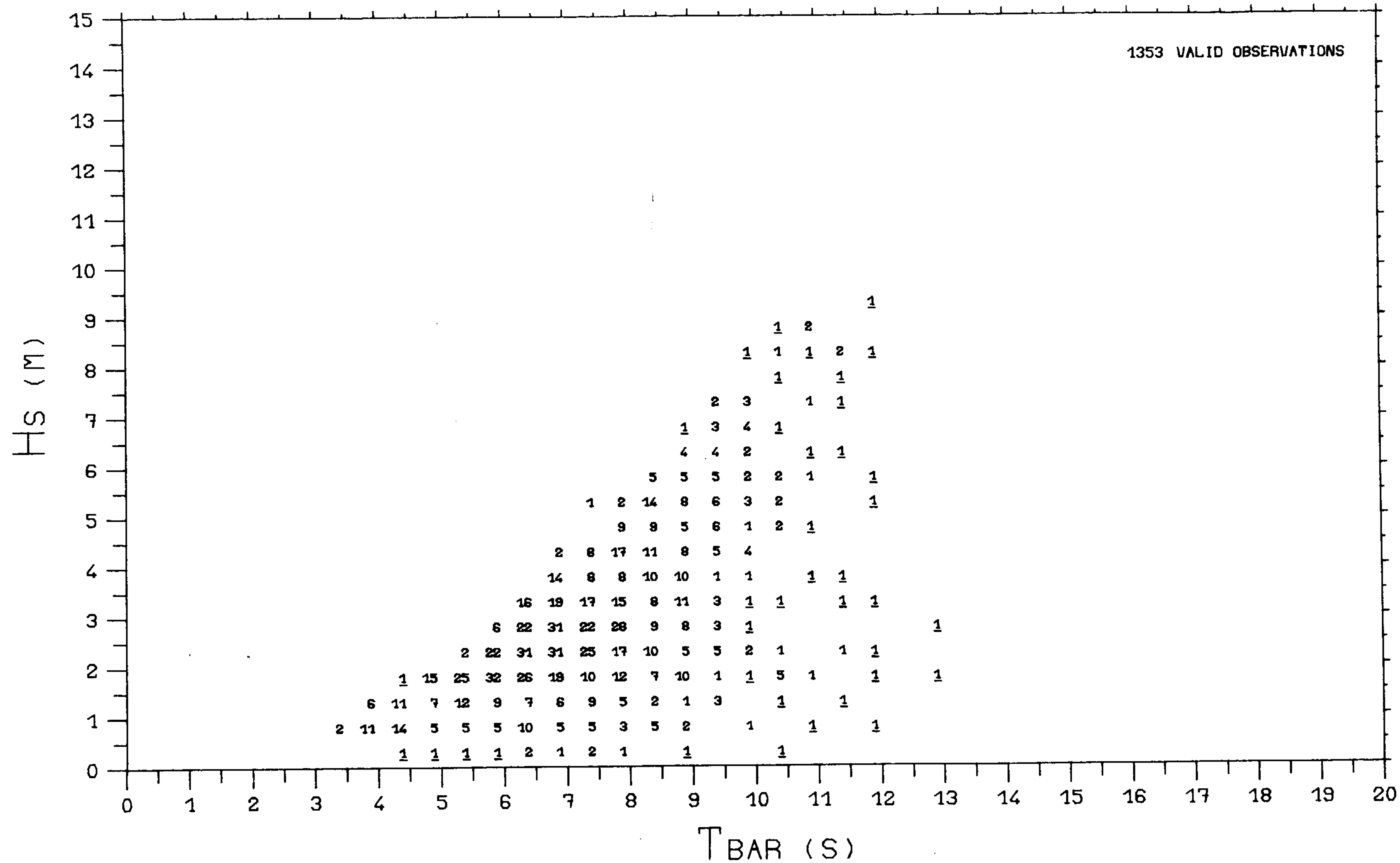

SCATTER DIAGRAM OF H_S AND T_{BAR} (PPT)

SOUTH UIST AUTUMN 1976 , 1977

FIG 3.5.2.3

SU768

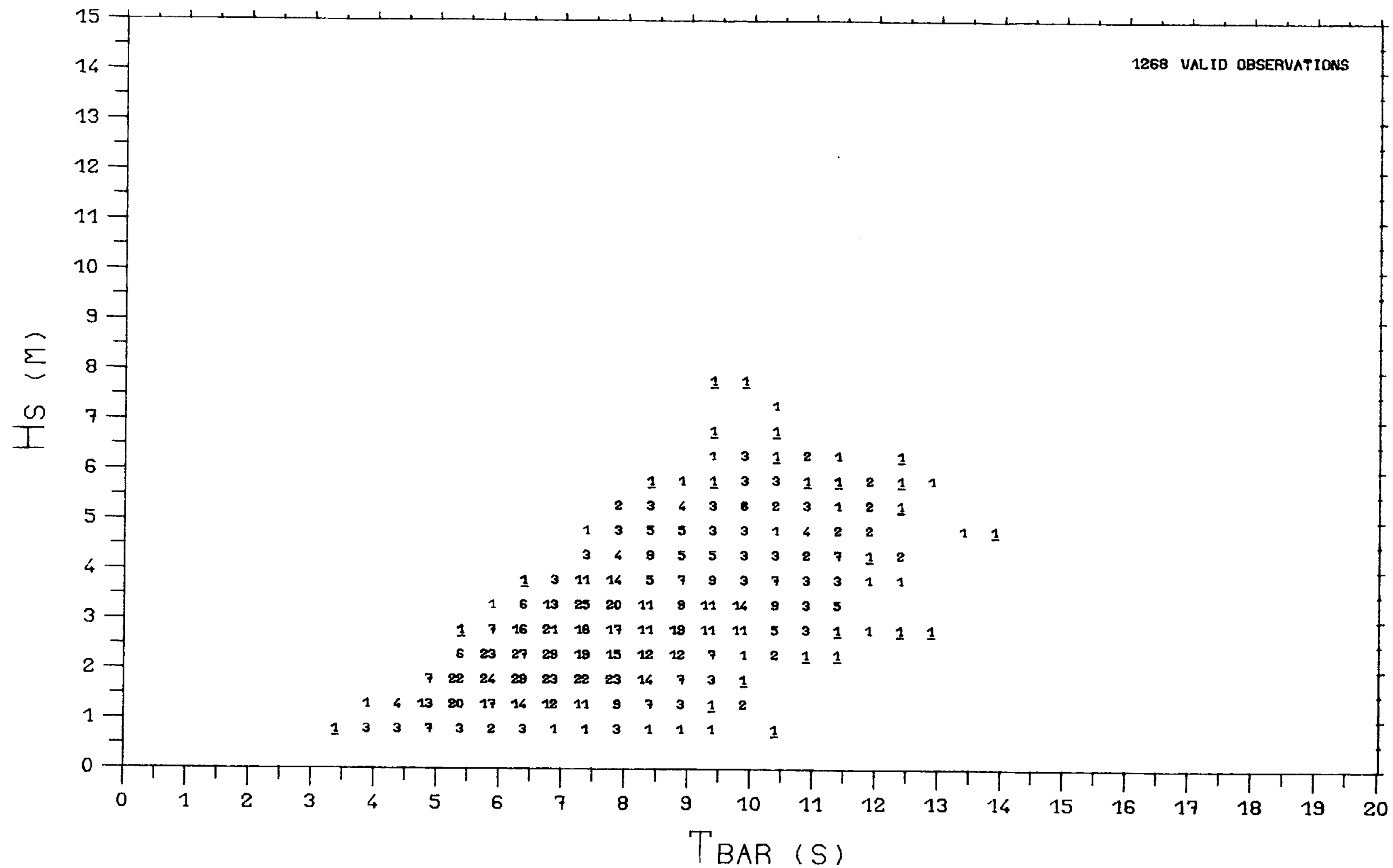

SCATTER DIAGRAM OF H_S AND T_{BAR} (PPT)

SU768

SOUTH UIST WINTER 1976/7, 1977/8

FIG 3.5.2.4

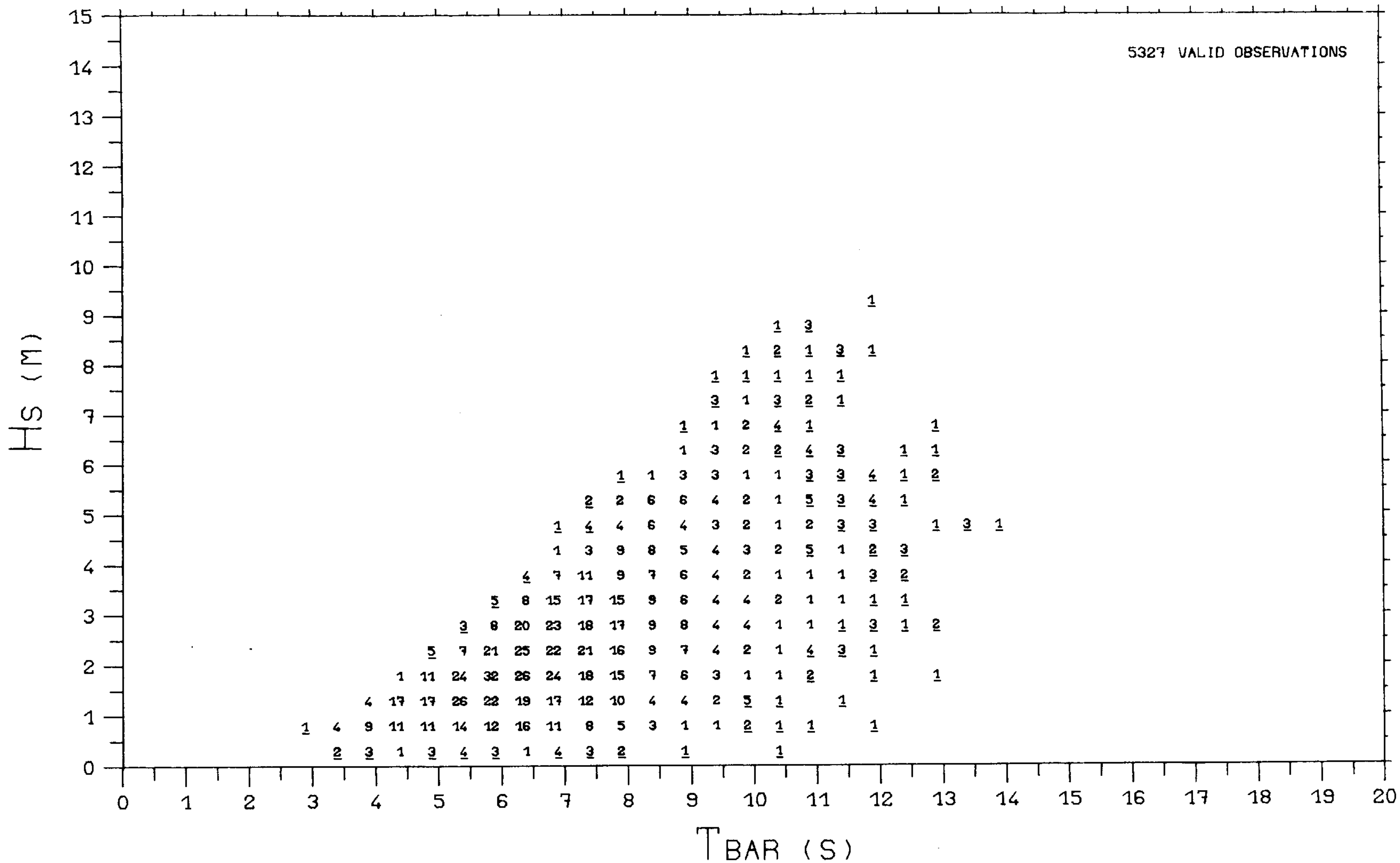

SCATTER DIAGRAM OF H_S AND T_{BAR} (PPT)

SOUTH UIST MAR 1976 - FEB 1978

FIG 3.5.2.5

SU768

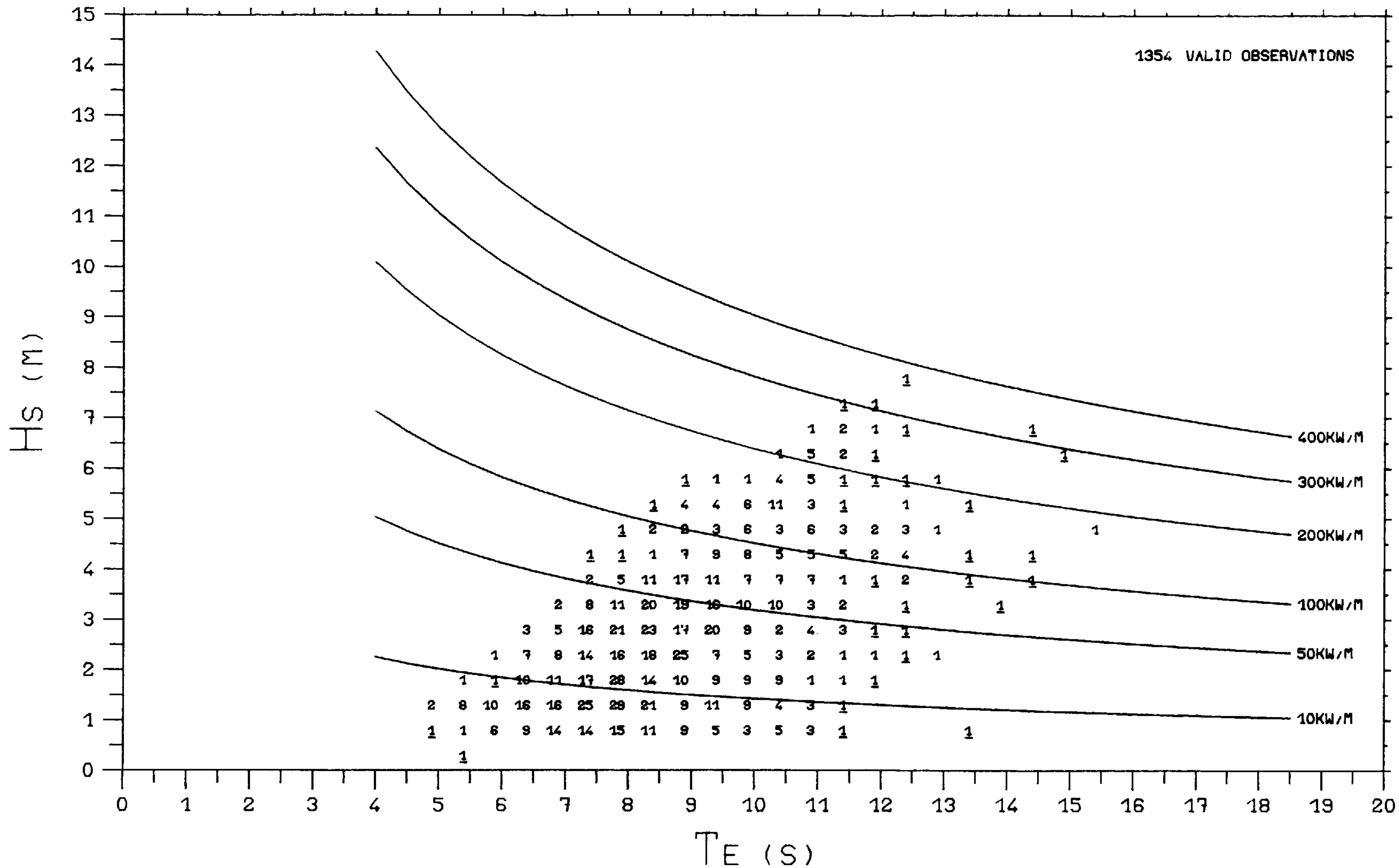

SCATTER DIAGRAM OF H_S AND T_E (PPT)

SOUTH UIST SPRING 1976 , 1977

FIG 3.5.3.1

SU768

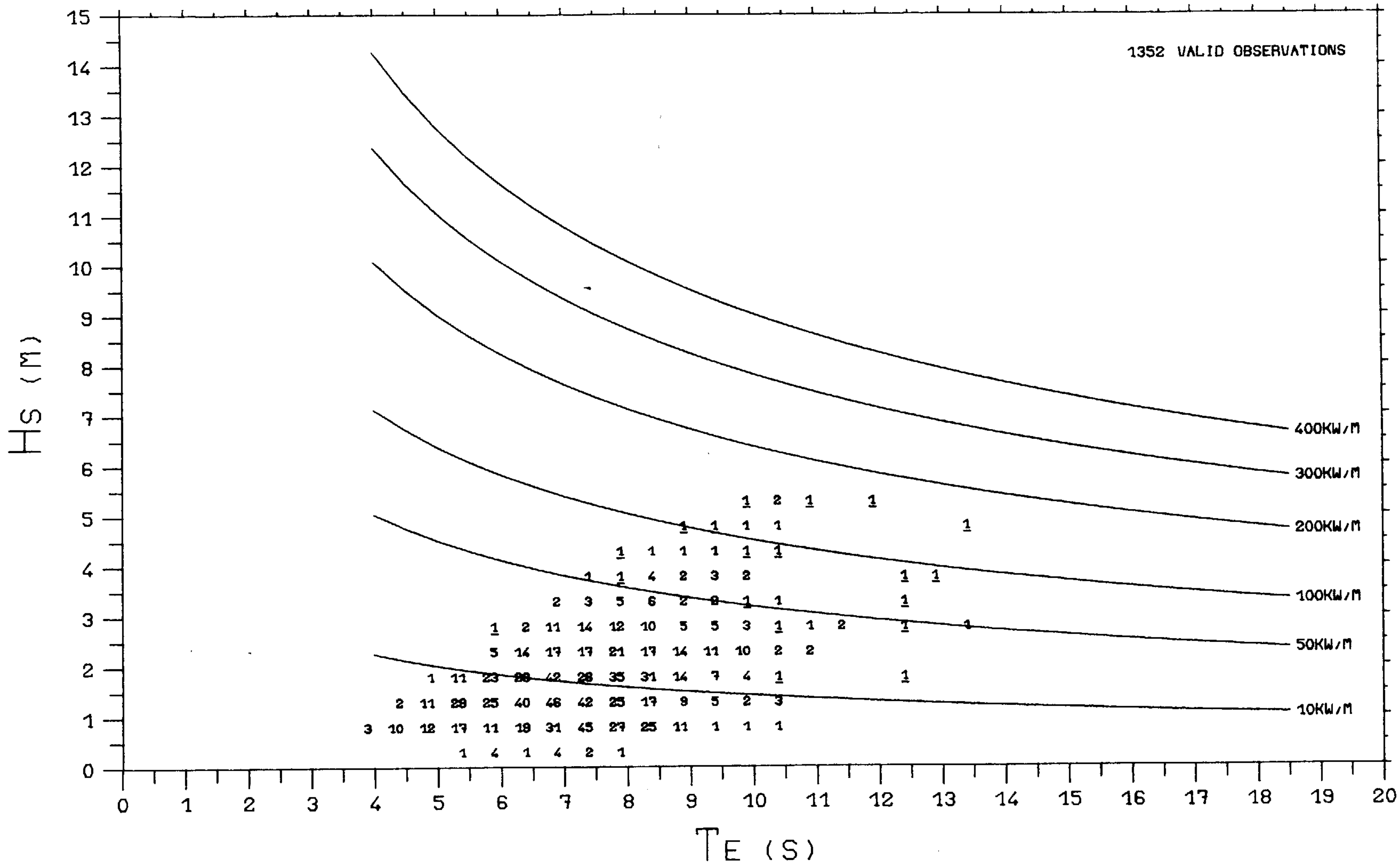

SCATTER DIAGRAM OF H_S AND T_E (PPT)

SOUTH UIST SUMMER 1976 , 1977

FIG 3.5.3.2

SU768

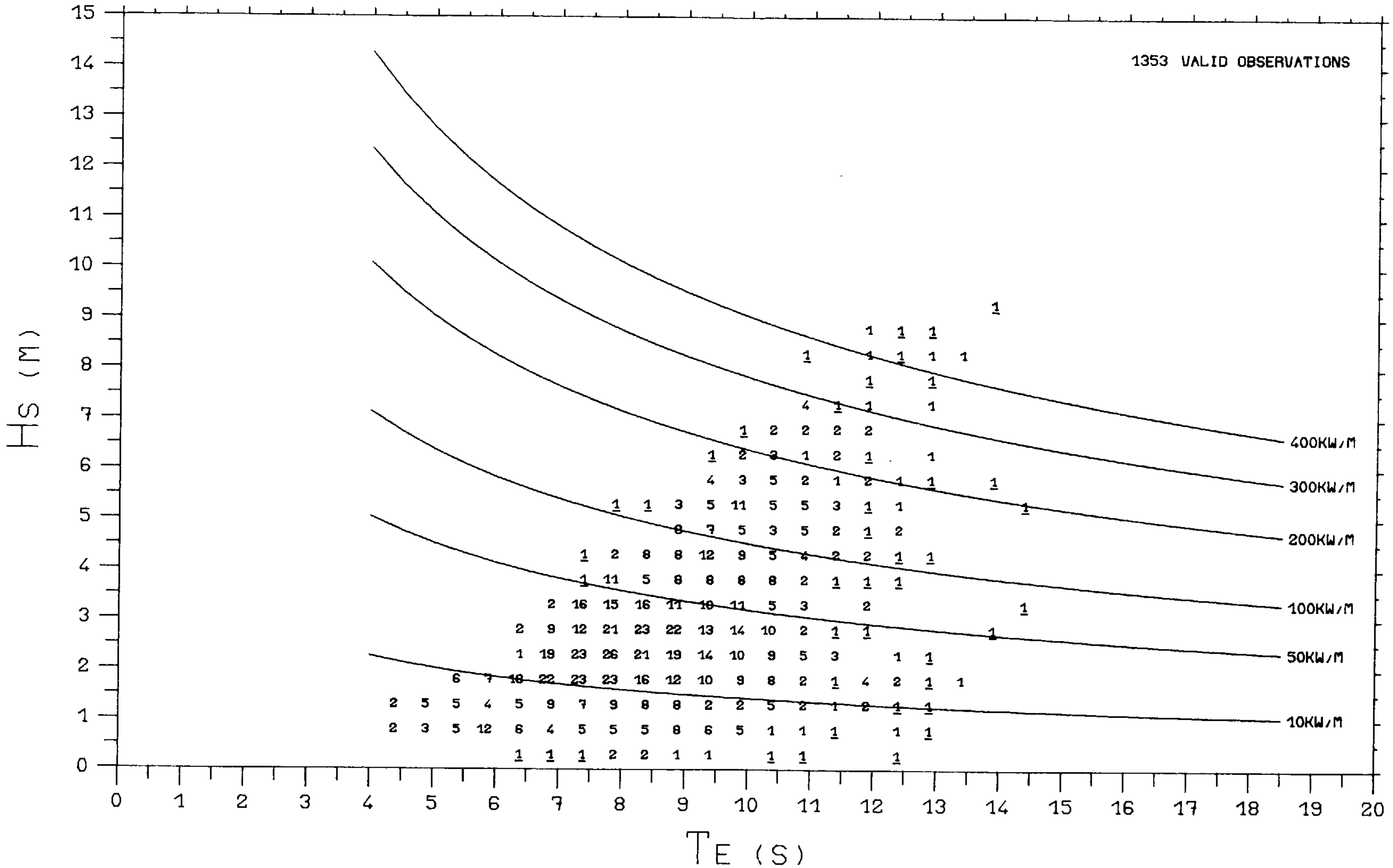

SCATTER DIAGRAM OF H_S AND T_E (PPT)

SU768

SOUTH UIST AUTUMN 1976 , 1977

FIG 3.5.3.3

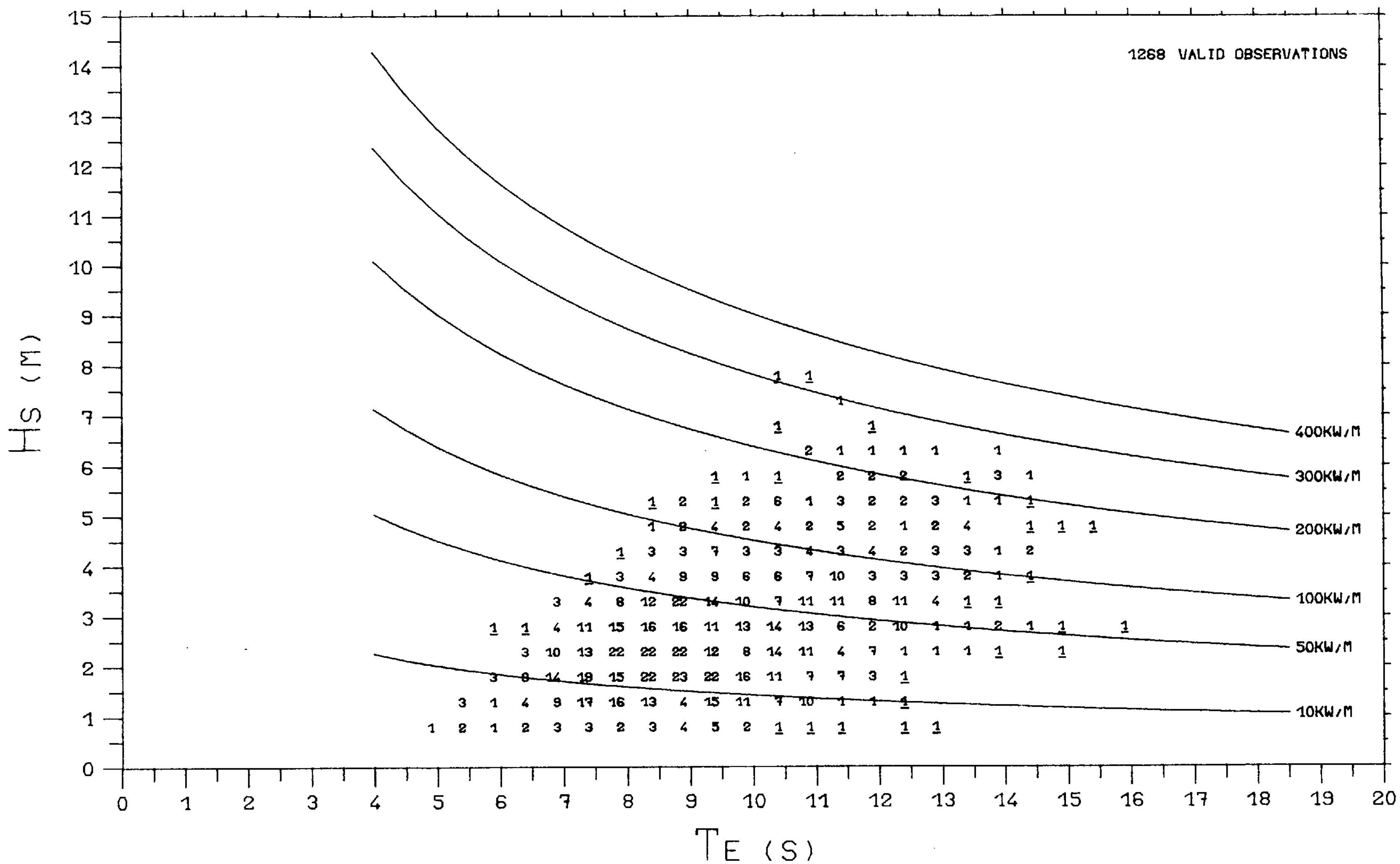

SCATTER DIAGRAM OF Hs AND Te (PPT)

SOUTH UIST WINTER 1976/7, 1977/8

FIG 3.5.3.4

SU768

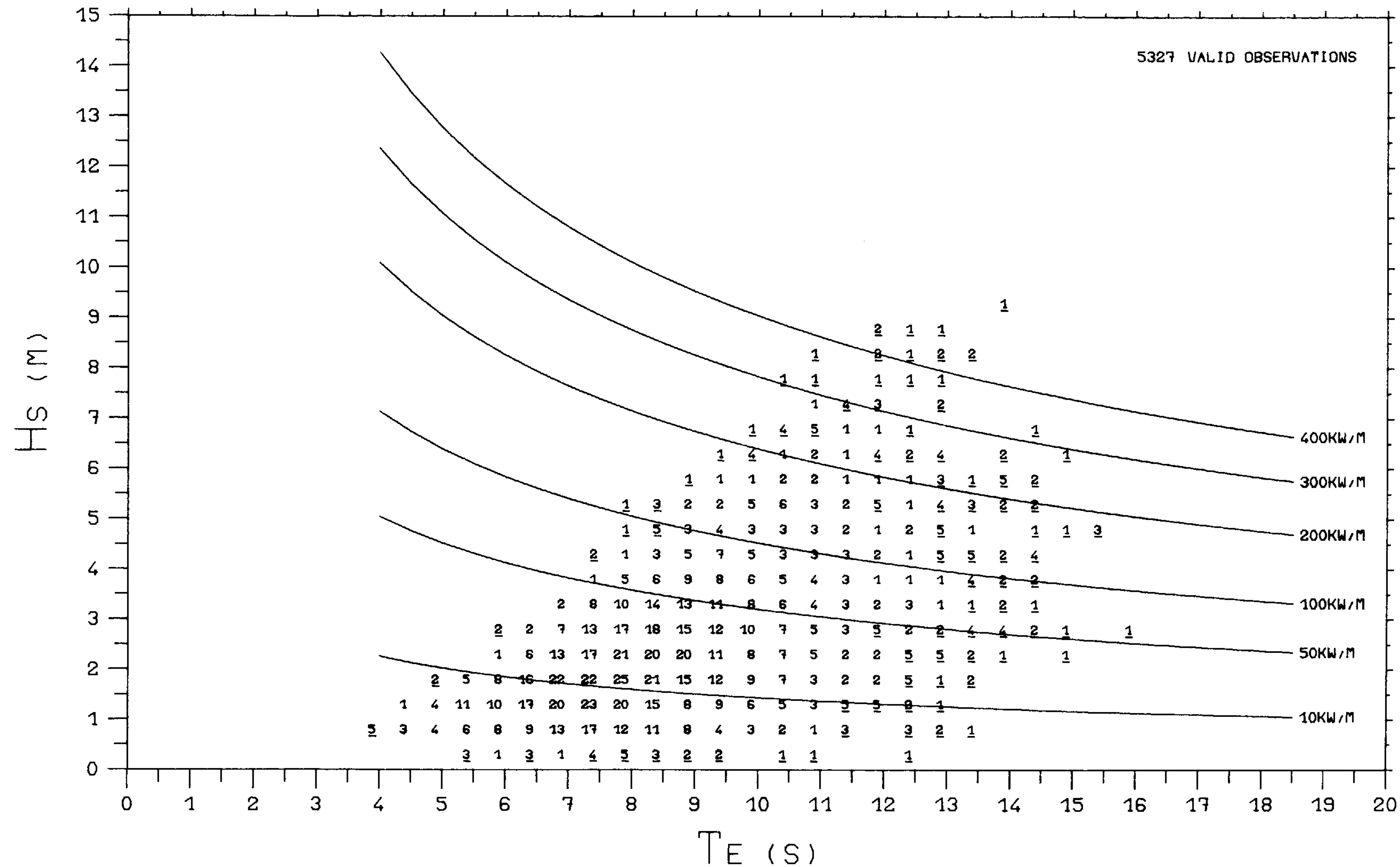

SCATTER DIAGRAM OF H_S AND T_E (PPT)

SOUTH UIST MAR 1976 - FEB 1978

FIG 3.5.3.5

SU768

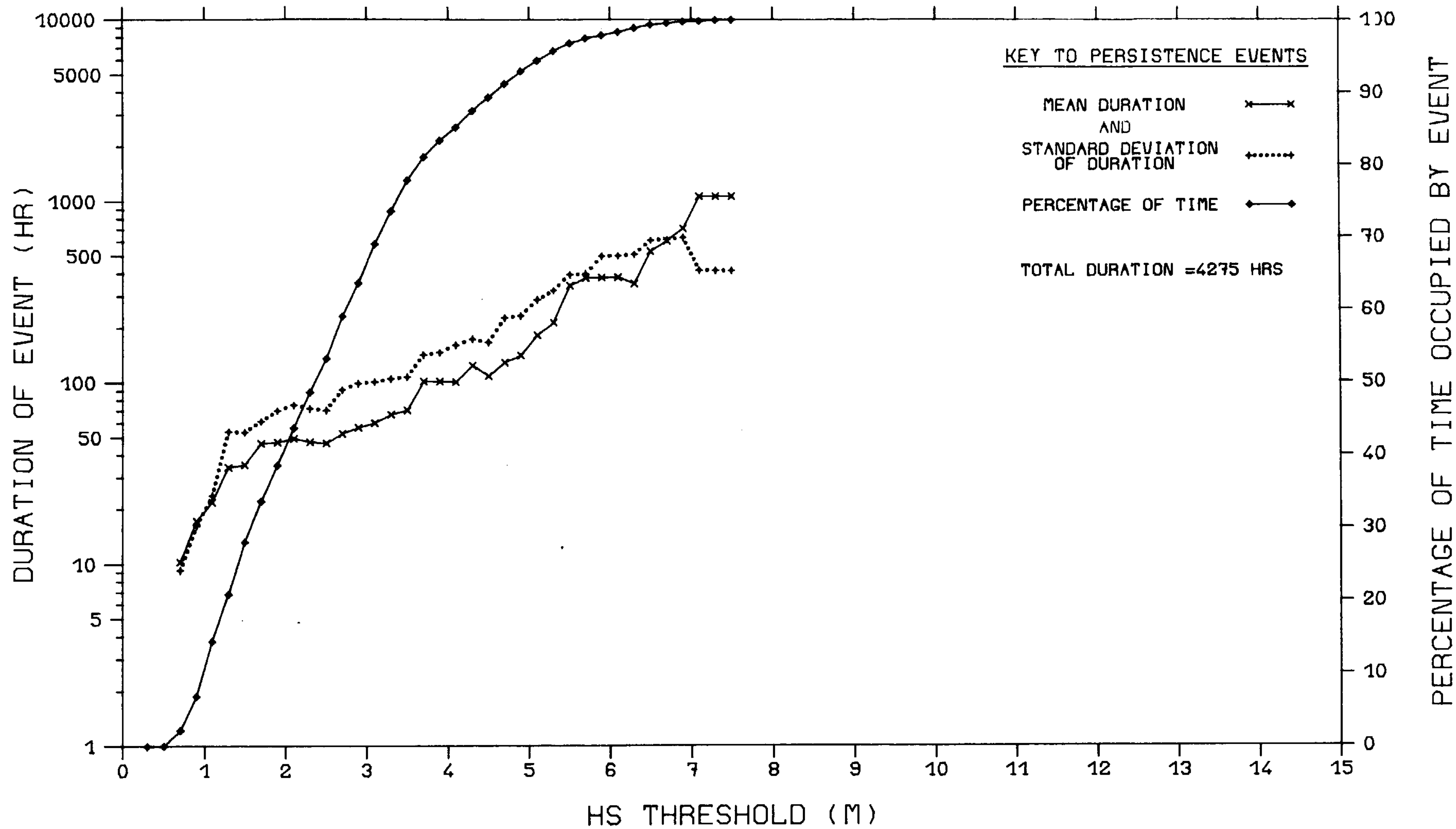

SOUTH UIST WAVE DATA - SPRING - 1976,77

CALMS

FIG 3.6.1.1

SU768

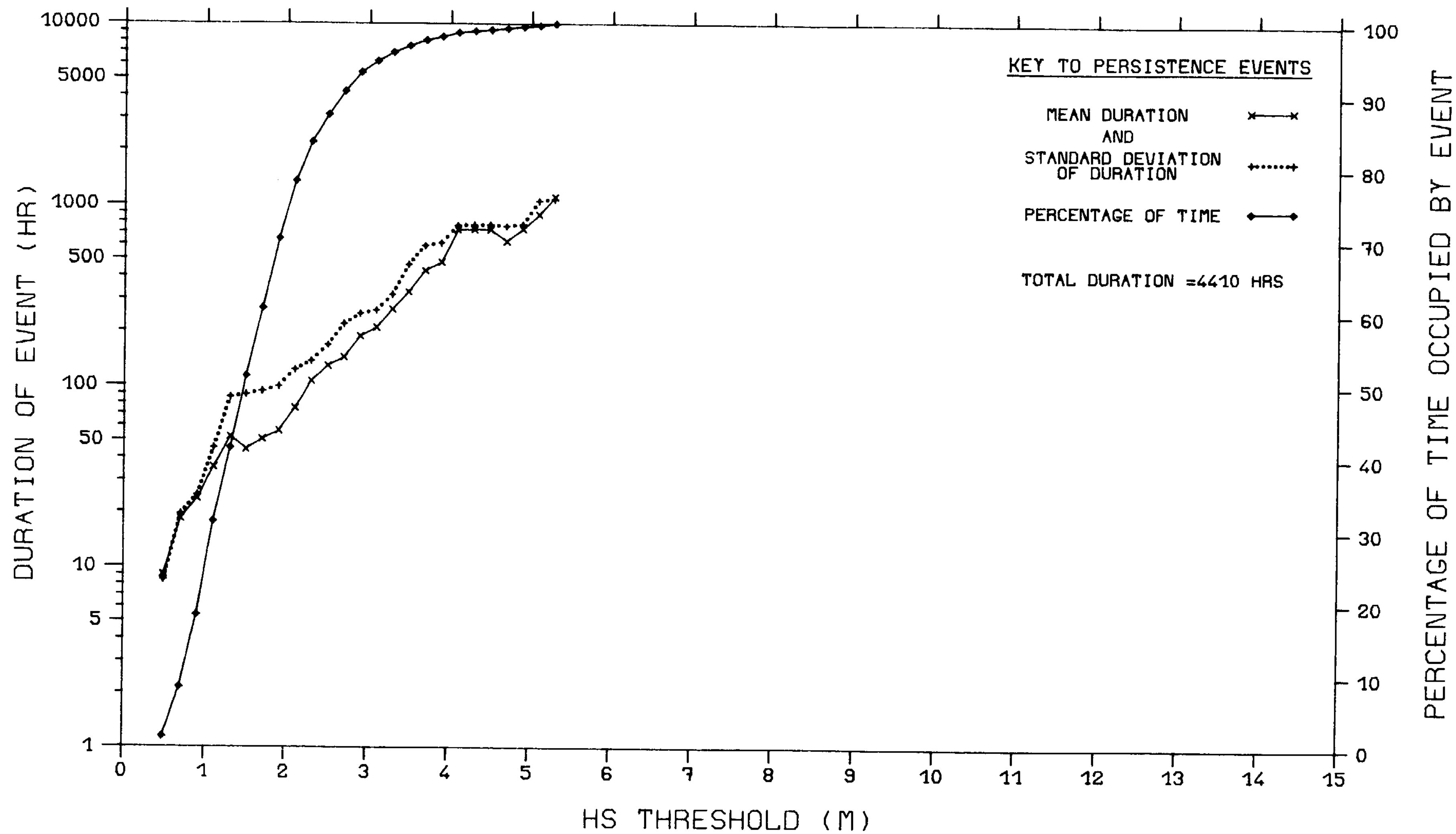

SOUTH UIST WAVE DATA - SUMMER - 1976,77

CALMS

FIG 3.6.1.2

SU768

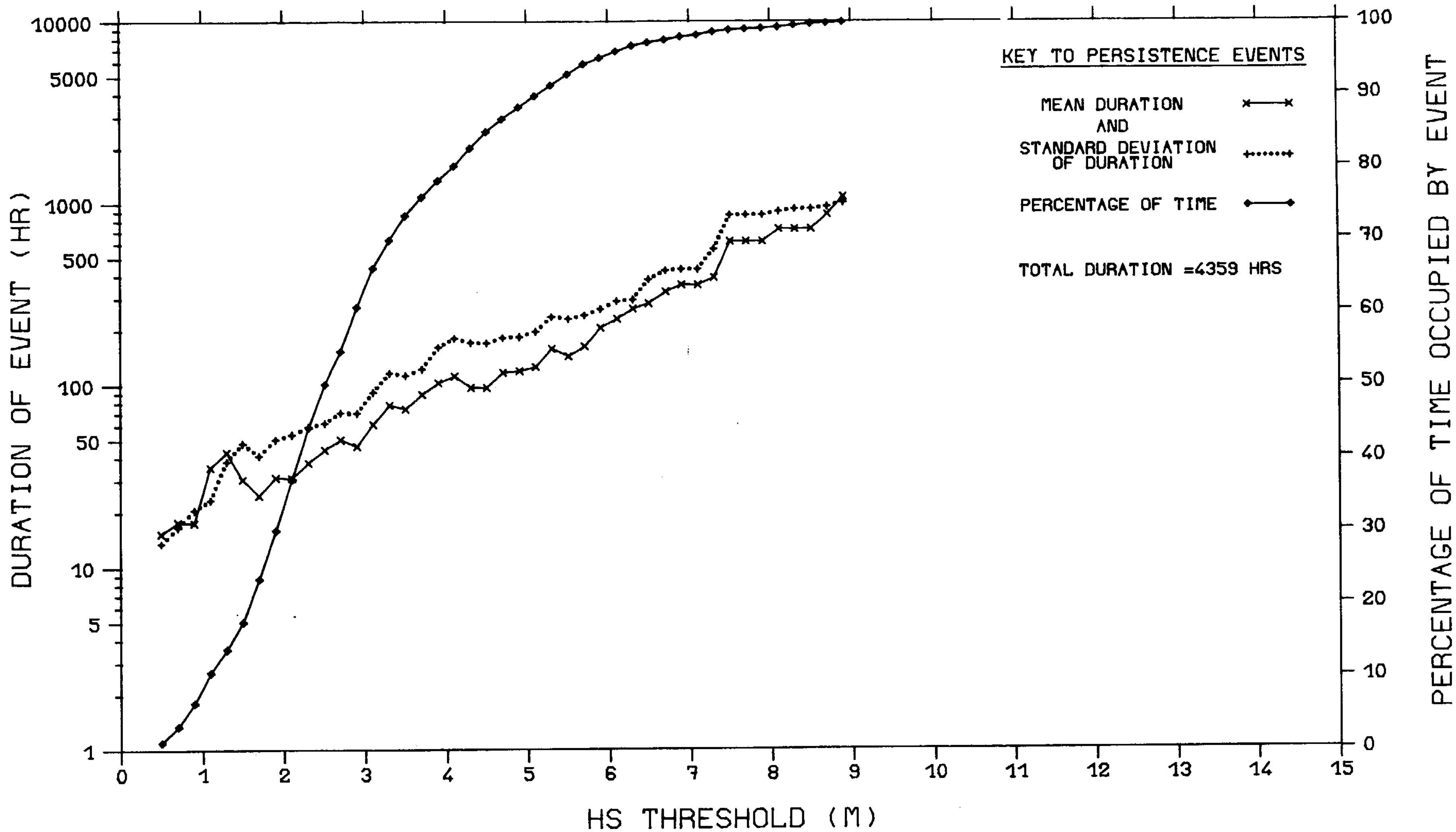

SOUTH UIST WAVE DATA - AUTUMN - 1976,77

CALMS

FIG 3.6.1.3

SU768

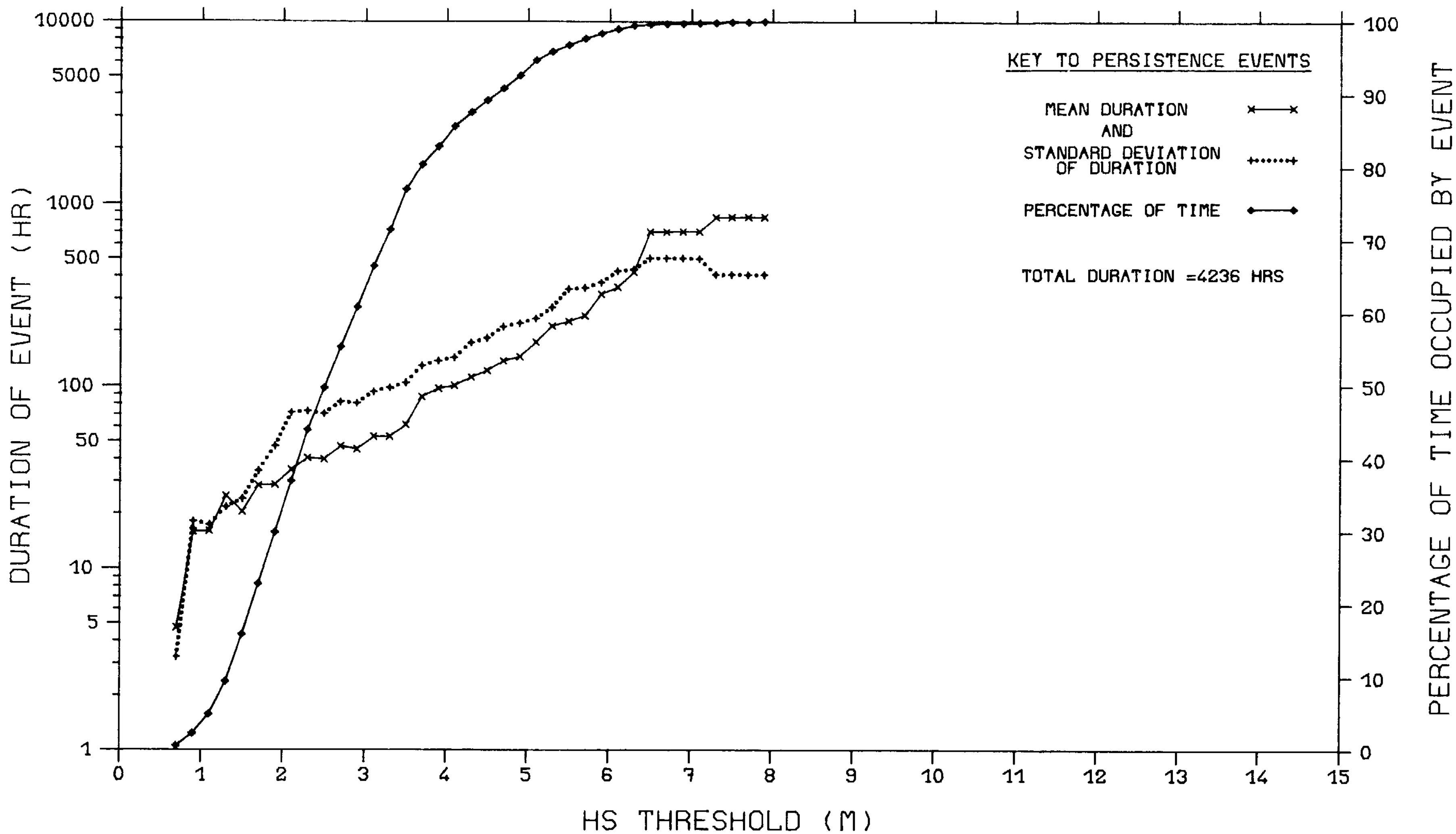

SOUTH UIST WAVE DATA - WINTER 1976/7,1977/8

CALMS

FIG 3.6.1.4

SU768

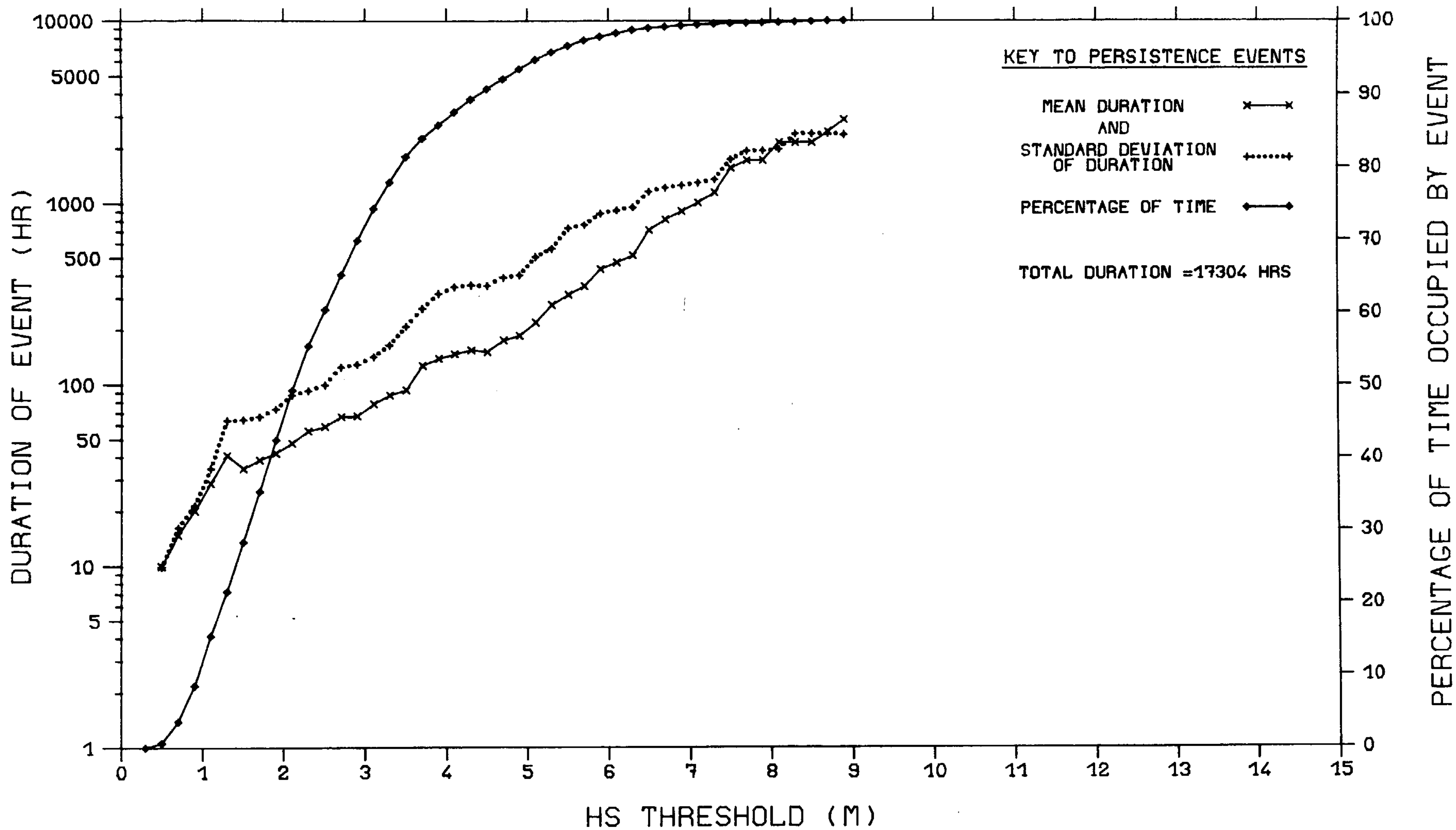

SOUTH UIST MAR 1976 - FEB 1978

CALMS

FIG 3.6.1.5

SU768

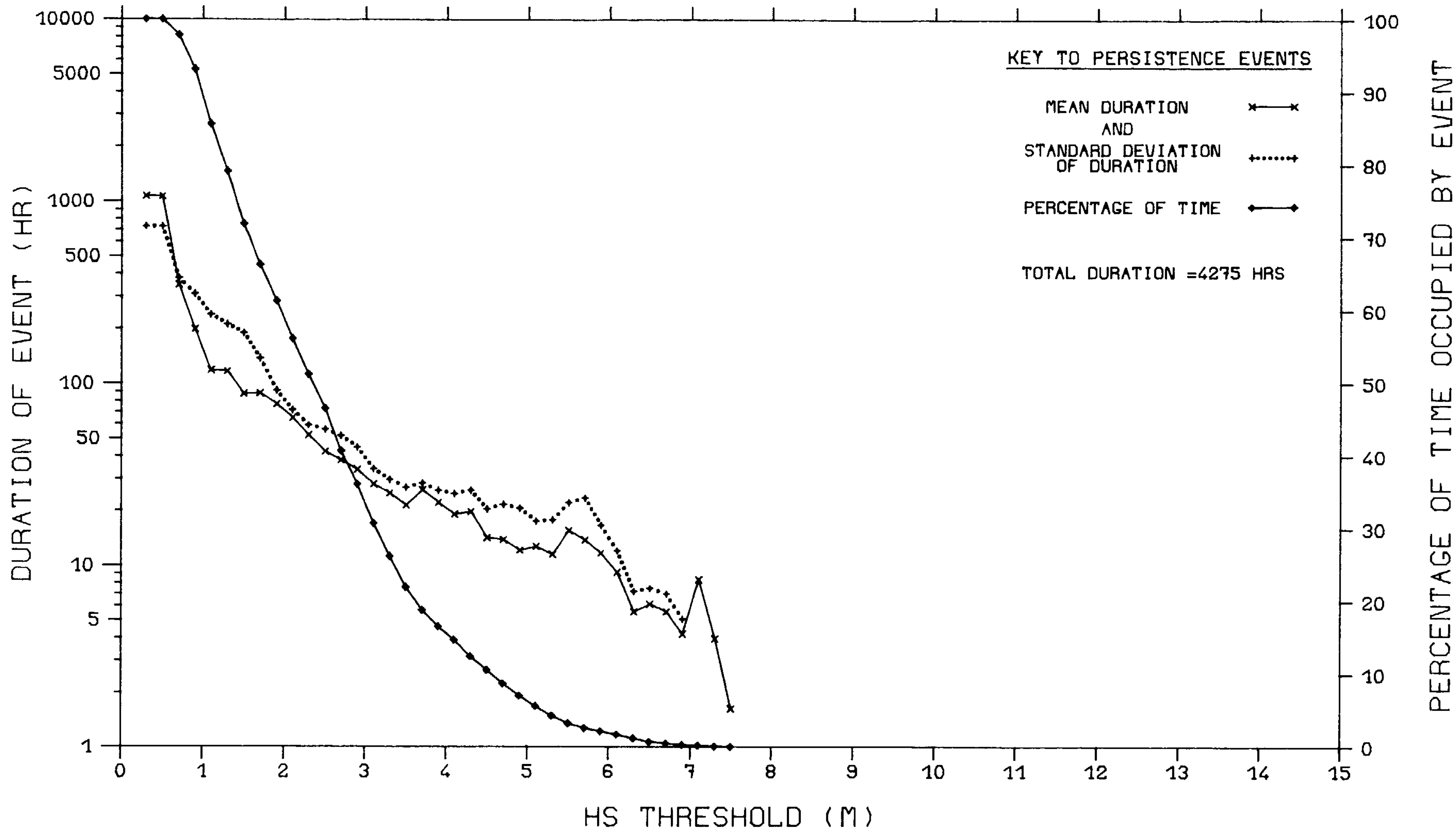

SOUTH UIST WAVE DATA - SPRING - 1976,77

STORMS

FIG 3.6.2.1

SU768

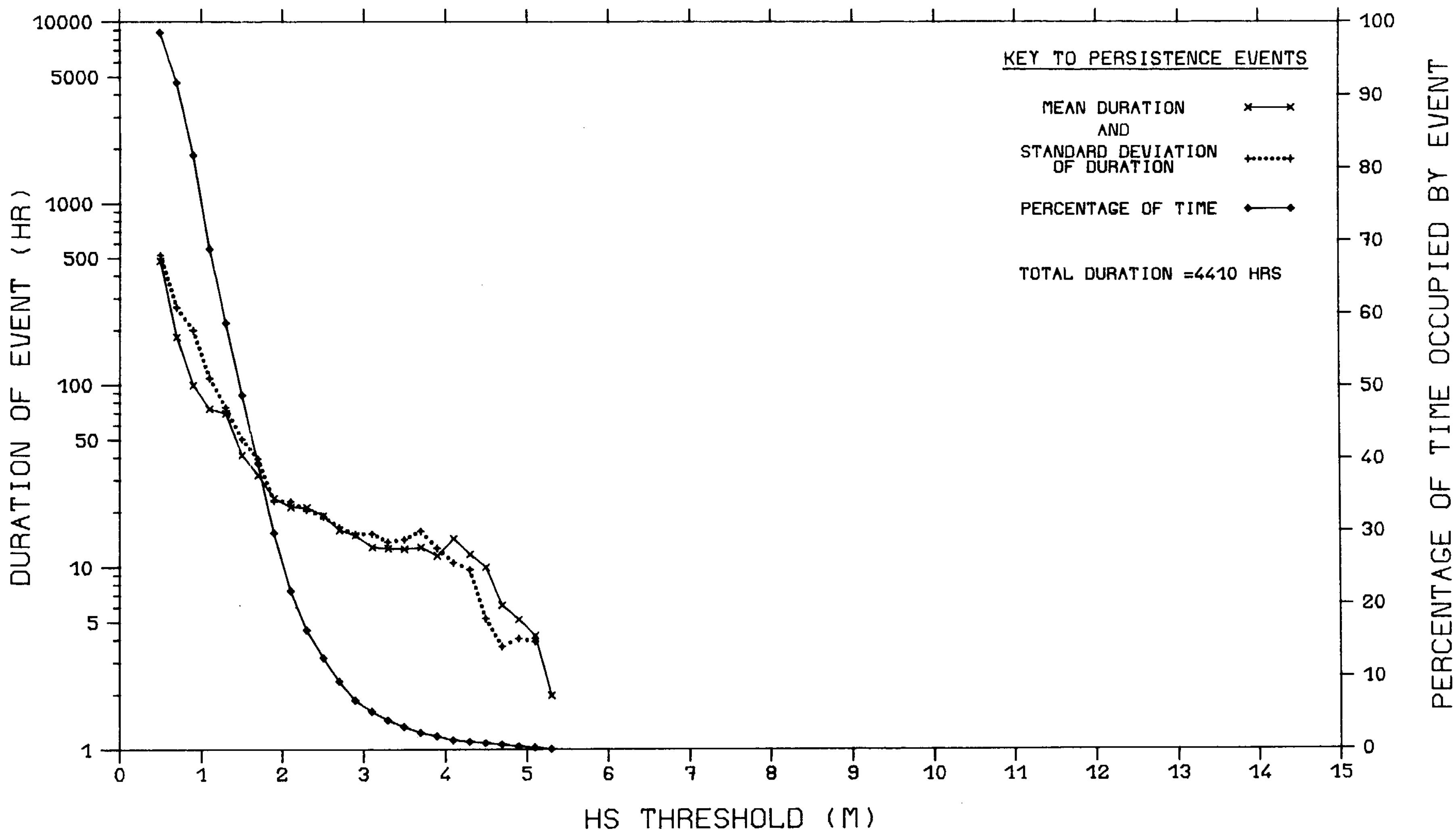

SOUTH UIST WAVE DATA - SUMMER - 1976,77

STORMS

FIG 3.6.2.2

SU768

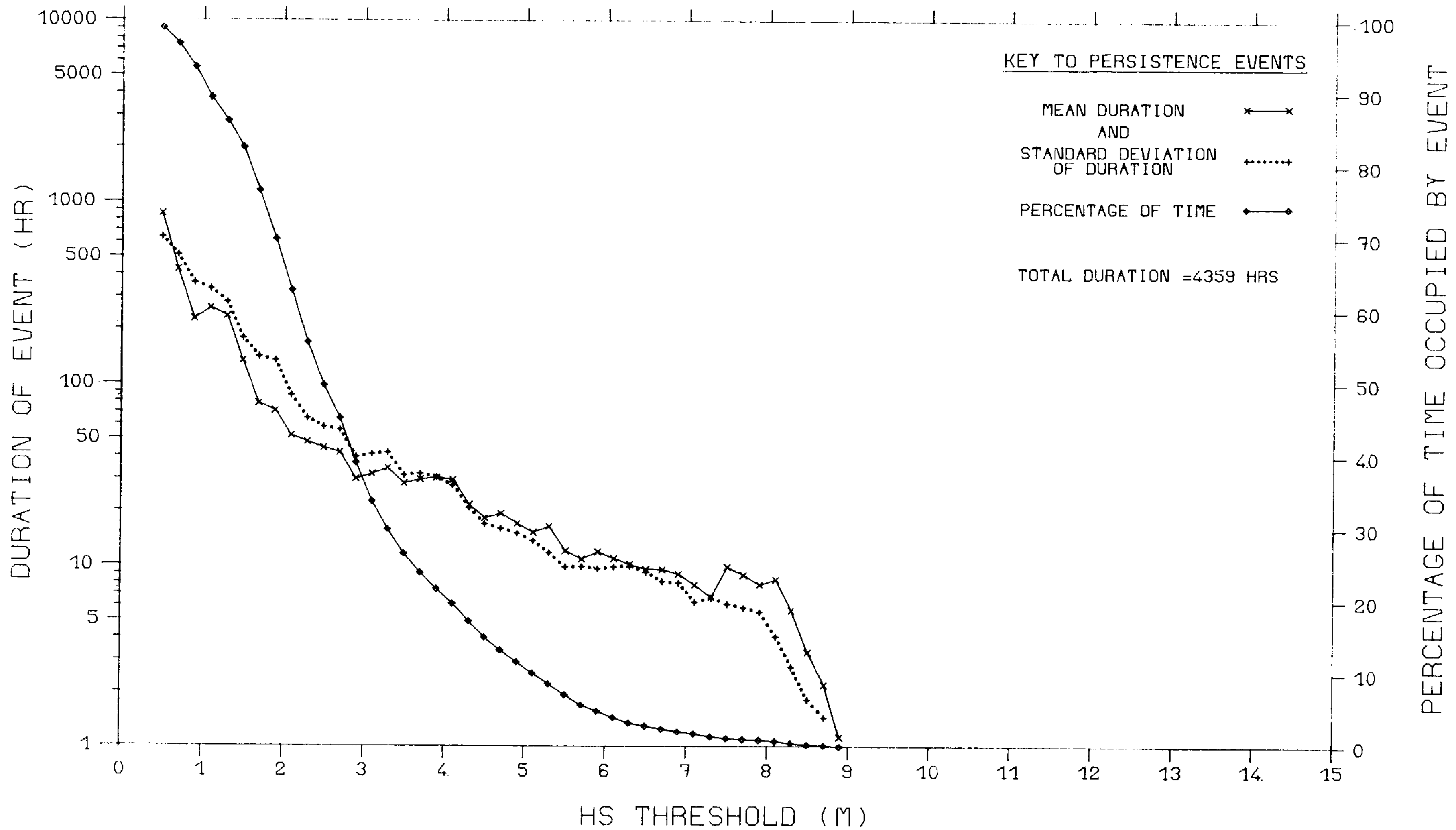

SOUTH UIST WAVE DATA - AUTUMN - 1976,77

STORMS

FIG 3.6.2.3

SU768

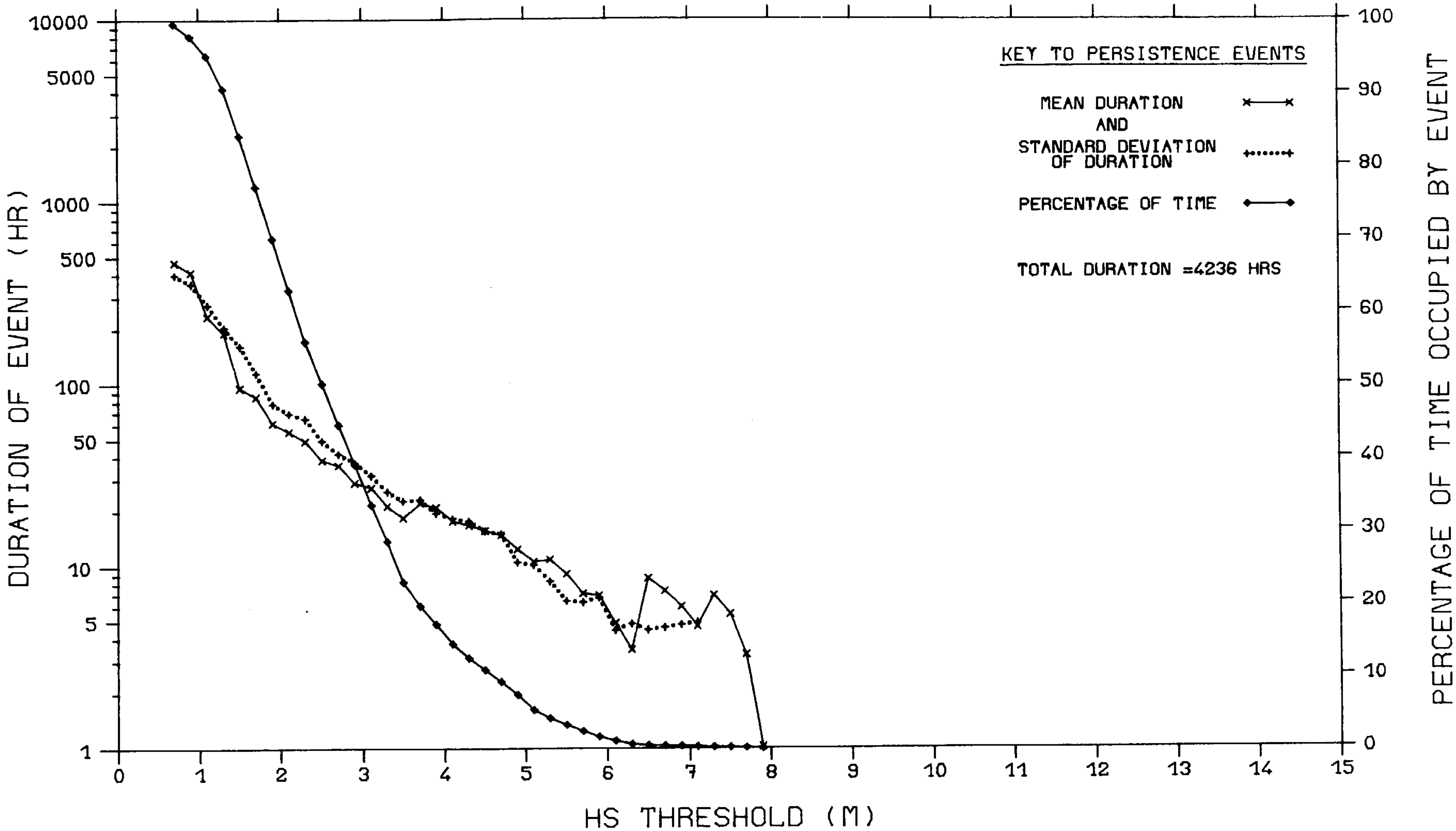

SOUTH UIST WAVE DATA - WINTER 1976/7,1977/8

STORMS

FIG 3.6.2.4

SU768

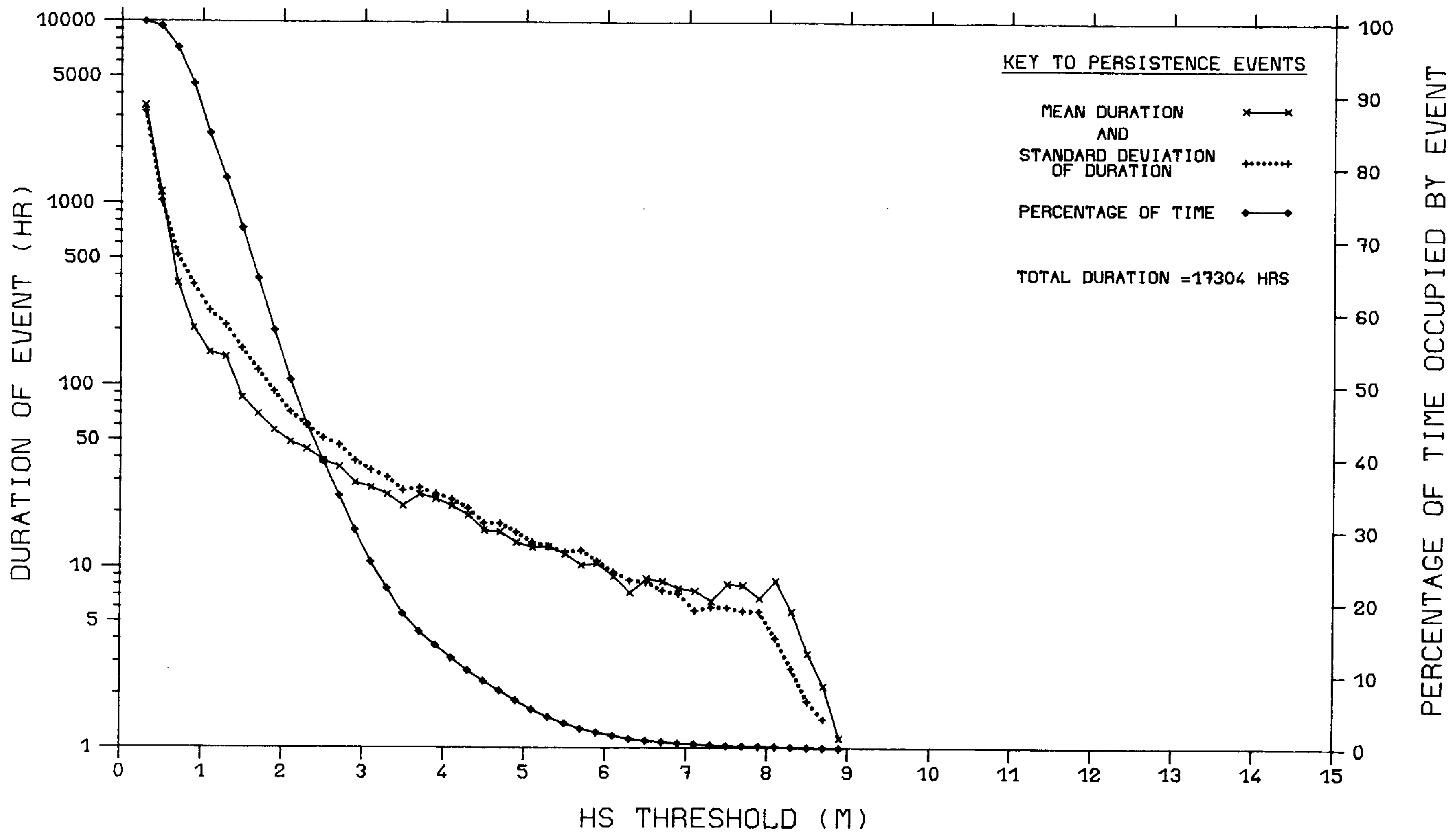

SOUTH UIST MAR 1976 - FEB 1978

STORMS

FIG 3.6.2.5

SU768

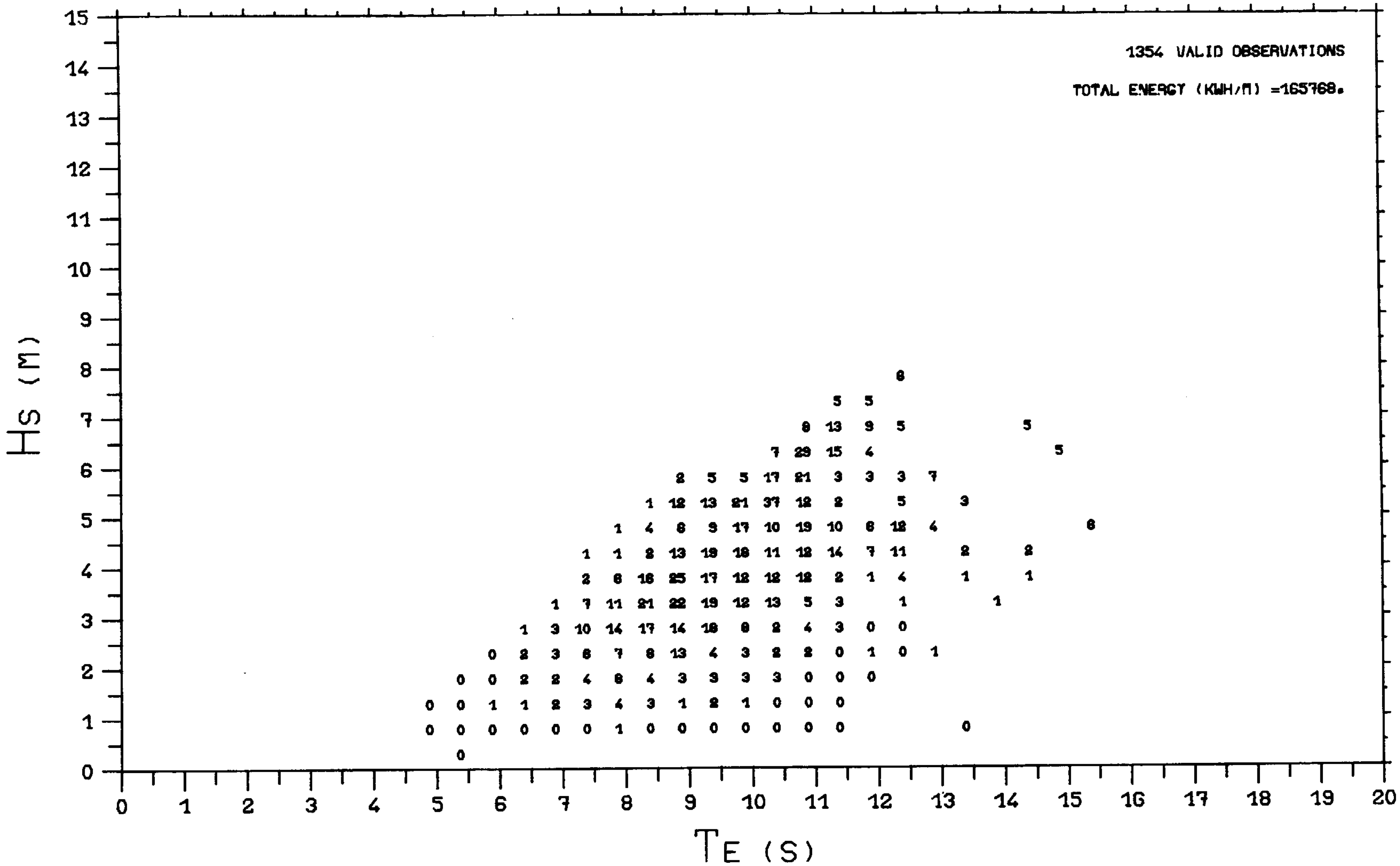

DISTRIBUTION OF TOTAL MEASURED WAVE ENERGY
WITH H_S AND T_E (PPT)

SOUTH UIST SPRING 1976 , 1977

FIG 3.7.1

SU768

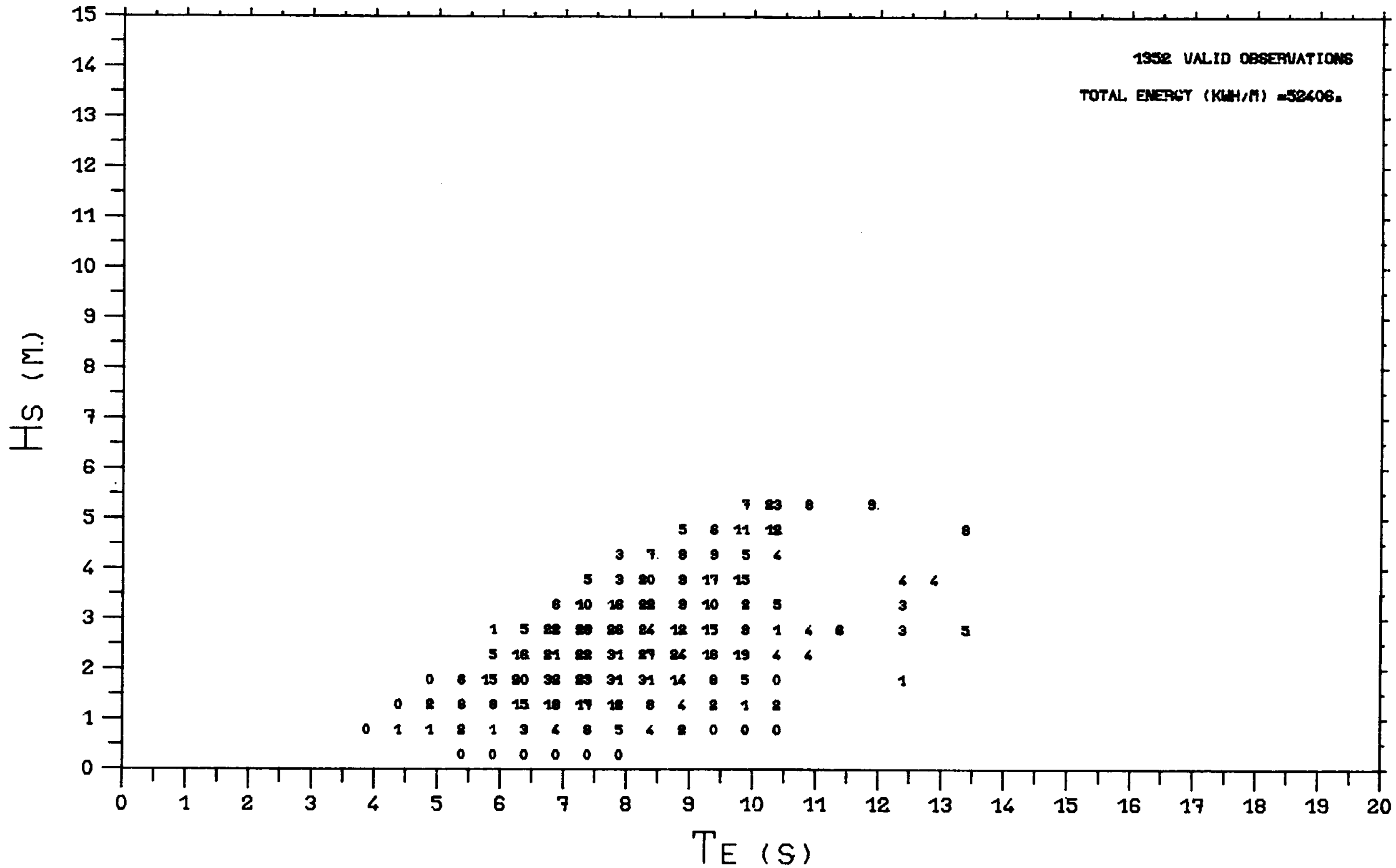

DISTRIBUTION OF TOTAL MEASURED WAVE ENERGY
WITH Hs AND Te (PPT)

SOUTH UIST SUMMER 1976 , 1977
FIG 3.7.2

SU768

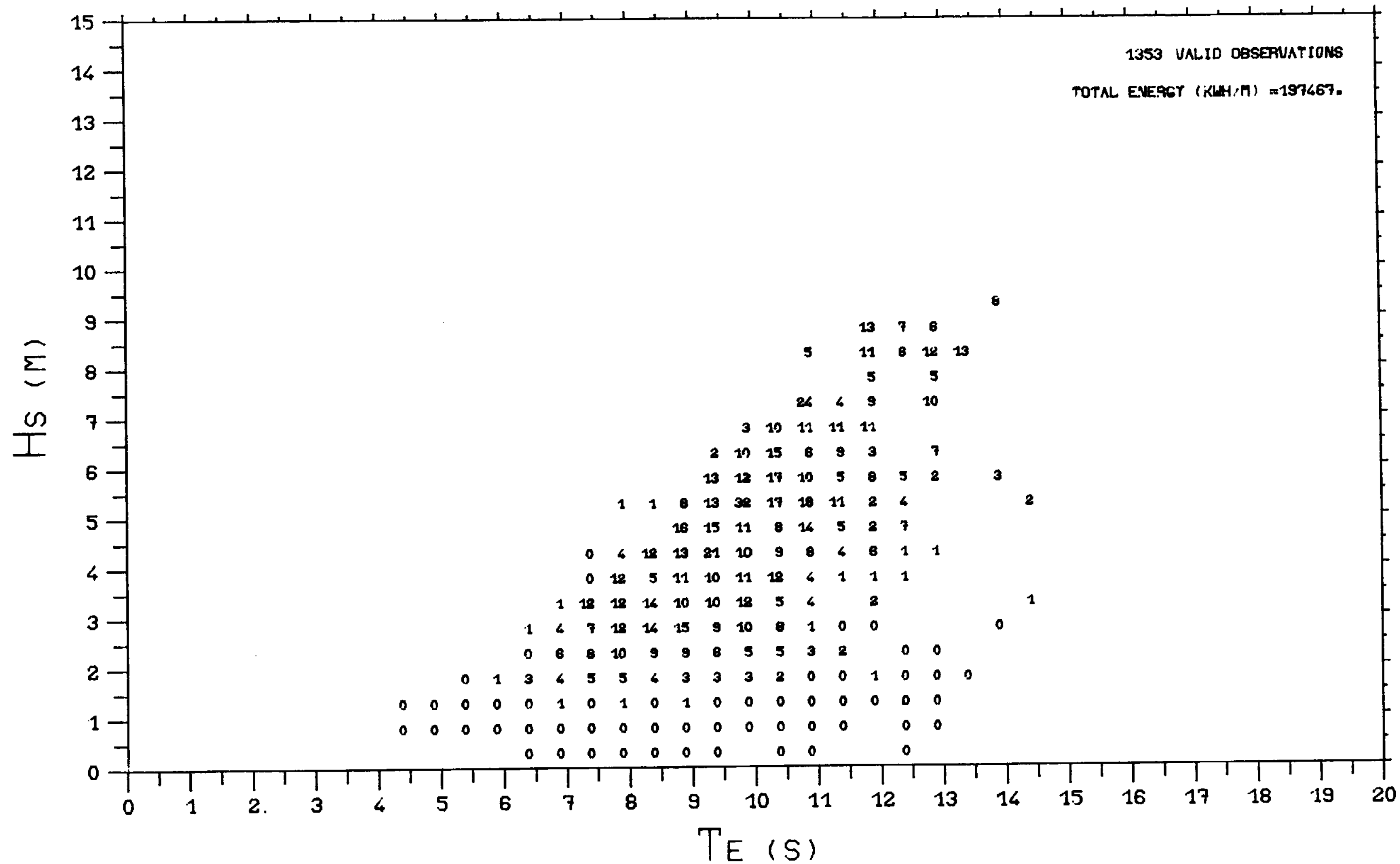

DISTRIBUTION OF TOTAL MEASURED WAVE ENERGY
WITH HS AND TE (PPT)

SOUTH UIST AUTUMN 1976 , 1977

FIG 3.7.3

SU768

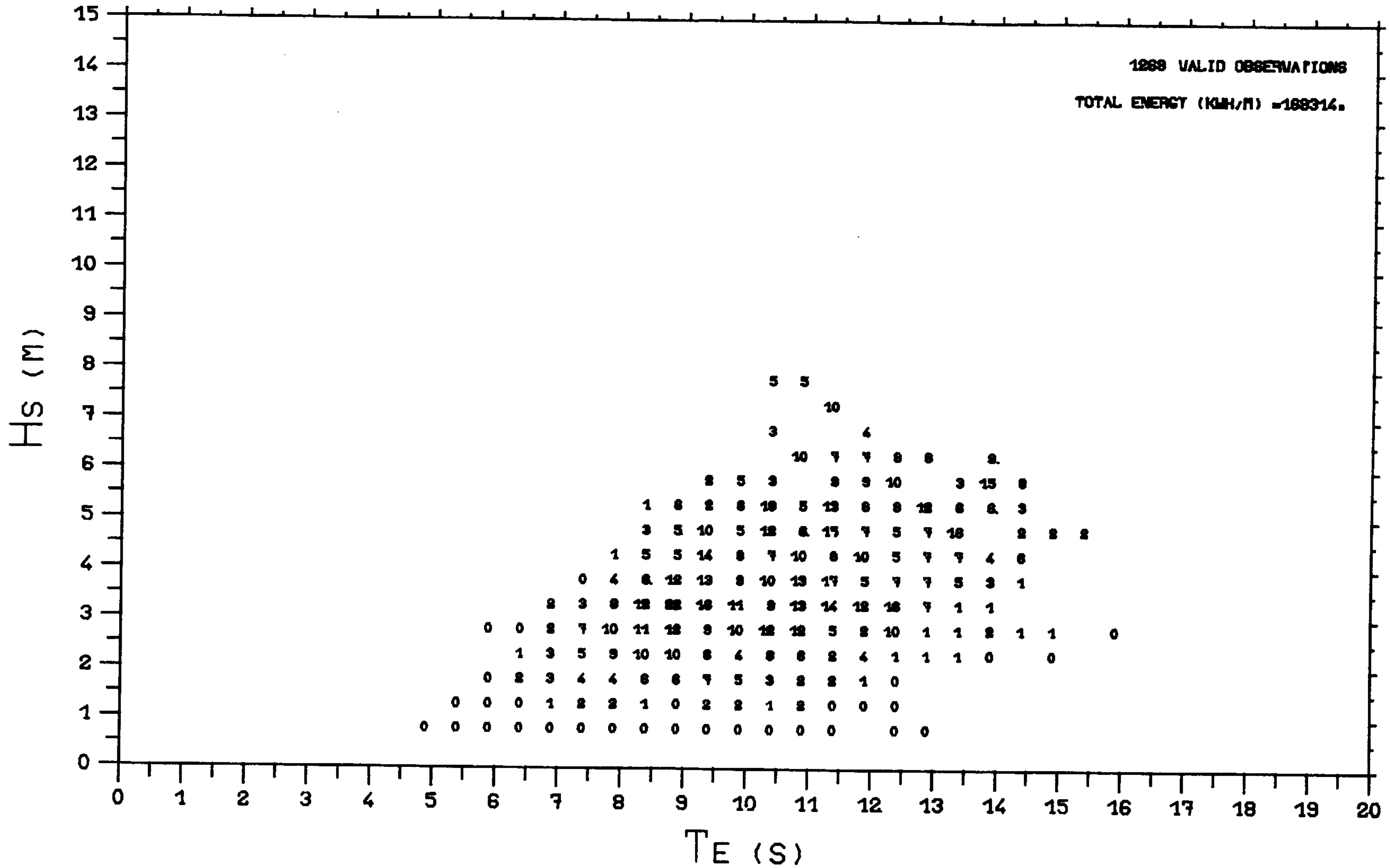

DISTRIBUTION OF TOTAL MEASURED WAVE ENERGY
WITH Hs AND Te (PPT)

SOUTH UIST WINTER 1976/7, 1977/8

FIG 3.7.4

SU768

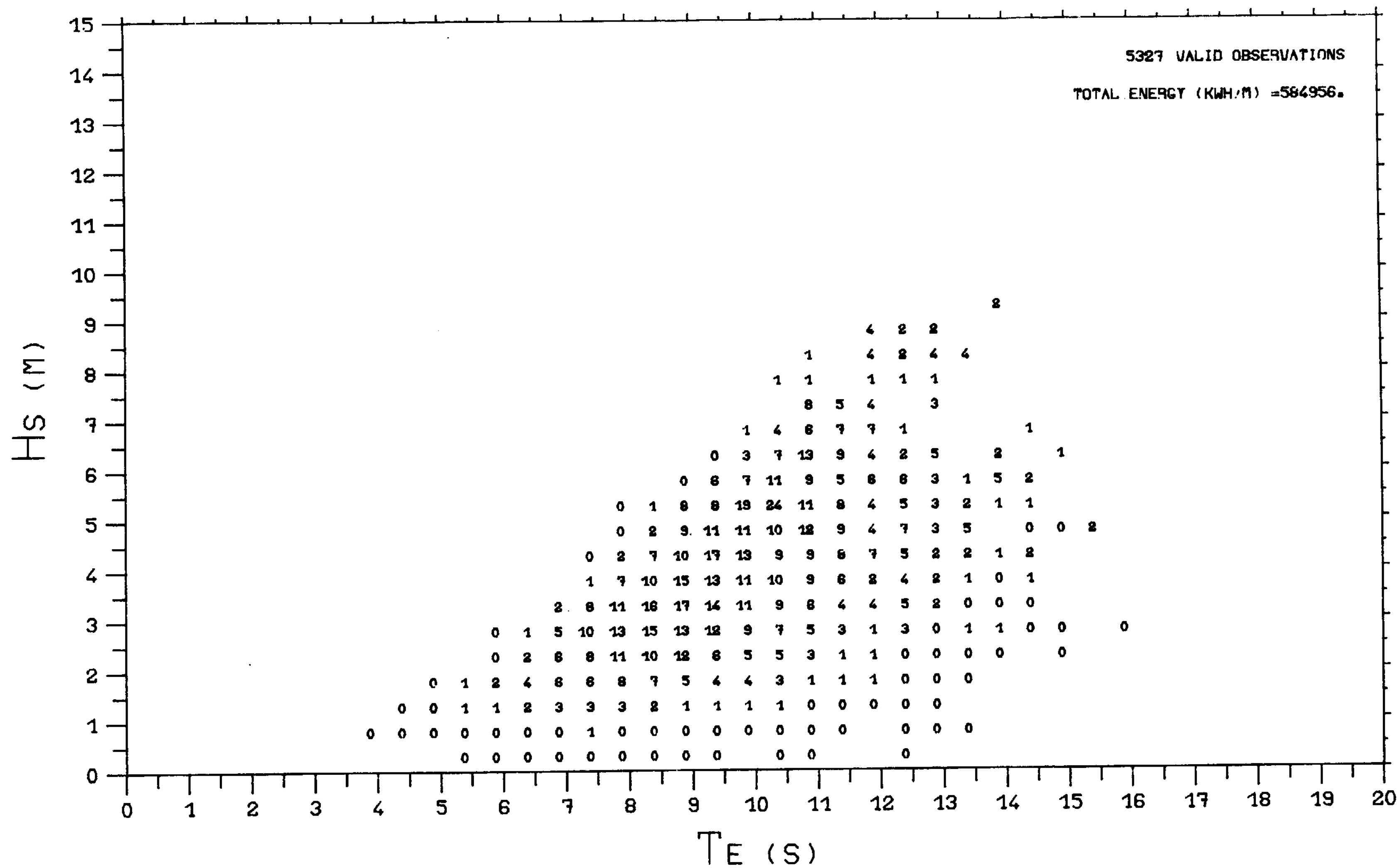

DISTRIBUTION OF TOTAL MEASURED WAVE ENERGY
WITH Hs AND Te (PPT)

SOUTH UIST MAR 1976 - FEB 1978

FIG 3.7.5

SU768